# Deepwater Container Terminal T3: Sediment Transport and Water Quality Numerical Modelling Study

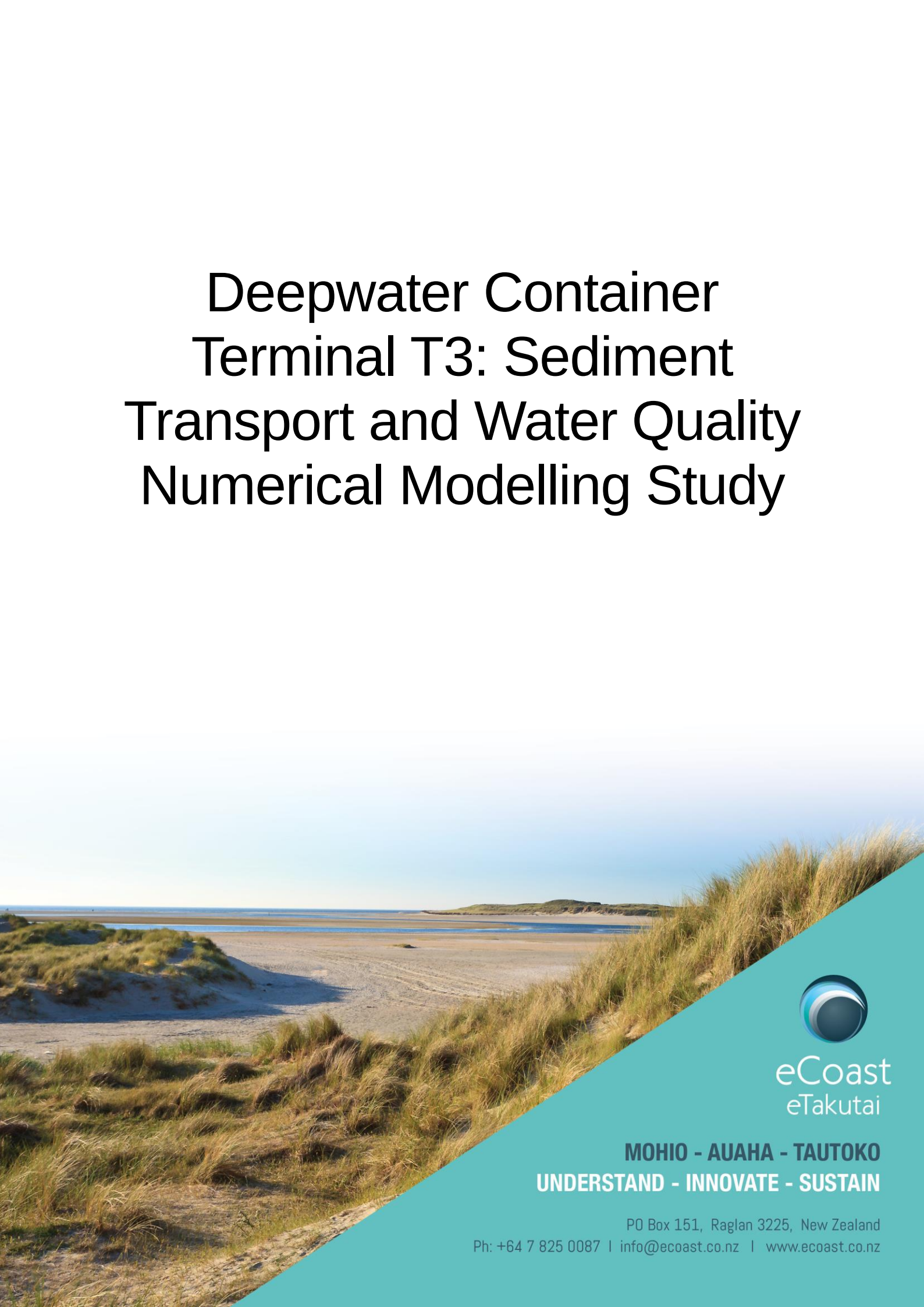

eCoast
eTakutai

MOHIO - AUAHA - TAUTOKO
UNDERSTAND - INNOVATE - SUSTAIN

PO Box 151, Raglan 3225, New Zealand
Ph: +64 7 825 0087 | info@ecoast.co.nz | www.ecoast.co.nz

# Deepwater Container Terminal T3: Sediment Transport and Water Quality Numerical Modelling Study

**Report Status**

| Version | Date | Status | Approved by |
|---|---|---|---|
| V1 | 10 June 2022 | Draft | SDG |
| V2 | 27 June 2022 | Final | SDG |
| | | | |

It is the responsibility of the reader to verify the version number of this report.


Authors:

Dougal Greer MSc
Jose C. Borrero Ph.D.
Rhys Mcintosh MSc
Jai Davies Campbell MSc


Client

**Arup**


The information contained in this document, including the intellectual property, is confidential and propriety to Ecological and Physical Coastal Consultants Limited (T/A eCoast). It may be used by the persons to whom it is provided for the stated purpose for which it is provided and must not be imparted to any third person without prior written approval from eCoast. eCoast reserves all legal rights and remedies in relation to any infringement of its right in respect of its confidential information. eCoast 2022

# Executive Summary

The Port of Gdańsk is a seaport located in the city of Gdańsk on the southern coast of the Gulf of Gdańsk and is one of the largest seaports on the Baltic Sea. The Gdańsk Deepwater Container Terminal (DCT) is the only truly deep-water container terminal in the Baltic Sea and is the primary gateway for Polish traffic and Baltic transhipment operations.

The existing facility is divided into two main operating areas, known as Terminal 1 (T1) and Terminal 2 (T2). In 2020, two extra segments were added to the existing breakwater. DCT currently has plans for the future development of a Terminal 3 (T3) which will include capital dredging and land reclamation. The area of T3 is approximately 37 ha (0.37 $km^2$).

Stogi Beach lies directly to the east of the Port of Gdańsk and is a popular bathing beach with swimming water quality rated as excellent. It also provides habitat for a number of threatened bird species.

This study includes:

- A beach morphology evolution study using numerical models to assess potential adverse impacts on the adjacent beach due to the development of T3 and the expansion of the offshore detached breakwaters.
- A numerical modelling study investigating potential water quality issues affecting the coastal zone due to the development of T3.

The numerical modelling components considered three scenarios:

1. The port layout prior to 2020 with T1 and T2 in place but without the breakwater extensions that were built in 2020. None of the proposed dredging is included in this scenario.
2. The port layout as it is currently with T1 and T2 in place and with the breakwater extensions in place as well as the dredging associated with the approach channels and turning circles.
3. The same as Scenario 2 with the addition of the T3 development including dredging of the T3 berthing area.

The scenarios are shown graphically in Figure 5.2.

**Beach Morphology**

The construction of the T1 terminal in 2005 led to the accretion of the western end of Stogi Beach (adjacent to T1) at a rate of approximately 3.4 m per year from 2008 through 2018. The rate of accretion decreases with distance east of T1 and some erosion is seen in the central and east of central portion of the beach while the far-eastern portion of the beach is broadly stable. The rate of accretion at the western end of the beach is greater than the rate of erosion towards the centre and east of centre suggesting a net accumulation of sediment along the beach. While the source of this sediment is not clear, it most likely comes from offshore.

Results from the modelling indicate that the breakwaters that were constructed in 2020 will lead to changes to the sediment transport dynamics of Stogi Beach. They will reduce the wave driven accretion at the western end of the beach and will lead to a pattern of accretion along the central region of the beach. Erosion and accretion patterns at the eastern end of the beach will remain largely unaffected.

The T3 development will lead to continued accretion of the shoreline in the far western end of Stogi Beach which will be exacerbated by wind driven sand transport. The T3 reclamation will not affect sediment transport patterns on the beach to the east of this region.

**Water Quality Modelling**

The modelling results indicate that the freshwater plume from the Vistula River disperses widely over the southern Gulf of Gdańsk and reaches the Port of Gdańsk particularly under high flow conditions and easterly wind conditions. The intrusion of the river water in the marine area between the T3 terminal and Stogi Beach is reduced with the T3 development in place due to its effect on ambient current patterns. River water is likely to be one of the largest contributors of bacterial loads

to the marine environment. Construction of the T3 development is unlikely to lead to higher bacterial or river borne pollutant concentrations at the western end of Stogi Beach.

The modelling also shows that in the same area, while there is some variability in current patterns under different wind conditions, flushing in this area is on average 7 times slower with the T3 development in place. While Vistula River water is less likely to enter the region between the T3 terminal and Stogi beach with the T3 terminal in place, once waterborne pollutants enter this area, they will take on average 7 times as long to be removed under natural influences. There is consequently a strong likelihood that this region will become a sink for litter and debris.

# Contents

# Figures

# Tables

# 1 Introduction

## 1.1 Definitions and Conventions

**Units** – Unless otherwise stated all measurements are in SI units except for temperature where degrees Celsius is used.

**MSL** – Mean Sea Level. All depths are stated relative to this datum unless otherwise stated.

**$H_s$** – Significant wave height (m).

**$T_p$** – Peak wave period (s).

**$D_p$** – Peak wave direction (deg true).

## 1.2 Background

The Port of Gdańsk is a seaport located in the city of Gdańsk on the southern coast of the Gulf of Gdańsk and is one of the largest seaports on the Baltic Sea (Figure 1.1). The Gdańsk Deepwater Container Terminal (DCT) is the only truly deep-water container terminal in the Baltic Sea and is the primary gateway for Polish traffic and Baltic transhipment operations. The terminal has previously undergone an expansion project to extend the facility to include a second deep water terminal to ensure can accommodate all shipping line vessels efficiently. The existing facility is divided into two main operating areas, known as Terminal 1 (T1) and Terminal 2 (T2). DCT currently has plans for the future development of Terminal 3 (T3) which will include capital dredging and land reclamation (Figure 1.2).

In 2020, two extra segments were added to the existing breakwater (Figure 1.3). Proposed dredging activities are presented in Figure 1.4. The size of the T3 dredge area is approximately 38 ha (0.38 $km^2$). The dredging for the access channel and turning circle is not part of the T3 development and therefore is not considered as part of the T3 development effects. The maximum dredge depth is -17.5 m (MSL); however, the dredge tolerances bring this value to -17.8 m (MSL) in the berthing area buffer zone and -19.5 m (MSL) in the rest of the berthing area. The maximum amount of spoil is estimated to be 4,000,000 $m^3$ (ED, 2019). In terms of land reclamation, the size of the T3 reclamation is approximately 37 ha (0.37 $km^2$). Future terminal expansions T4 and T5, planned in the longer term after the completion of T3 development, are not considered in this study. The T4 and T5 developments will bring the total reclamation area to 80 ha (0.80 $km^2$).

The popular Stogi Beach lies directly to the east of the Port of Gdańsk and is a popular bathing beach. It also provides habitat for a number of threatened bird species (Arup, 2022). It is a medium sand beach ($D_{50}$ = 0.386 mm), 4 km long, 130 m wide at the western end and less than 30 m wide at places on the eastern end (Figure 1.5). The beach is particularly popular in summer months and has excellent/very good water quality for bathing purposes with 2021 water quality sampling showing E. coli counts of 29 cfu (NPL) / 100 ml and Enterococci counts of cfu (NPL)/100 ml[1].

The T3 development forms a semi enclosed basin between the T3 reclamation and Stogi beach (Figure 1.2) which we will refer to as the ‘T3 Shadow Zone’ throughout this report.

[1] Gdańsk Stogi water quality reporting


**Figure 1.1: The Port of Gdańsk, Poland and relevant landmarks.**

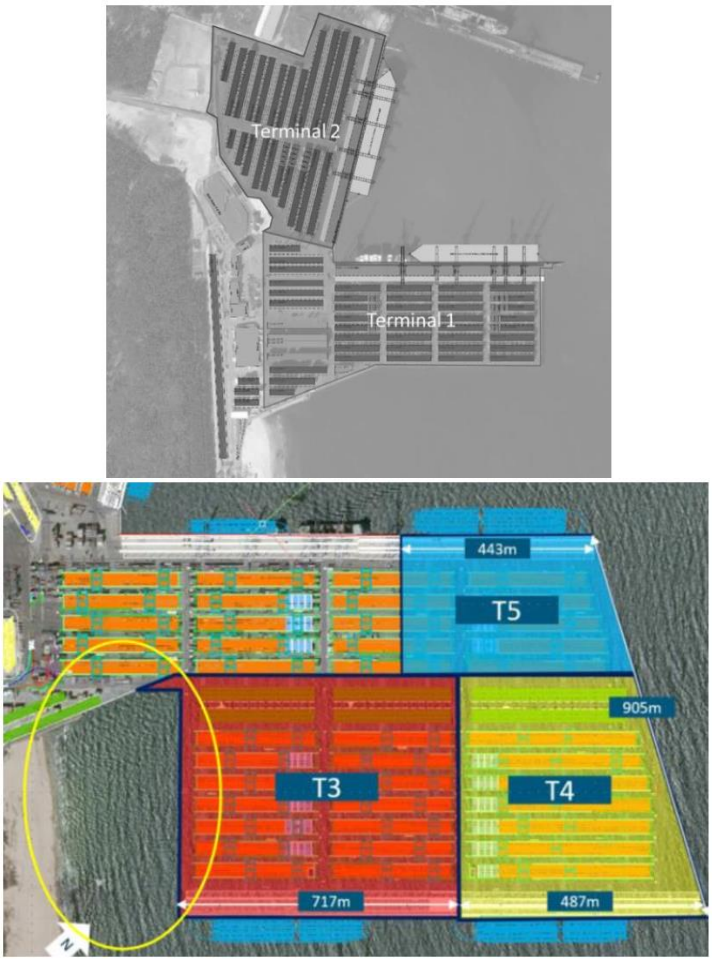


**Figure 1.2: Existing facility at the Port of Gdańsk (top) and the proposed expansion (bottom). The yellow circle highlights the enclosed body of water (the 'T3 shadow zone') that will be created following construction of the T3 development.**

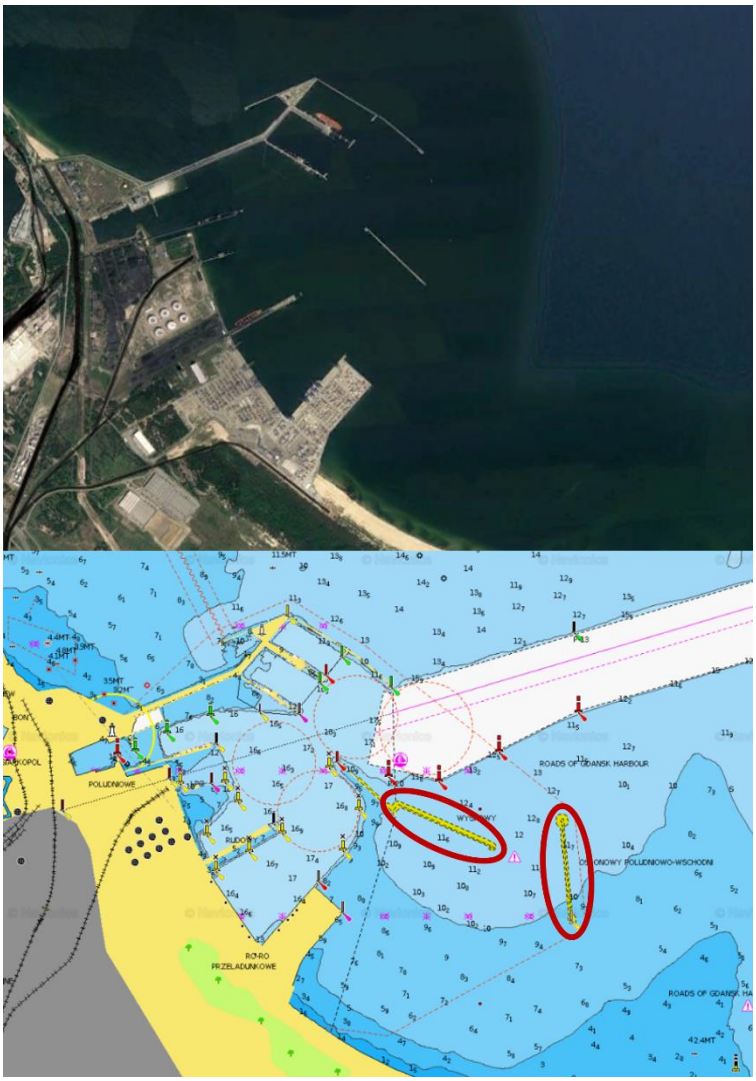


**Figure 1.3: The port layout in 2018 (top) and the extra breakwaters added in 2020 (bottom).**


**Figure 1.4: The location of the proposed T3 terminal (yellow), dredging for the T3 berthing area (purple), berthing area buffer zone (brown) and approach channels and turning circles (green).**

**Figure 1.5: Stogi Beach (top) and visitor infrastructure at the beach (bottom).**

## 1.3 Purpose

The purpose of this study is to undertake:

- A beach morphology evolution study using numerical models to assess potential adverse impacts on the adjacent beach due to the development of T3 and the expansion of the offshore detached breakwaters.
- A numerical modelling study investigating potential water quality issues affecting the coastal zone due to the development of T3.

# 2 Data Sources

The following data sources were used to inform the study presented in this report.

**Bathymetry data** (see Figure 2.1) were sourced from digitised hydrographic charts, port surveys of the T2 and T3 areas provided by DCT, The 2018 EMODnet (resolution ~115 m latitudinal × 47–68 m longitudinal) digital bathymetric dataset (Jakobsson et al., 2019) and a beach topography survey (down to a depth of -1 m) undertaken in May 2022 as part of this study.

**Wind and wave data** were sourced from the NOAA Wave Watch III 30-year Hindcast Phase 1[2] from the North Sea Baltic 4 min sub-grid (Figure 2.2) for the years of 1979 to 2009. For time periods after 2009, wind data were derived from the ECMWF ERA5 hindcast model (Hersbach et al., 2020).

**T3 and dredging specifications** were derived from AutoCAD files provided by DCT.

**Sediment grain size data** were derived from a sediment analysis study[3] undertaken in May 2022 as part of this study. The study analysed samples at 19 locations along Stogi Beach (Figure 2.4).

**Satellite imagery** was sourced from the Google Earth historical archive and from the Landsat database[4].

**River flow data** at an hourly sampling rate from the Tczew flow gauge for 2014 to 2021 was provided by the Institute of Meteorology and Water Management - National Research Institute (Poland).

[2] https://polar.ncep.noaa.gov/waves/hindcasts/nopp-phase1.php

[3] Undertaken by Geoteko Projekty I Konsultacje Geotechniczne (Geoteko Projects and Consultations Geotechniczne), Study number 83/5755/22.

[4] https://www.usgs.gov/landsat-missions

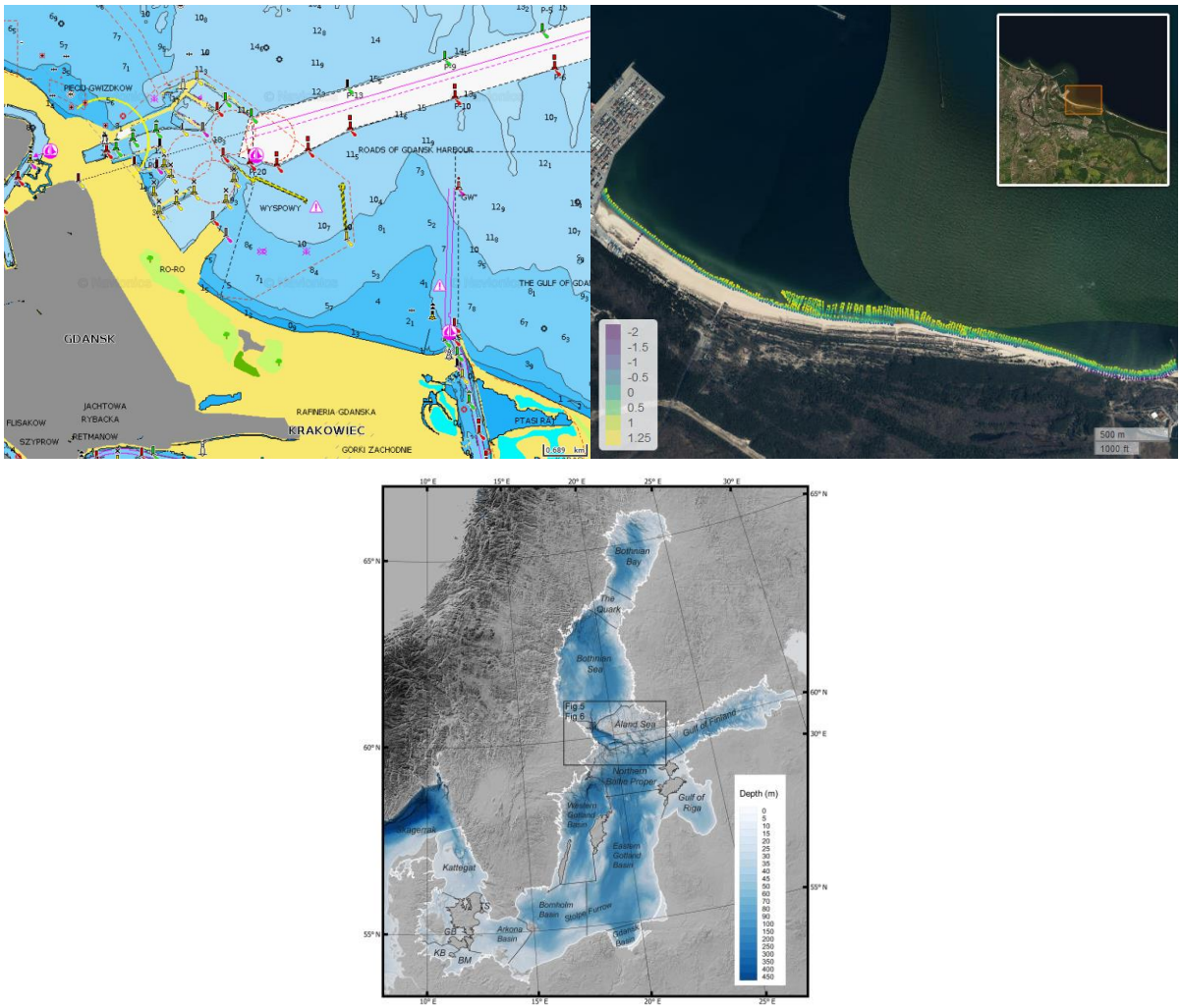


**Figure 2.1: Example hydrographic chart (top left), Stogi beach survey (2022) (top right) and the EMODnet bathymetric dataset for the Baltic Sea (bottom).**

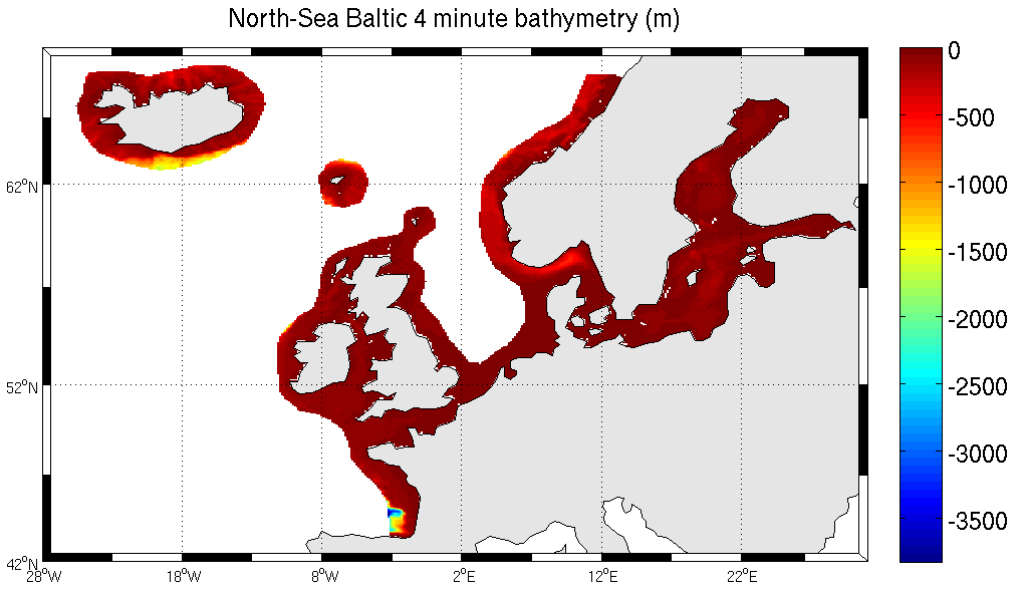


**Figure 2.2: NOAA Wave Watch III 30-year Hindcast Phase 1 from the North Sea Baltic 4 min sub-grid (source: NOAA).**

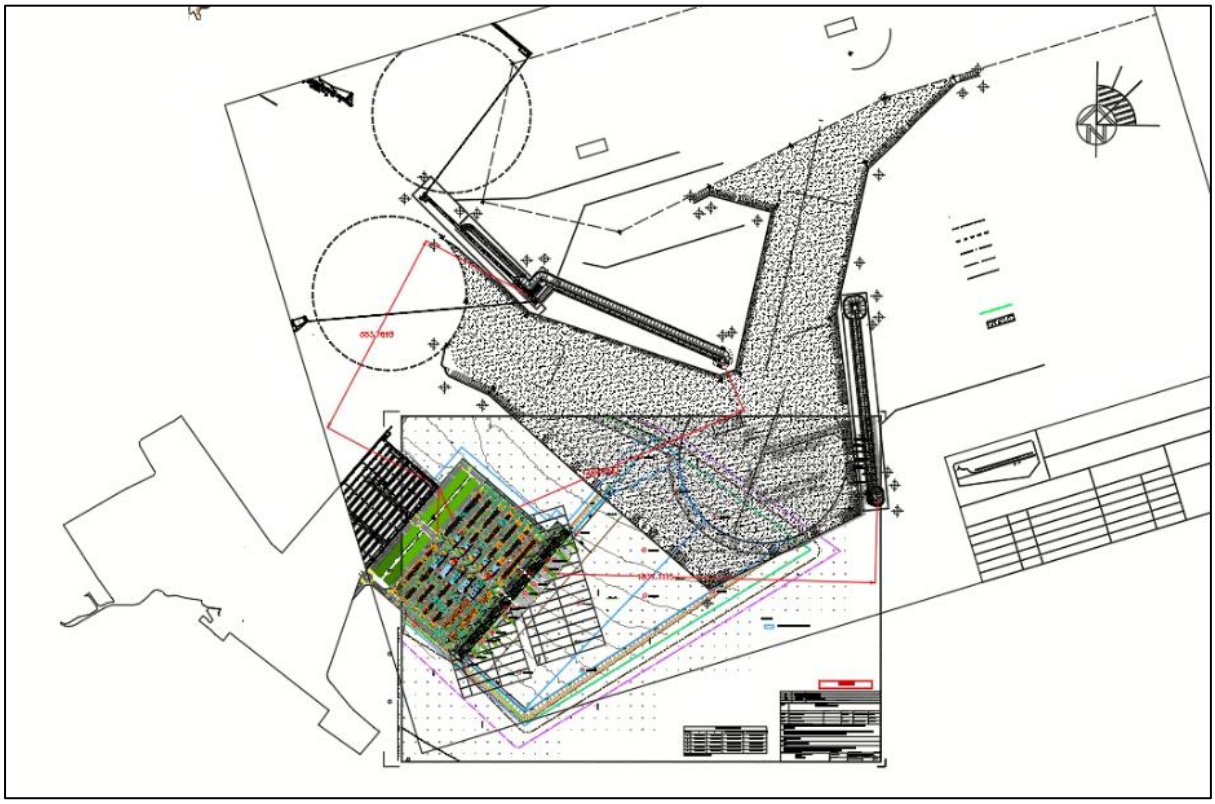

**Figure 2.3: AutoCAD drawing of the port developments including the T3 terminal and dredge areas (source: DCT).**


**Figure 2.4: The 19 sampling locations used for sieve analysis of sediment.**

# 3 Literature Review and Site Description

The Port of Gdańsk is located in the south of the Gulf of Gdańsk which is in the south of the Baltic Sea. The Gulf of Gdańsk is a waterbody that is formally shared between Poland and Russia. It is a north facing bay with a large sandspit (the Vistula Spit) across the western side of the mouth. The mouth of the Vistula River lies 14 km to the east of the port. It is the longest river of those received by the Baltic Sea (1,047 km) and the second largest by catchment area (183,176 $km^2$).

## 3.1 Wind and Waves

As part of this study, wind and wave records were extracted from a long-term 30-year wave model at a grid node corresponding to 54.8 N, 19.2 E (Figure 3.1) which is summarised in Figure 3.2 to Figure 3.4. Wind is observed to come from all directions though it is most commonly from the west and southwest with a speed typically less than 14 $ms^{-1}$. Some seasonality is seen in the wind climate with lighter winds observed from April to June. Wave directions are primarily from the northwest though northerly waves are also commonly observed. Other wave directions are observed, but considerably less frequently.

Significant wave heights ($H_s$) are typically less than 2 m with an associated peak period ($T_p$) less than 10s. Scatter plots show that $H_s$ and $T_p$ are strongly associated with wind speed and occasionally, though rarely, $H_s$ exceeds 6 m associated with winds speeds greater than approximately 17 $ms^{-1}$. These large waves are associated with $T_p$ of nearly 12 s and are from the north. These waves are associated with the largest fetch in the Baltic Sea for the Gulf of Gdańsk (approximately 600 km). It is expected that the wave characteristics at the study site in the southwest of the Gulf will be strongly affected by the large spit at the western entrance of the gulf and by the port infrastructure to the west of the study site.


**Figure 3.1: Wave model extraction location (54.8N, 19.2E) from the North Sea Baltic 4-minute model which is part of the NOAA Phase 2 wave watch 3 30-year hindcast.**

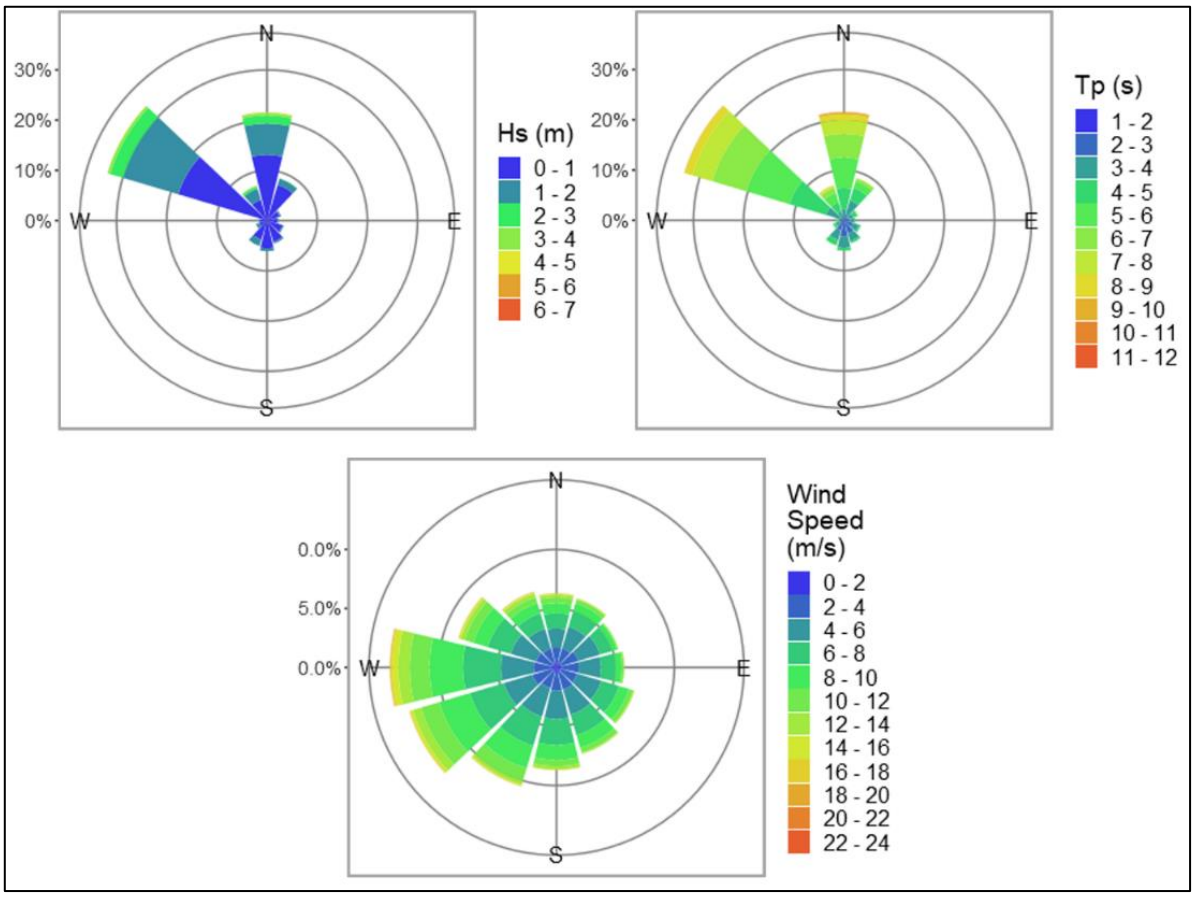


**Figure 3.2: Wind and wave roses for 30-year data extracted from the North Sea Baltic 4-minute model which is part of the NOAA Phase 2 wave watch 3 30-year hindcast at a grid node located at 54.8N, 19.2E.**

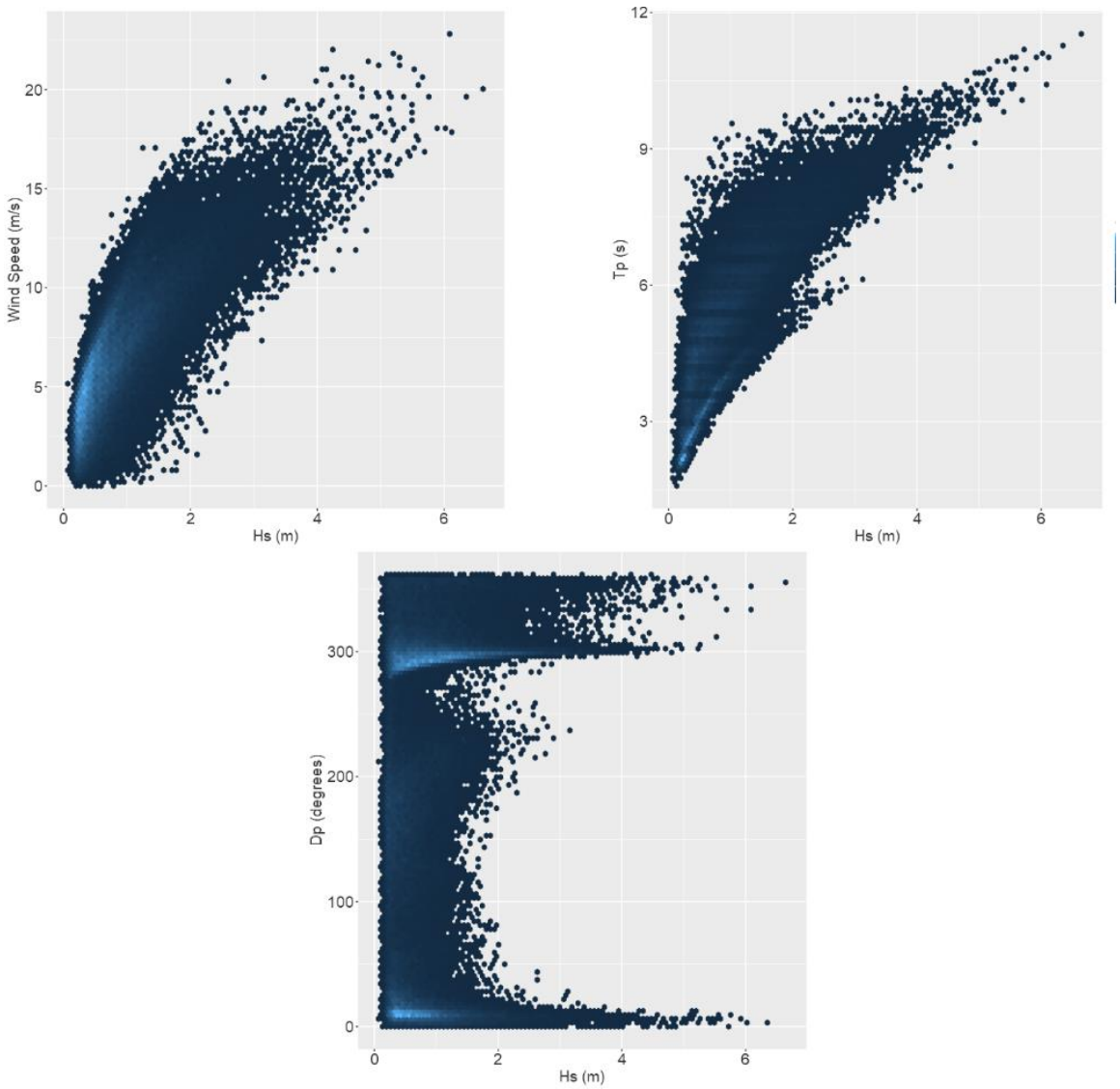


**Figure 3.3: Wind and wave scatter plots for 30-year data extracted from the North Sea Baltic 4-minute model which is part of the NOAA Phase 2 wave watch 3 30-year hindcast at a grid node located at 54.8N, 19.2E.**

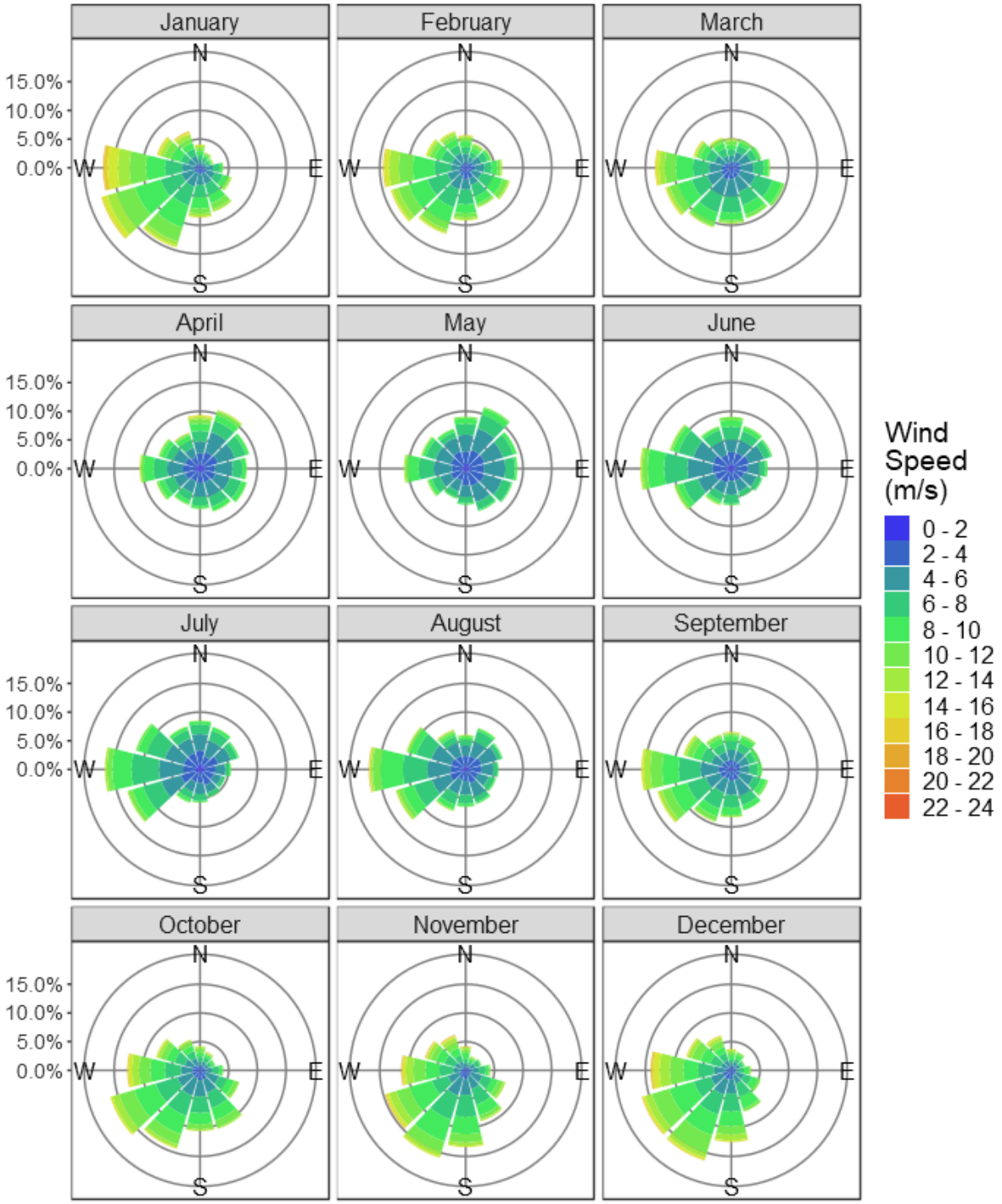


**Figure 3.4: Wind roses by month for 30-year data extracted from the North Sea Baltic 4-minute model which is part of the NOAA Phase 2 wave watch 3 30-year hindcast at a grid node located at 54.8N, 19.2E**

## 3.2 Sea Level

The tidal range in the Baltic Sea is very small due to the low connectivity with the North Sea. Overall, tidal ranges are mostly between about 0.02 m and 0.05 m although in the western sea areas, tidal ranges of up to 0.1 m and 0.3 m are observed (Weisse et al., 2021). Non-tidal sea level variability can be significant and maximum sea levels at the Port of Gdańsk of 0.38 m are observed with a return period of 1 year. This increases to 1.06 m and 1.20 m for 5- and 10-year return intervals respectively (Royal Haskoning DHV, 2020).

## 3.3 Water Quality

The mean Vistula River water discharge into the Gulf of Gdańsk is 1080 $m^3$ $s^{-1}$, with an average sediment suspension load of 14.6 mg $L^{-1}$ which varies between 8 and 40 mg $dm^{-3}$ (Damrat et al., 2013). According to Pruszak et al. (2005), the annual sediment load into the Gulf of Gdańsk ranges from 0.6 to 1.5 million $m^3$ of sediment.

Eutrophication is one of the greatest ecological threats to the Baltic Sea environment[5]. Eutrophication is the increase in the supply of organic matter to an ecosystem through nutrient enrichment and is induced by excessive availability of nitrogen and phosphorus for primary producers (algae, cyanobacteria and benthic macro-vegetation). Most of the nutrients in the Baltic Sea are delivered via freshwater sources (HELCOM, 2018). At the study site, the main source of these nutrients is likely to be the Vistula River which has the highest area specific nutrient loading in the Baltic Sea (HELCOM, 2021a). The input of total nitrogen from the Vistula River (118,000 t $y^{-1}$, on average) amounts to 15%, and the input of total phosphorus (7,000 t $y^{-1}$, on average) consists of 19% of the total riverine discharge into the Baltic Sea. The high contribution from the Vistula River is due to the nature of its drainage area, 60% of which is agricultural land. The Vistula River basin is inhabited by 20 million people, i.e. 27% of the entire population inhabiting the drainage area of the Baltic Sea. As a result of anthropogenic pressure, the ecosystem of the Gulf of Gdańsk has been subject to significant changes during the last 50 years. The Inspectorate of Environmental Protection (2020) has undertaken regular sampling of indicators of eutrophication in the Gdańsk Basin including phosphorus, nitrogen, chlorophyll a, water clarity and dissolved oxygen which it presents dating back to 2010. In general, nitrate concentrations have decreased over time while phosphates have increased. This study indicates that chlorophyll a has broadly decreased, though a HELOCM study (2018) indicates that is levels have not changed significantly. Water clarity has shown a slight negative trend. Near the study site monitoring indicates that the spring blossom continues to be the most intensive and higher chlorophyll a concentrations are recorded during this time than in summer. However, the total weight of phytoplankton in the bay in summer is very large (Atkins, 2014).

In terms of bathing water quality, during the last ten years, several sewage treatment plants have been constructed. As a result of this effort, only 20% of the Polish coast of the Gulf of Gdańsk is unavailable for bathing; this is in comparison to the fact that all beaches were closed in the 1980s (Andrulewicz and Witek, 2002). However, Stogi Beach has been rated as having excellent/very good water quality for bathing in recent years.

Marine litter is a considerable and growing problem worldwide. In 2015, a 3-year pilot program for monitoring waste in the marine environment of the southern Baltic Sea was implemented at several locations along the Polish Baltic Sea coastline (see Figure 3.5) (Inspectorate of Environmental Protection, 2020). Since 2018, regular monitoring of waste collected on the shoreline, floating on the water surface and on the seabed has been carried out. While results vary from year to year, the 2020 survey shows that the largest amount of waste was found in Gdańsk (Figure 3.6).

[5] http://stateofthebalticsea.helcom.fi/pressures-and-their-status/eutrophication/


**Figure 3.5: Locations of waste surveys. (Source: Inspectorate of Environmental Protection, 2020).**

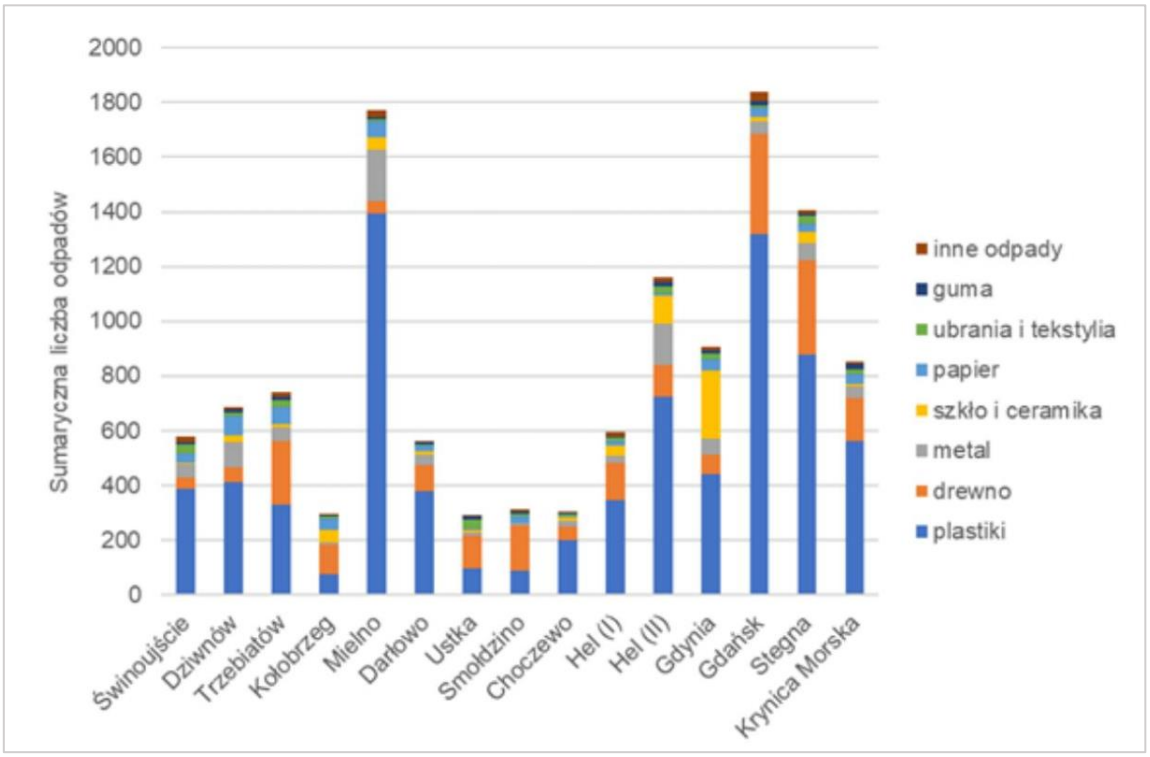


**Figure 3.6: Total number of waste items (from four study periods) recorded on individual sections in seven main categories in 2020. The largest number of waste items were found at Gdańsk in 2020. (Source: Inspectorate of Environmental Protection, 2020).**

## 3.4 Climate Change

### 3.4.1 Waves

A study of climate change effects on wave climate by Bonaduce et al. (2019) predicted only small changes in wave height in the Gulf of Gdańsk by the end of the 21st century (2075-2100) (Figure 3.7). These results show a slight reduction (between 5% and 10%) in winter and little change in summer. HELCOM (2021b) reports that changes in Baltic Sea wave climate are strongly linked to changes in wind climate and are highly uncertain. There is high confidence on reduced ice cover which may increase fetch, and perhaps change the wave climate. By 2100, changes in significant wave height are projected to be around 5% higher than today, particularly in the north and east of the Baltic Sea. However, such changes are superimposed by substantial multi-decadal and inter-simulation variability and are not conclusive.

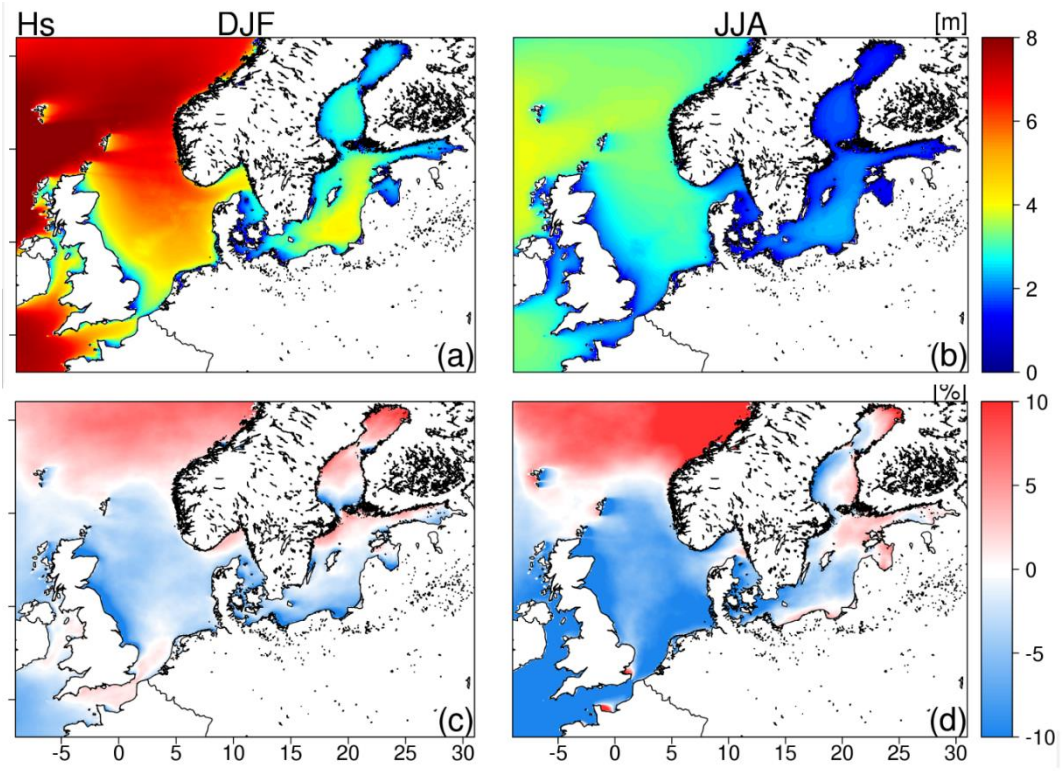


**Figure 3.7: Mean future significant wave height (top) during winter (DJF) and summer (JJA) and difference with present day wave climate (bottom) (source: Bonaduce et al.,2019)**

### 3.4.2 Sea Level

Global sea level rise will accelerate. Current projections estimate Baltic Sea level rise to about 87% of the global rate. Estimates for global mean sea level rise by 2100 are 43 cm (RCP2.6) to 84 cm (RCP8.5). The likely ranges for these estimates are 29 to 56 cm (RCP2.6) and 61 to 110 cm (RCP8.5) HELCOM, (2021b).

### 3.4.3 River runoff

HELCOM, (2021b) reports that no statistically significant change in total annual river runoff has been detected during the last centuries and the large decadal and regional variations occur. In the northern Baltic Sea and the Gulf of Finland, larger river runoff is statistically

associated with warmer air temperature and increased precipitation, while further south, decreased annual runoff is associated with rising air temperatures. Over the 20th century, winter discharge has increased, while spring floods have decreased.

The total runoff to the Baltic Sea has been projected to increase from present day by 2-22% with warming temperatures. The increase will take place mostly in the North, with potentially decreasing total runoff in the South while winter runoff will increase due to intermittent melting. On average rivers terminating in the southeast of the Baltic Sea will likely experience a reduction in discharge of approximately 18.25% by 2081 to 2100 (Šarauskienė et al., 2017).

### 3.4.4 Nutrient Loading of Rivers

Projections suggest that river discharge will decrease in the southern Baltic Sea region thus potentially decreasing waterborne nutrient inputs, respectively (HELCOM, 2021b).

### 3.4.5 Wind

Projected changes in wind climate are highly uncertain due to large natural variability in the Baltic Sea area. Climate model simulations project a slight but significant wind speed increase in autumn and a decrease in spring (HELCOM, 2021b).

# 4 Model Scenarios

The numerical modelling components considered three scenarios:

4. The **Previous** scenario: the port layout prior to 2020 with T1 and T2 in place but without the breakwater extensions that were built in 2020. None of the proposed dredging is included in this scenario.
5. The **Present** scenario: the port layout as it is currently with T1 and T2 in place and with the breakwater extensions in place as well as the dredging associated with the approach channel and turning circles.
6. The **Future** scenario: the same as the Present scenario with the addition of the T3 development including dredging of the T3 berthing area.

The scenarios are shown graphically in Figure 5.2.

The ‘Previous’ scenario has been undertaken since the breakwater extensions were constructed recently (2020) and they are expected to have a significant impact on Stogi Beach incident wave climate and sediment transport. A comprehensive assessment of the expected changes to waves and sediment transport due to the T3 development needs to account for the effects of the breakwater extensions in isolation.

# 5 Beach Morphology

A beach morphology evolution study has been carried out to understand the effects of the T3 development on the local sediment transport regime.

## 5.1 Methods

This study has been undertaken in three stages:

1. **Historical Shoreline Analysis** using satellite imagery to identify trends in accretion and erosion along Stogi Beach.
2. **Long Term Wave Modelling** to provide a wave record at the study site with and without developments in place.
3. **Sediment Transport Modelling** to understand the changes in the sediment transport regime along Stogi beach with and without developments in place.

For the beach morphology modelling, an additional scenario was included to investigate the effects of climate change which uses the same parameterisation as the *Future* scenario but with incident wave energy reduced by 10% in line with conservative predictions from Bonaduce et al. (2019).

### 5.1.1 Historical Shoreline analysis

Shoreline analysis was undertaken by examination of historical satellite photography. Imagery was sourced from the Google Earth historical archive and from the Landsat database[6]. Imagery was collated to provide coverage of the whole of Stogi Beach with emphasis on the western end towards the T1 terminal.

The Google Earth imagery provides high resolution but sporadic coverage of the beach from 2008 to 2018. No full coverage Google Earth images of Stogi Beach were available beyond 2018. Landsat imagery was collated from between 1986 and 2020 at varying resolutions. Even at the highest resolution of 10 m, it was not of sufficient quality to make reliable measurements of beach width, though it was useful for identifying construction timelines for local coastal infrastructure.

Beach width was assessed at 14 locations (Figure 5.1) over 24 images and the results are presented in Table 5.2. The first measurement location was chosen at a location 100 m east of the T1 terminal. Examination of the imagery showed this to be a stable location away from the intermittent variable erosion and accretion at the edge of the T1 rock revetment. Subsequent transects were located every 300 m thereafter. Results for this analysis are presented in Section 5.2.1.

Note that these erosion/accretion measurements have been made in the absence of the extra breakwater infrastructure which was built in 2020. The timing of this construction was found by examination of Landsat imagery. The presence of these breakwaters and of the T3 terminal are likely to further change the sediment transport regime in this area.

[6] https://www.usgs.gov/landsat-missions


**Figure 5.1: Beach width measurement locations used to assess historical changes in the width Stogi Beach.**

## 5.1.2 Long Term Wave Modelling

Wave modelling was undertaken using the SWAN wave model (Holthuijsen et al., 2004) which is an industry standard for simulating wave generation and propagation. SWAN is a third-generation ocean wave propagation model which solves the spectral action density balance equation for frequency-directional spectra.

The model setup used a 3-stage nested bathymetry scheme shown in Figure 5.2. Note the large raised bathymetric feature offshore from the eastern end of the beach. The dimensions for each grid are presented in Table 5.1. The nesting scheme allows for increasing model resolution with proximity to the study site. Wave conditions were specified on the northern boundaries using $H_s$, $T_p$ and $D_p$ extracted from the NOAA Wave Watch III 30-year Hindcast (Section 3.1) at 19.200 E, 54.933 N. Winds were extracted from the same model at 19.200 E, 54.667 N. The 30-year wave hindcast was forced through the model for the 3 model scenarios providing detailed wave conditions at the study site. No measured wave data were available with which to calibrate the wave model and standard settings were used for model parameterisation. Model results are presented in Section 5.2.2.

**Table 5.1: Specifications of the SWAN model grids used in this project.**

| | nx | ny | Cell size (m) |
|---|---|---|---|
| **Grid 1** | 107 | 69 | 1000 |
| **Grid 2** | 111 | 66 | 200 |
| **Grid 3** | 176 | 141 | 40 |

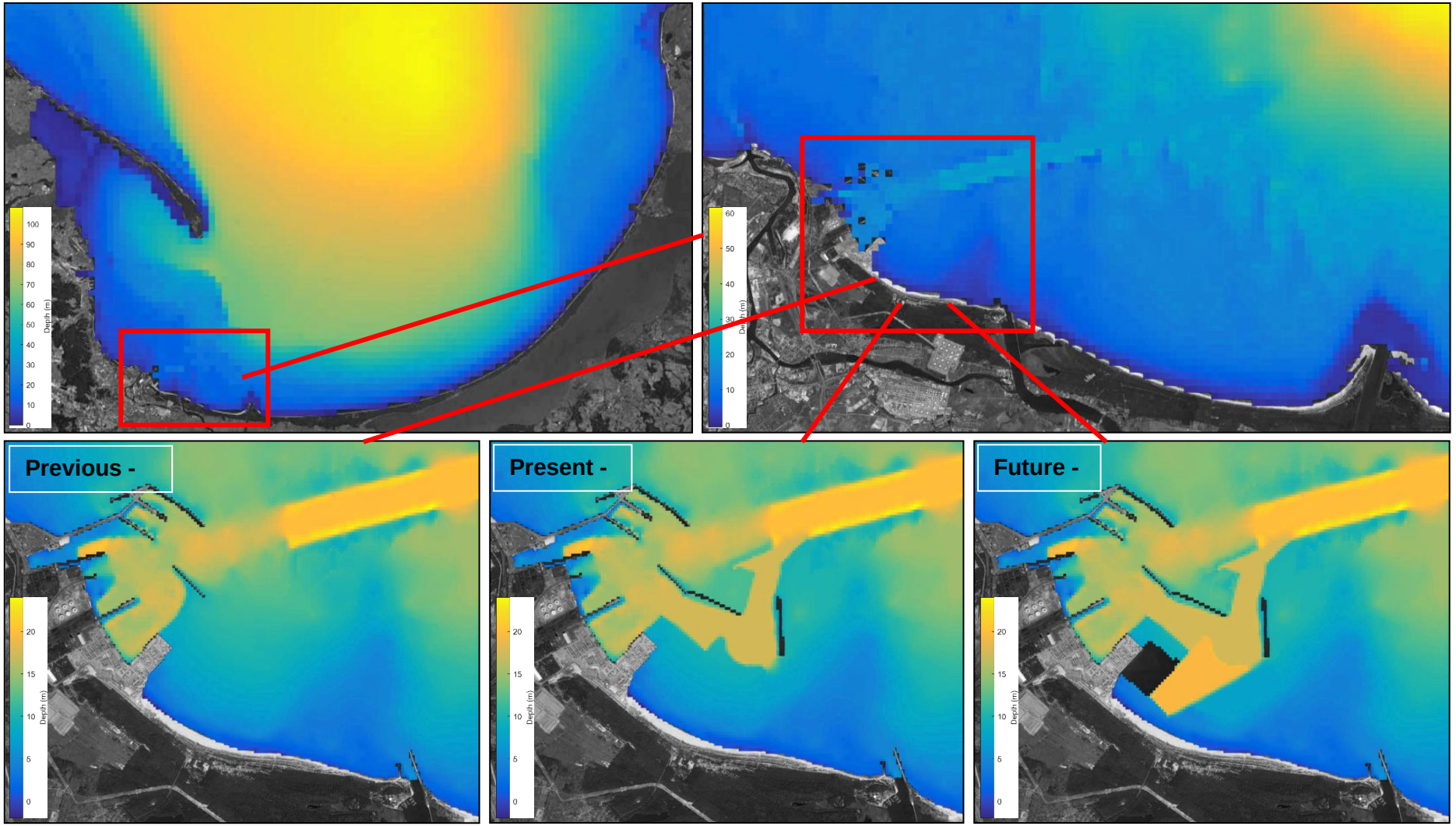


**Figure 5.2: SWAN bathymetry grids used in the wave modelling study for the three scenarios.**

### 5.1.3 Beach Morphology Modelling

Beach morphology was modelled using a one-line modelling approach. One-line models are 1-dimensional and they assess longshore sediment flux based on an isobath-normal topography/bathymetry transect. The wave climate was extracted from the long-term wave model at the offshore end of the transects. The wave characteristics extracted from the model were significant $H_s$, $T_p$ and $D_p$. The wave record was binned to create a table of representative wave conditions for each transect. These were used as boundary conditions for the model.

For this study we used the GENIUS sediment transport model. GENIUS predicts refraction, breakpoint wave conditions and longshore sediment transport on beaches. It is similar to its well-known counterpart GENESIS (Hanson and Kraus, 1989) but with some extra features including frictional attenuation of wave height and a physics-based treatment of wave transmission across submerged reefs.

The sediment grain size was determined from a survey of Stogi Beach sands undertaken as part of this study (see Section 2). The analysis sampled beach sediment at 19 locations along the beach and showed a very uniform grain size. The average $D_{50}$ grain size across the 19 sampling locations was 0.386 mm.

The one-line model was applied at the 14 locations that were analysed in the historical shoreline analysis (Section 5.1.1). Cross-shore transects at these locations are shown in Figure 5.3. Each transect extends out to the 7 m isobath except for Transects 1 and 2 which are truncated to accommodate the T3 reclamation in the *Future* scenario.

The output from the one-line model is the total along-shore sediment transport rate at discrete points on each transect. Sediment transport rates were aggregated over the time series of wave conditions to calculate the net transport rate over the model period. The model output quantifies the overall magnitude and direction of sediment transport for each transect.

Using the results from the '*Previous'* scenario, a relationship was established between the accretion and erosion rates from the historical shoreline analysis and the modelled sediment transport rates at each transect. This relationship was then used to predict shoreline evolution in the '*Present'* and '*Future'* scenarios. Beach morphology model results are presented in Section 5.2.3.

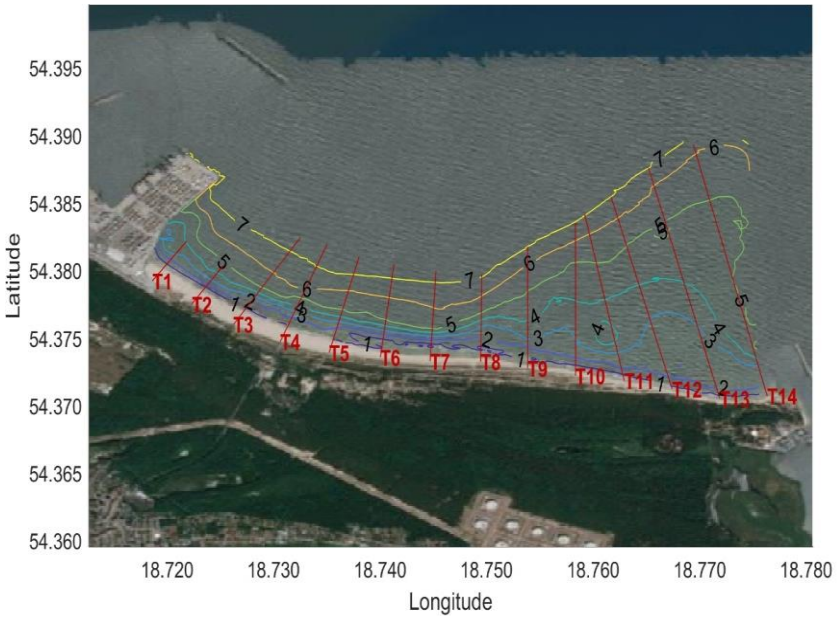


**Figure 5.3: Transects for used in the one-line sediment transport modelling superimposed on a bathymetric map. 'T' in the legend here indicates 'Transect'.**

### 5.1.4 Limitations

Historical shoreline analysis was undertaken based only on available historical imagery. If more up to date imagery had been available, it would have been beneficial to analyse the shoreline change since the construction of the additional breakwater structures in 2020. It would also have been useful to have had additional data to understand the change in beach morphology prior to the construction of the T1 terminal.

The boundaries of the wave model used wave parameters ($H_s$, $T_p$ and $D_p$) rather than spectral wave boundaries. While spectral boundaries are generally preferable, in this instance wave energy distribution is almost always unimodal due to the fetch limiting characteristics of the Baltic Sea and this reduces the need for spectral boundaries.

One-line wave models do not simulate complex current patterns generated by wave propagation (e.g. rip cells). Nonetheless, Stogi Beach is reasonably straight and uniform therefore it is appropriate for use with a one-line model.

Extrapolating shoreline changes into the future does not account for the changing bathymetric orientation relative to the angle of wave attack. The orientation of the shoreline usually alters over time to be perpendicular to the angle of wave attack at which time a state of equilibrium is reached. For this reason, caution should be applied when extrapolating shoreline change results far into the future.

Measured erosion and accretion rates on Stogi beach indicate that there is net accretion of sediment along the beach and that the beach is likely being nourished by sand from further offshore and this may be connected to the large shallow bathymetric feature offshore from the eastern end of the beach. This extra source of sediment is not included in the one-line model.

No calibration data were available for the long-term wave model. Normally comparison of the model with measured data is an industry standard for wave modelling. However, the wave climate at this location is reasonably simple compared with locations in the open ocean where long period swells coexist with locally generated wind swells.

Berthed ships were not included in the modelling. While it is expected that they will lead to some attenuation of wave energy, they are unlikely to strongly influence the sediment transport regime.

Beach morphology was based on wave driven effects. Aeolian (wind driven) sediment transport was not included in the model.

## 5.2 Sediment Transport Modelling Results

This section presents the results from the historical shoreline analysis, long term wave modelling and sediment transport modelling.

### 5.2.1 Historical Shoreline Analysis

Examination of the Google Earth images provides reasonably high resolution (approximately 1 m by 1 m) imagery of Stogi Beach. This imagery was used for examination of beach width evolution between 2008 to 2018. The images are shown for the western end of Stogi beach in Figure 5.9 to Figure 5.11. A zoomed-out version of the same imagery covering Stogi Beach in its entirety is presented in Appendix A. The archive also contains one image from 1985 which shows that the beach was considerably narrower prior to the construction of T1, noting that this image predates the 2005 construction of the T1 terminal by some 20 years.

Through analysis of the imagery, ephemeral bars were observed to occasionally form along the mid-section of Stogi Beach (example in Figure 5.5). The bars often form at an oblique angle to the coastline and are occasionally emergent.

The evolution of beach width over time is shown in Figure 5.6. Results presented here divide the beach into the western, central and eastern sections as depicted in Figure 5.4. There is evidence of ongoing accretion at the western end of the beach (west of Transect 6) throughout the images between 2008 and 2018. The centre and east of centre of the beach (Transect 7 to Transect 11) has shown a trend of ongoing erosion. This erosional trend has been proportionally smaller than the accretion in the west. Apart from fluctuations, the far eastern end of Stogi Beach (Transect 12 to Transect 14) has been reasonably stable (Appendix A) through the analysis period.


**Figure 5.4: Stogi Beach to the east of the Port of Gdańsk. The labels provide the naming convention used throughout this report. 'T' in the legend here indicates 'Transect'.**

For each transect linear regression was used to calculate the change in beach width per year for each measurement location. An example of this is shown in Figure 5.7 for Transect 1. In this instance the beach is accreting at a rate of 3.4 m/year (95% confidence interval 2.66 to 4.15 m/year). The largest erosion rate (-2.36 m/year) is seen at Transect 8. Beach

erosion and accretion rates are summarised in Table 5.3. The regression plots for all the transects are presented in Appendix B.

While considerable accretion has been seen on the western end of Stogi Beach over the available 10-year record of satellite images, proportional erosion has not been seen at the centre and east of centre of the beach. This indicates that there is a source of sediment that is adding to the total volume of beach sand though the source of this additional sediment is not immediately clear. The sediment transport is predominantly from east to west (this in confirmed in later sediment transport modelling – Section 5.1.3). The training walls at the mouth of the Marta Wisla (east) appear to block sediment transport from the east; however, no filet of sand is observed against the eastern training wall (see Figure 5.8) indicating firstly that east to west sediment transport is not significant to the east of the wall and secondly that sand does not bypass the wall in a significant quantity in the nearshore. It is therefore most likely that the additional sediment on Stogi Beach builds up through cross-shore transport (i.e. accretion of sand moved ashore from deeper water offshore). It is possible that the source of this additional sediment is the raised bathymetric feature offshore from the eastern end of the Stogi Beach.


**Figure 5.5: Ephemeral emergent bars that observed along the central section of Stogi Beach.**

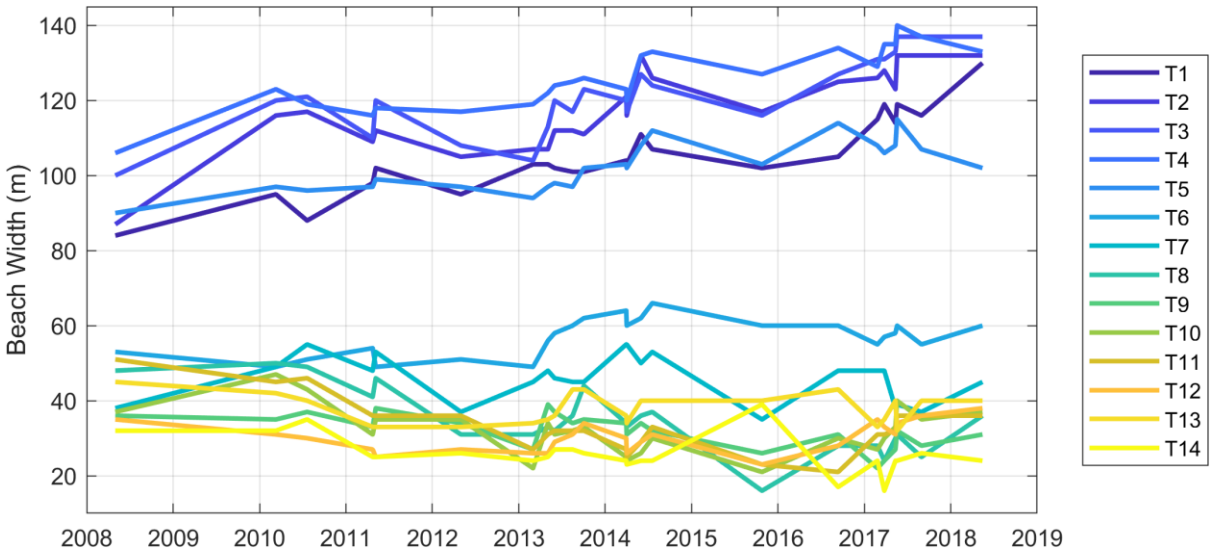


**Figure 5.6: Beach width over time at the 10 transects. 'T' in the legend here indicates 'Transect'.**

**Table 5.2: Measured beach widths at the 14 measurement locations (see Figure 1.1).**

| Date | T1 | T2 | T3 | T4 | T5 | T6 | T7 | T8 | T9 | T10 | T11 | T12 | T13 | T14 |
|---|---|---|---|---|---|---|---|---|---|---|---|---|---|---|
| **15/12/1985** | 25 | 37 | 67 | 90 | 82 | 43 | 42 | 36 | 75 | 67 | 76 | 88 | 116 | 49 |
| **1/05/2008** | 84 | 87 | 100 | 106 | 90 | 53 | 38 | 48 | 36 | 37 | 51 | 35 | 45 | 32 |
| **11/03/2010** | 95 | 116 | 120 | 123 | 97 | 49 | 49 | 50 | 35 | 47 | 45 | 31 | 42 | 32 |
| **21/07/2010** | 88 | 117 | 121 | 119 | 96 | 51 | 55 | 49 | 37 | 43 | 46 | 30 | 40 | 35 |
| **24/04/2011** | 98 | 109 | 110 | 116 | 97 | 54 | 48 | 41 | 33 | 31 | 36 | 27 | 33 | 25 |
| **7/05/2011** | 102 | 112 | 120 | 118 | 99 | 49 | 53 | 46 | 38 | 35 | 36 | 25 | 33 | 25 |
| **1/05/2012** | 95 | 105 | 108 | 117 | 97 | 51 | 37 | 31 | 34 | 35 | 36 | 27 | 33 | 26 |
| **2/03/2013** | 103 | 107 | 104 | 119 | 94 | 49 | 45 | 31 | 27 | 22 | 27 | 26 | 34 | 24 |
| **4/05/2013** | 103 | 107 | 113 | 122 | 97 | 56 | 48 | 33 | 39 | 34 | 31 | 26 | 35 | 25 |
| **1/06/2013** | 102 | 112 | 120 | 124 | 98 | 58 | 46 | 32 | 37 | 31 | 32 | 29 | 36 | 27 |
| **16/08/2013** | 101 | 112 | 117 | 125 | 97 | 60 | 45 | 36 | 34 | 32 | 32 | 31 | 43 | 27 |
| **3/10/2013** | 101 | 111 | 123 | 126 | 102 | 62 | 45 | 44 | 35 | 33 | 32 | 34 | 43 | 26 |
| **31/03/2014** | 104 | 121 | 120 | 123 | 103 | 64 | 55 | 34 | 34 | 25 | 27 | 30 | 36 | 24 |
| **2/04/2014** | 103 | 116 | 117 | 120 | 102 | 60 | 55 | 33 | 31 | 24 | 25 | 26 | 34 | 23 |
| **1/06/2014** | 111 | 132 | 127 | 132 | 108 | 62 | 50 | 36 | 34 | 26 | 29 | 29 | 40 | 24 |
| **19/07/2014** | 107 | 126 | 124 | 133 | 112 | 66 | 53 | 37 | 32 | 30 | 33 | 31 | 40 | 24 |
| **26/10/2015** | 102 | 117 | 116 | 127 | 103 | 60 | 35 | 16 | 26 | 21 | 23 | 23 | 40 | 39 |
| **12/09/2016** | 105 | 125 | 127 | 134 | 114 | 60 | 48 | 28 | 31 | 30 | 21 | 28 | 43 | 17 |
| **25/02/2017** | 115 | 126 | 131 | 129 | 108 | 55 | 48 | 28 | 22 | 27 | 31 | 35 | 33 | 24 |
| **26/03/2017** | 119 | 128 | 131 | 135 | 106 | 57 | 48 | 24 | 24 | 30 | 31 | 33 | 35 | 16 |
| **12/05/2017** | 114 | 123 | 133 | 135 | 108 | 58 | 38 | 30 | 27 | 33 | 32 | 31 | 40 | 24 |
| **19/05/2017** | 119 | 132 | 137 | 140 | 115 | 60 | 39 | 31 | 32 | 40 | 36 | 34 | 32 | 24 |
| **30/08/2017** | 116 | 132 | 137 | 137 | 107 | 55 | 37 | 25 | 28 | 35 | 36 | 36 | 40 | 26 |
| **15/05/2018** | 130 | 132 | 137 | 133 | 102 | 60 | 45 | 36 | 31 | 37 | 36 | 38 | 40 | 24 |

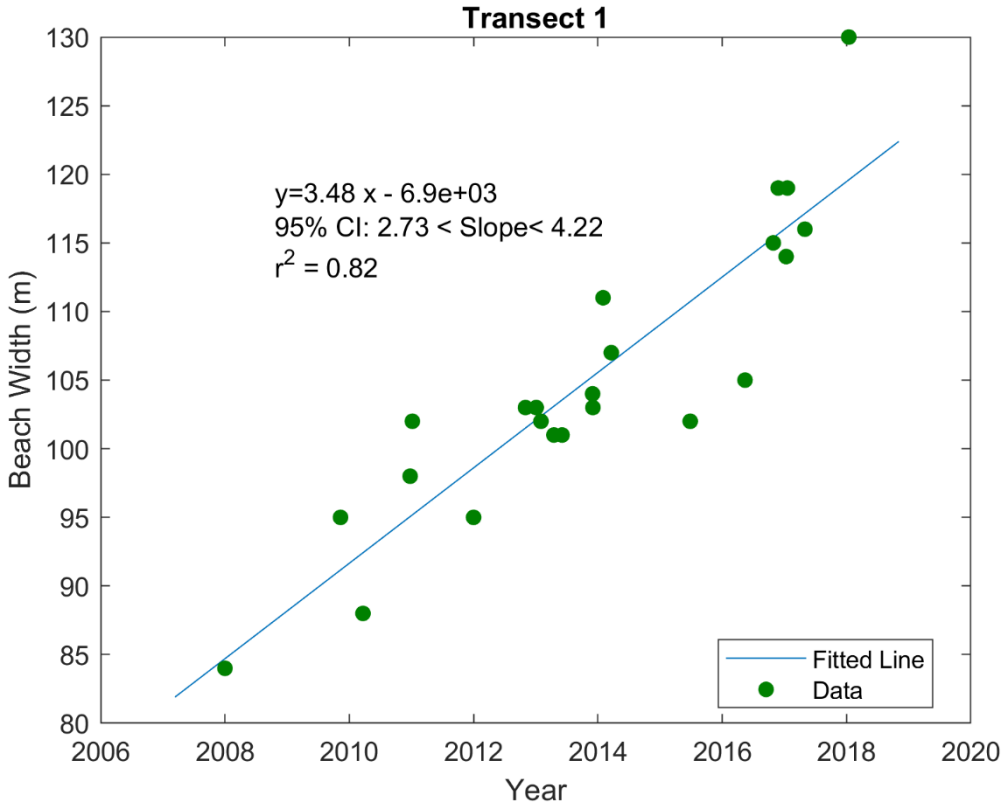


**Figure 5.7: Linear regression relating beach width to time. The slope of the line (3.4) indicates the rate of change of beach width in meters per year. The '95% CI' provides a 95% confidence interval around the slope.**

**Table 5.3: Erosion and accretion rates at each transect considered in this study.**

| | Rate (m/year) | 95% lower | 95% upper |
|---|---|---|---|
| **Transect 1** | 3.48 | 2.73 | 4.22 |
| **Transect 2** | 3.28 | 2.19 | 4.38 |
| **Transect 3** | 3.02 | 1.98 | 4.06 |
| **Transect 4** | 2.68 | 2.04 | 3.33 |
| **Transect 5** | 1.88 | 1.19 | 2.57 |
| **Transect 6** | 0.94 | 0.24 | 1.64 |
| **Transect 7*** | -0.53 | -1.54 | 0.48 |
| **Transect 8** | -2.36 | -3.30 | -1.43 |
| **Transect 9** | -1.13 | -1.69 | -0.57 |
| **Transect 10** | -0.73 | -1.74 | 0.29 |
| **Transect 11** | -1.50 | -2.46 | -0.54 |
| **Transect 12*** | 0.48 | -0.14 | 1.10 |
| **Transect 13*** | -0.17 | -0.84 | 0.50 |
| **Transect 14** | -0.89 | -1.62 | -0.16 |

*Confidence intervals bound 0 so likely no trend.


**Figure 5.8: The mouth of the Marta Wisla showing no notable fillet on the eastern training wall.**

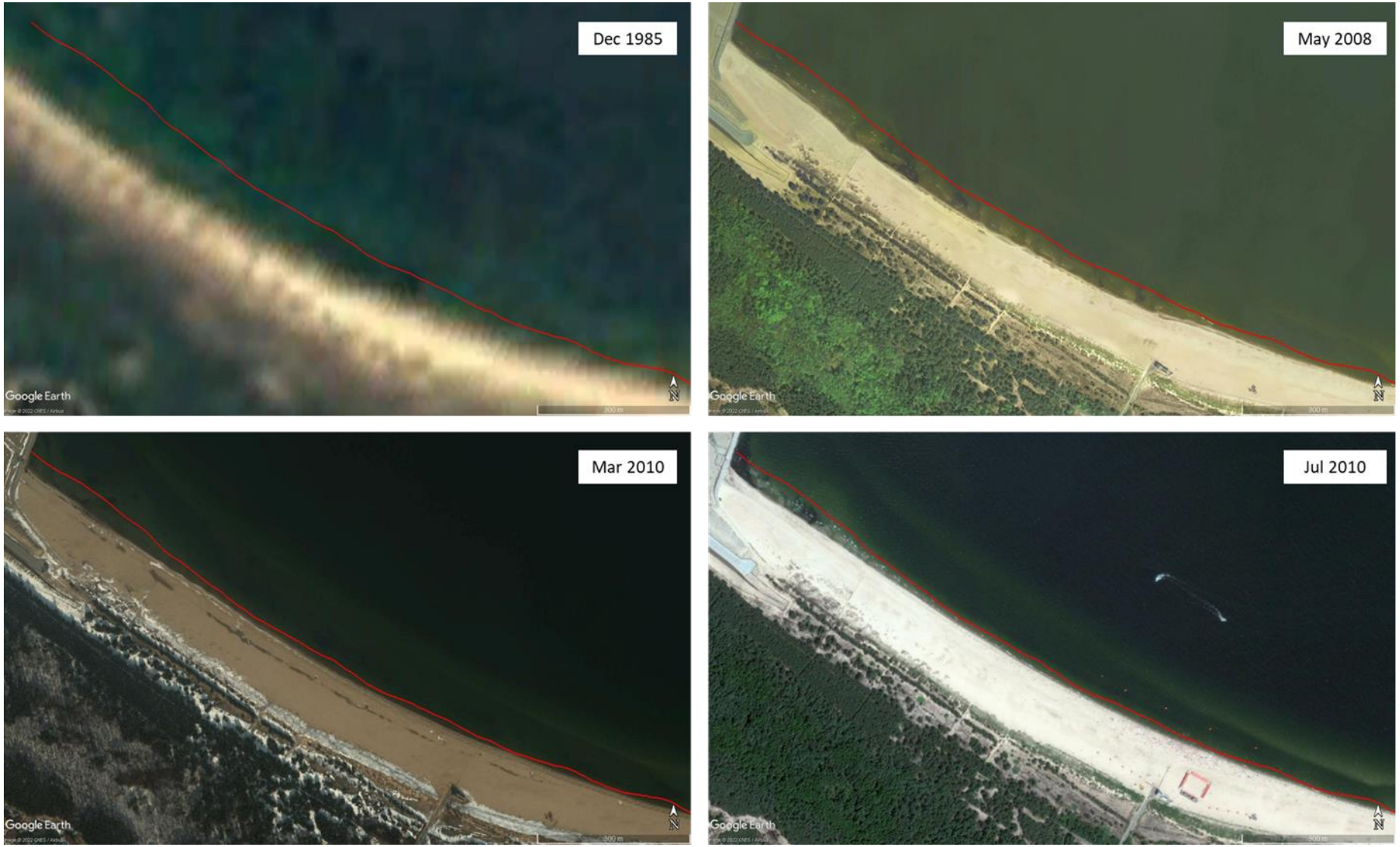


**Figure 5.9: The evolution of the western end of the Stogi Beach shoreline. The red line indicates the shoreline in May 2018 for comparison. Source: Google Earth.**

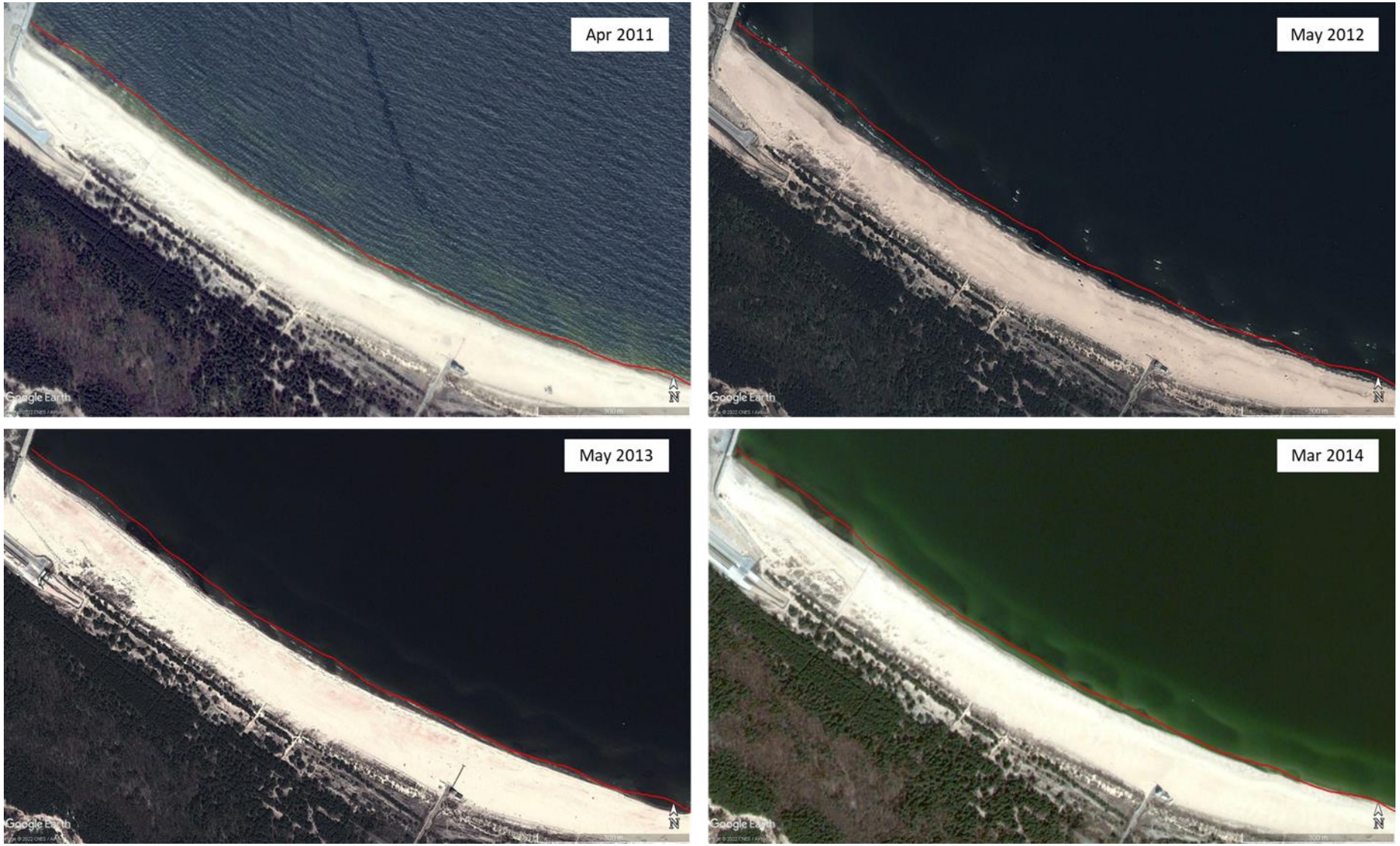


**Figure 5.10: The evolution of the Stogi Beach shoreline at the western end. The red line indicates the shoreline in May 2018 for comparison. Source: Google Earth.**

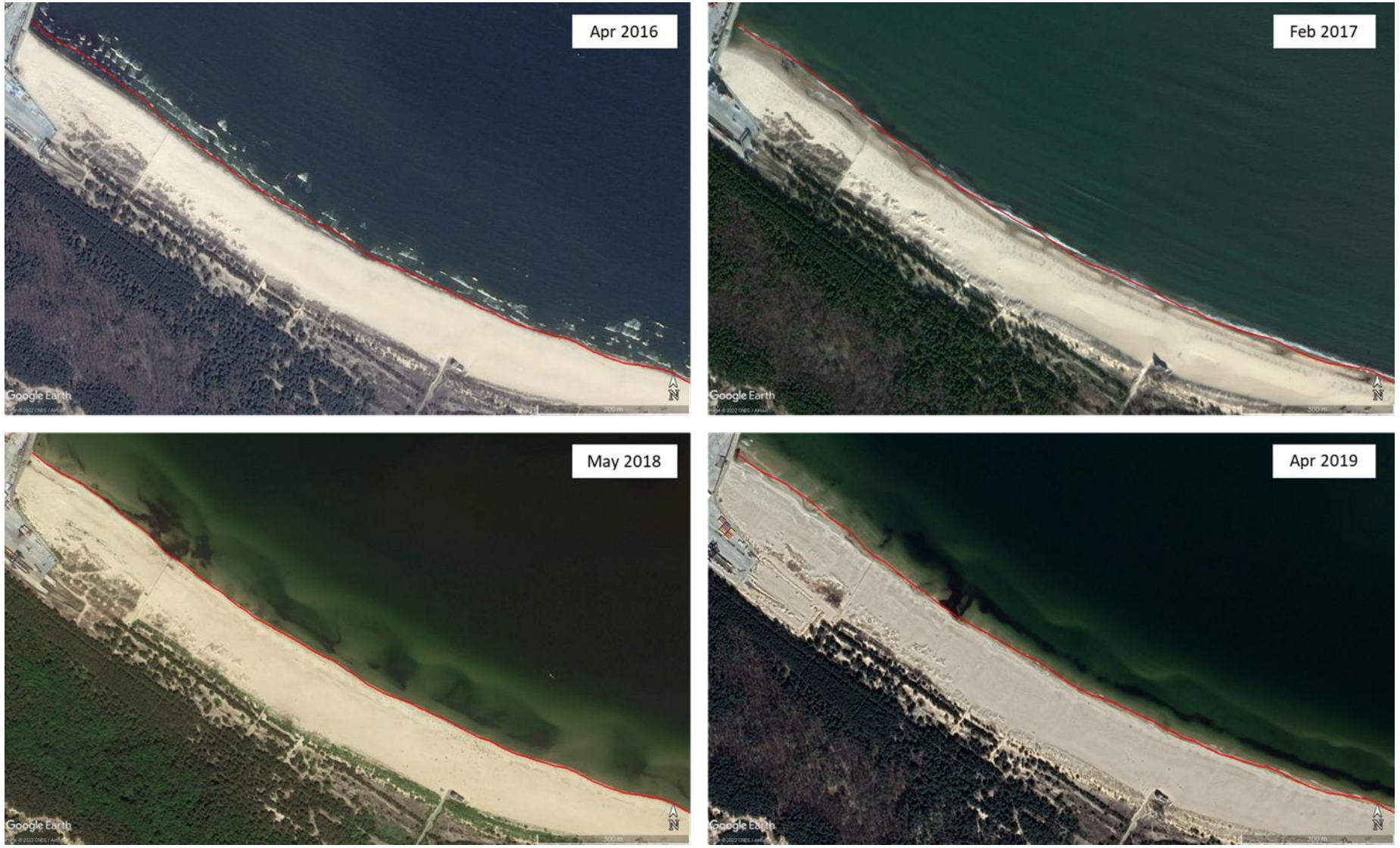


**Figure 5.11: The evolution of the Stogi Beach shoreline at the western end. The red line indicates the shoreline in May 2018 for comparison. Source: Google Earth.**

## 5.2.2 Long Term Wave Modelling

The long term wave modelling produced a 30-year record of wave conditions at the study site providing a comprehensive description of the variability of wave conditions at the port. A summary of wave conditions offshore from the port is shown in Figure 5.12. Overall, the waves are from the NE with most NW wave energy blocked by the Vistula Spit. Significant wave heights are generally less than 3 m and are usually between 0.5 and 1 m.

The variability in local wave energy around the port are shown for a moderate 0.5 m $H_s$ NE wave condition (Figure 5.13) and a large 3 m Hs NE wave condition (Figure 5.14) for the *Previous*, *Present* and *Future* scenarios. For the moderate wave condition, the breakwater extensions (*Present* scenario) reduce the wave energy reaching the western segment of the beach considerably though on the eastern segment, the wave conditions remain unchanged. The addition of the T3 development (*Future* scenario) leads to a further reduction in wave energy at the far western end of the beach. The same effect is seen in the large wave condition. In this case however the wave field is more strongly modified by wave-seabed interactions including strong focusing over the raised bathymetric feature offshore from the eastern end of the beach and refraction around the edges of the dredged channels.

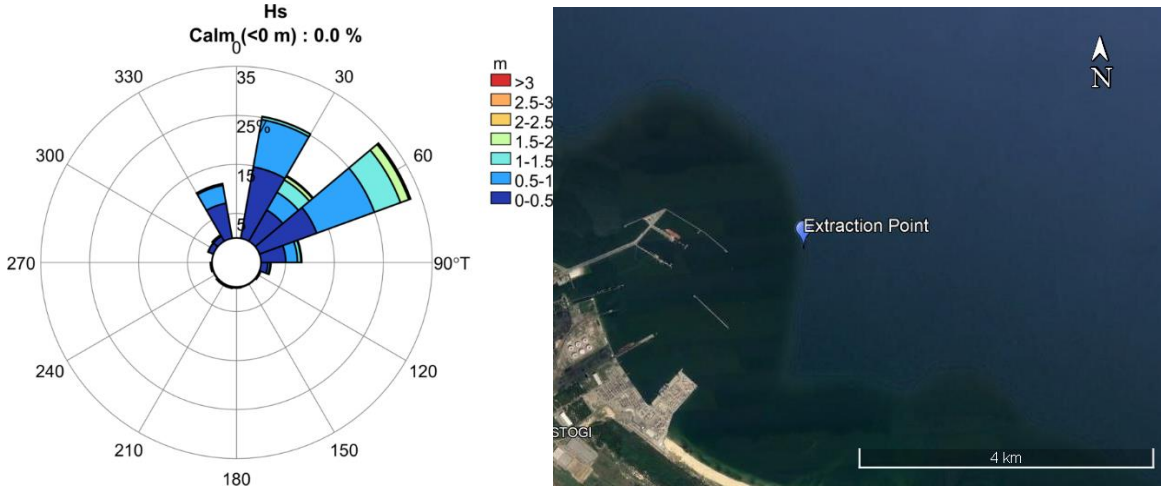


**Figure 5.12: Wave rose (left) summarising the wave climate directly offshore from the Port of Gdańsk (right).**

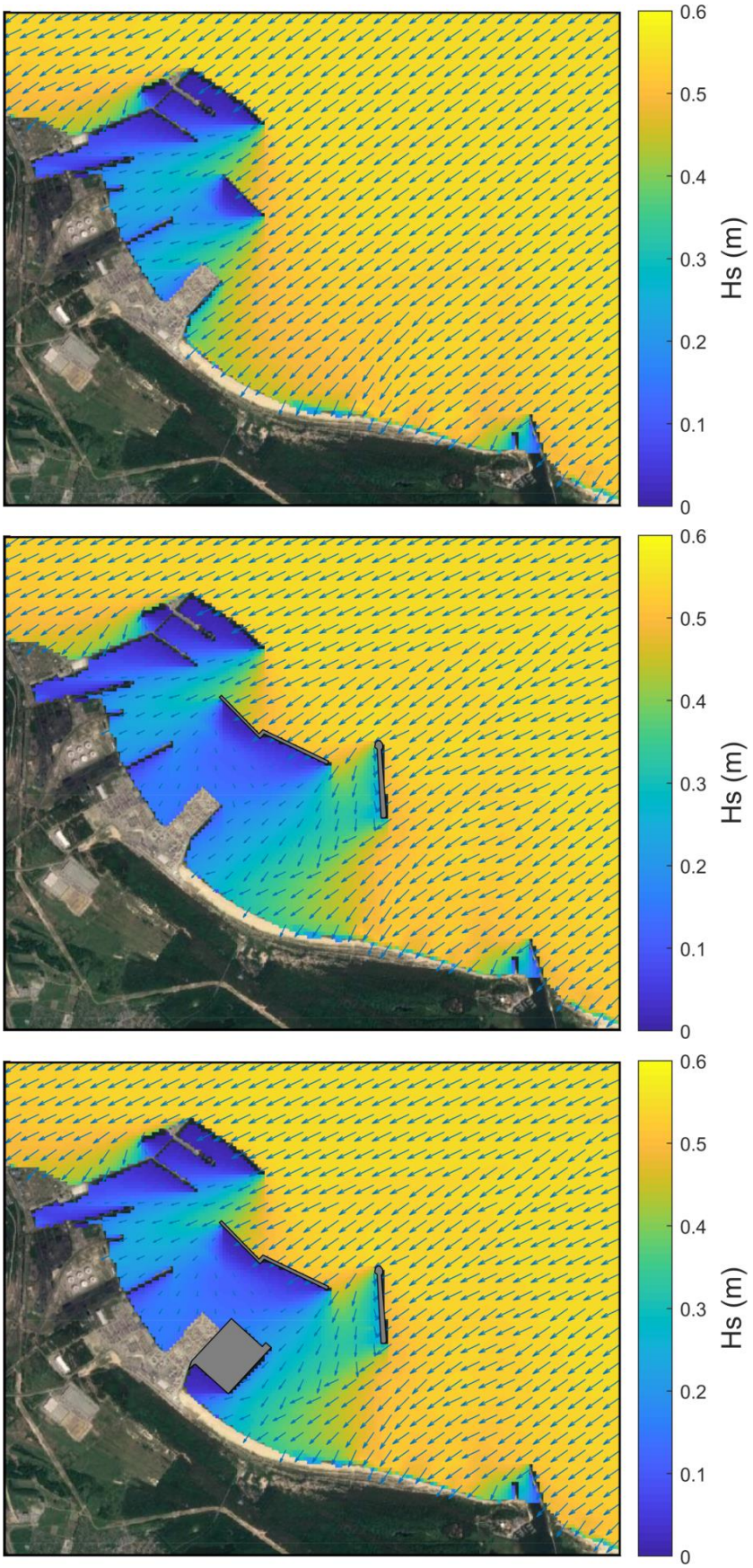


**Figure 5.13: Significant wave height for a moderate 0.5 m NE wave condition for the *Previous* (top), *Present* (middle) and *Future* (bottom) scenarios.**

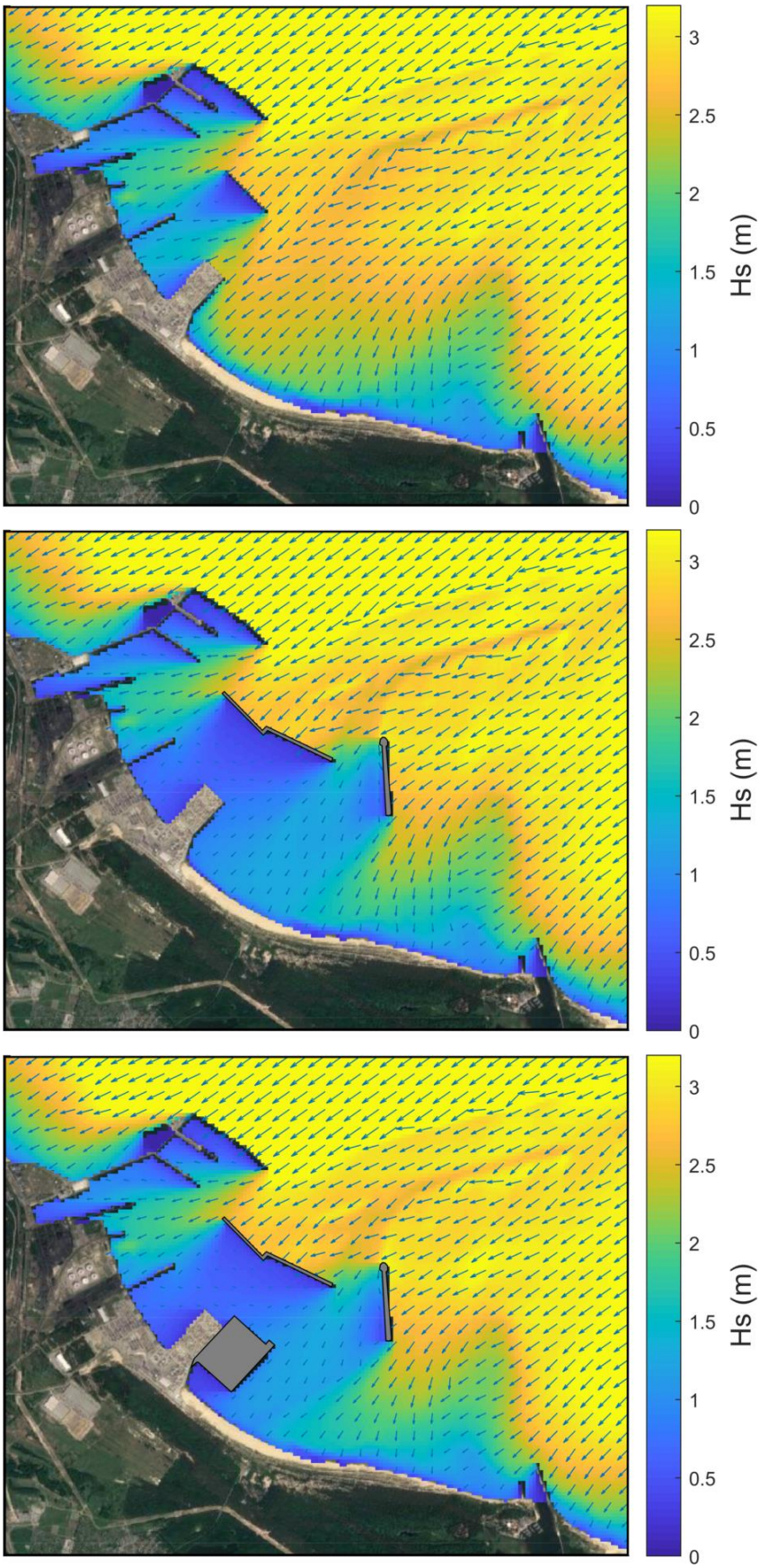


**Figure 5.14: Significant wave height for a large 3 m NE wave condition for the *Previous* (top), *Present* (middle) and *Future* (bottom) scenarios.**

### 5.2.3 Sediment Transport Modelling

The one-line sediment transport modelling approach provides an estimate of annual net sediment flux across each transect. The difference between the net flux at a transect and its neighbour provides an estimate of sediment flux anomaly for each transect (Figure 5.15). The sediment anomaly quantifies net accretion or erosion of sediment at that location. While this is useful for estimating the direction of movement of the shoreline it does not directly provide an estimate of shoreline change at each location. A relationship can be formed between sediment flux anomaly and the measured rate of shoreline change at each location (Section 5.2.1). This is shown graphically in Figure 5.16. This relationship can then be used to infer rates of shoreline change for other scenarios based on the modelled annual sediment flux.

Shoreline change is shown for the *Previous*, *Present* and *Future* scenarios in Figure 5.17 to Figure 5.19 for 10 and 20 years beyond the 2018 baseline case.

The *Previous* shoreline change shows accretion at the western end of the beach and less pronounced but nonetheless significant erosion towards the centre and east of centre of the beach. At the far eastern end of the beach, the shoreline is reasonably stable.

For the *Present* scenario, some erosion is seen at the far western end of the beach. The area of strong accretion moves from the western end of the beach eastwards towards the central area. A pattern of erosion is still seen eastwards from central region of the beach. As in the *Previous* scenario, no erosion is evident in the far eastern end of the model domain.

Shoreline change for the *Future* scenario is very similar to the *Present* scenario except for a return to a pattern of accretion at the far western end of the beach due to the wave shadowing effect of the T3 reclamation.

With the breakwaters in place very little wave energy reaches the western end of Stogi Beach and it is further reduced with the addition of the T3 reclamation. This means that very little wave driven sediment mobilisation is likely to occur in the T3 shadow zone. As noted in Section 5.1.4, Aeolian (wind driven) sediment transport is not included in the model though wind effects are likely to lead to additional accretion of sediment in the T3 shadow zone. The T1 and T3 reclamations will block wind energy from the west and northwest that may otherwise lead to the eastward transport of sediment from this region.

The effects of climate change on the Future scenario are presented in Figure 5.20. The reduced wave energy associated with future climate change will lead to reduced rates of erosion and accretion along the beach.

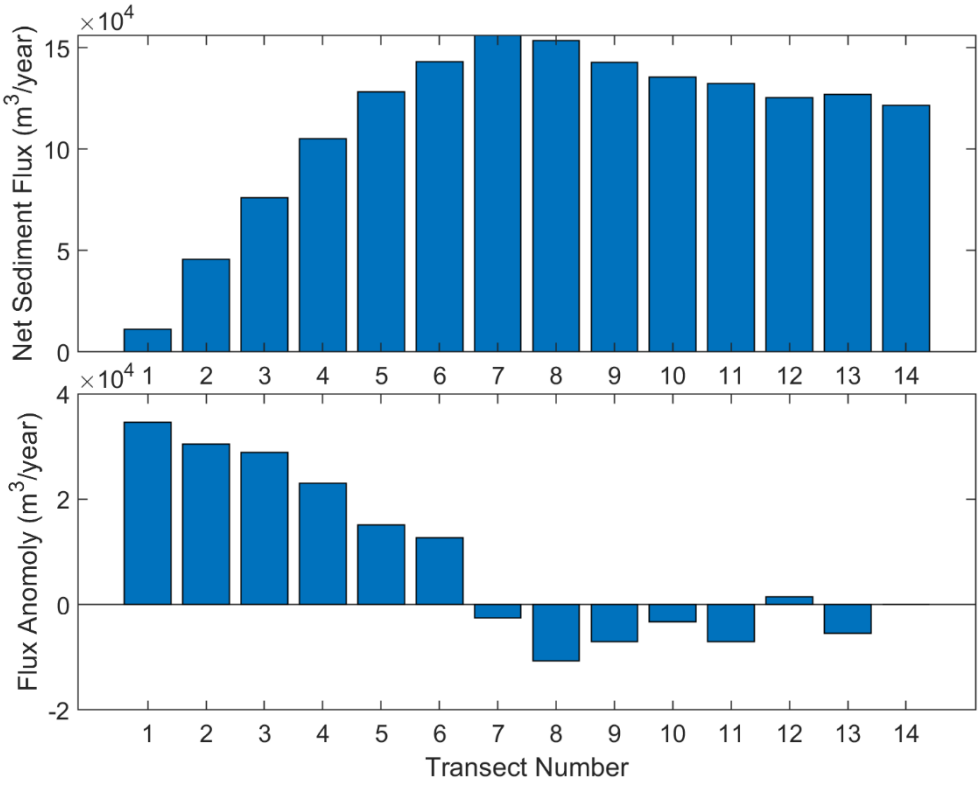


**Figure 5.15: Output from Genius showing the net flux at each transect (top) and flux anomaly at each transect (bottom).**

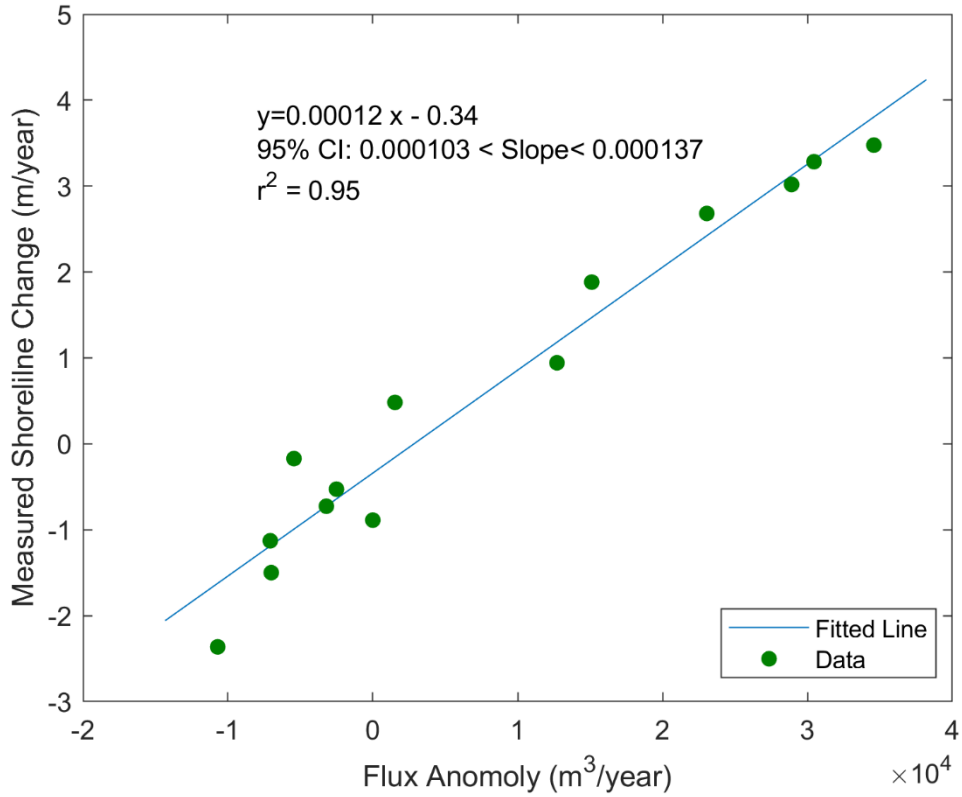


**Figure 5.16: Relationship between modelled sediment flux anomaly and beach width change from historical shoreline analysis.**

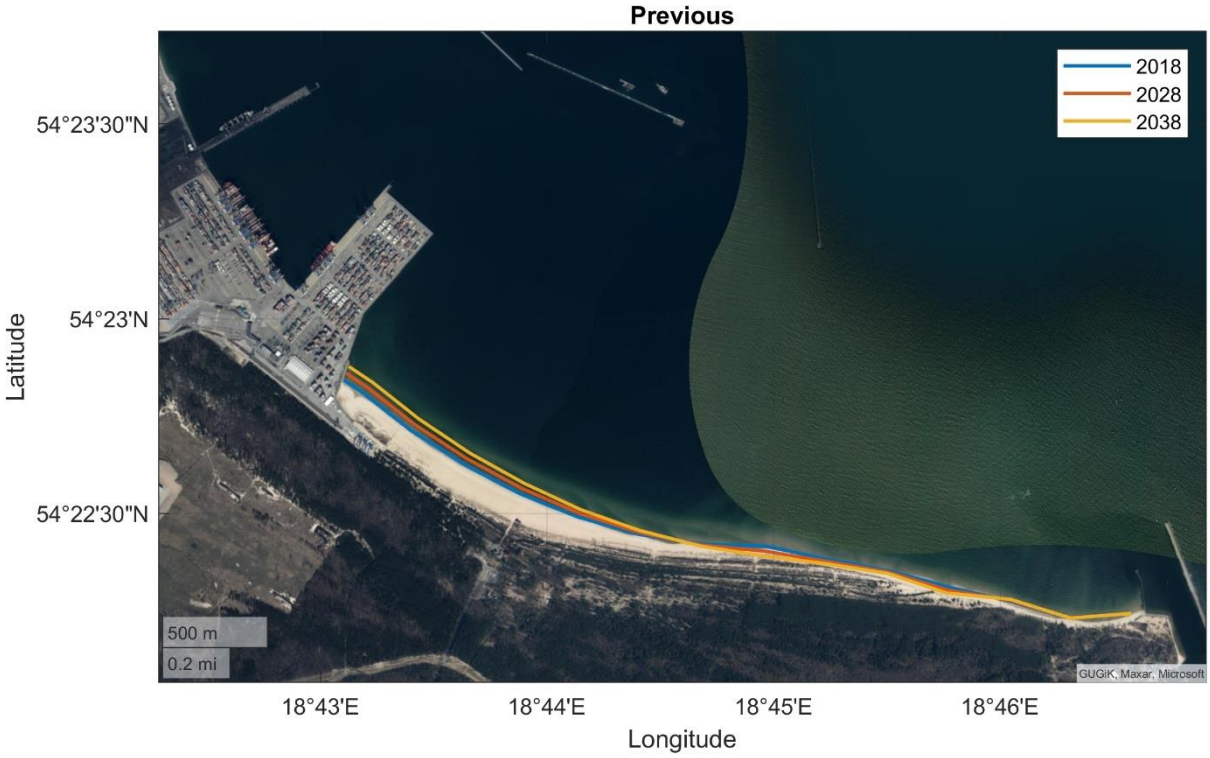


**Figure 5.17: Predicted shoreline change for the *'Previous'* scenario showing continued accretion at the western end of the beach and less pronounced erosion towards the east.**

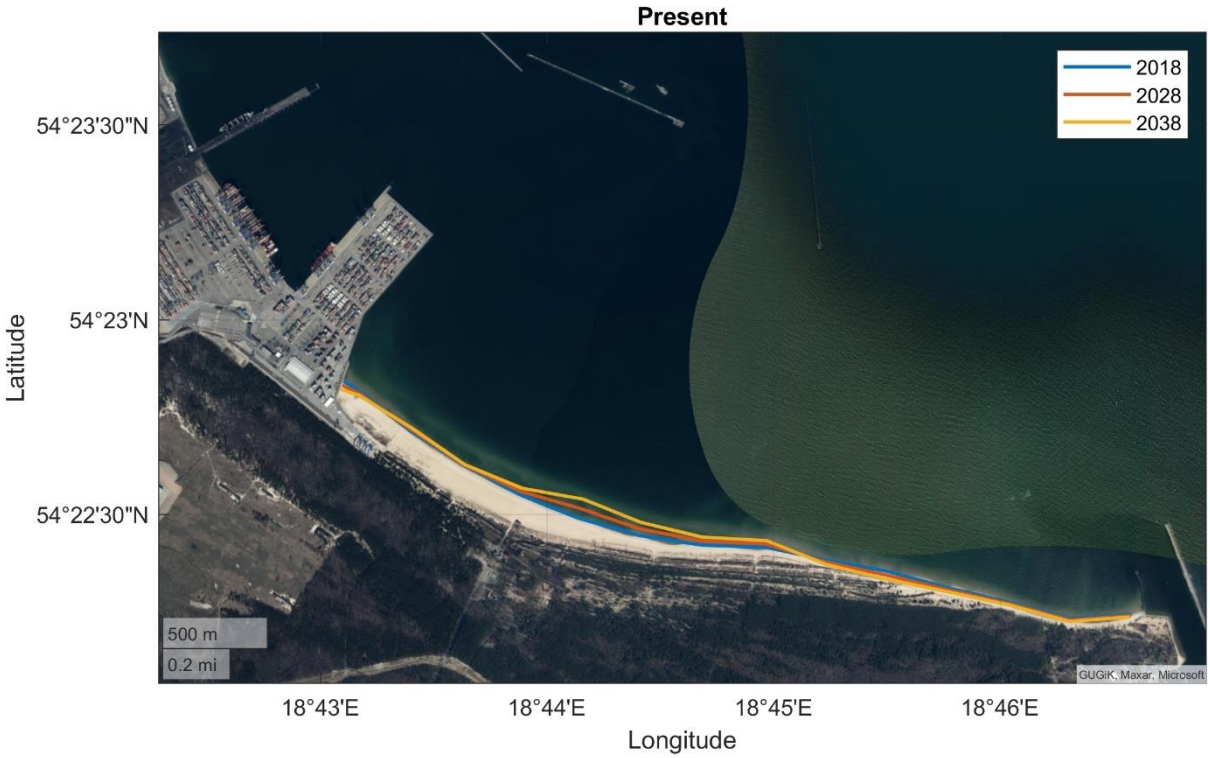


**Figure 5.18: Predicted shoreline change for the *'Present'* scenario.**

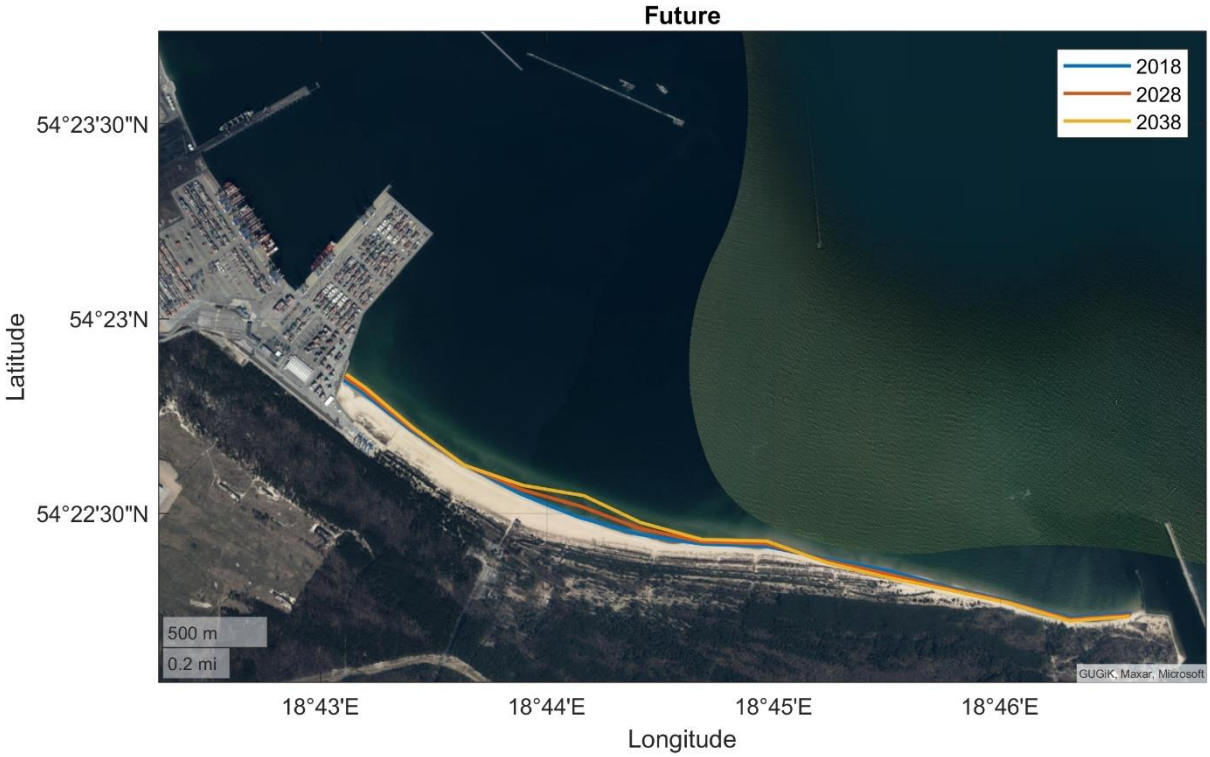


**Figure 5.19: Predicted shoreline change for the *'Future'* scenario.**

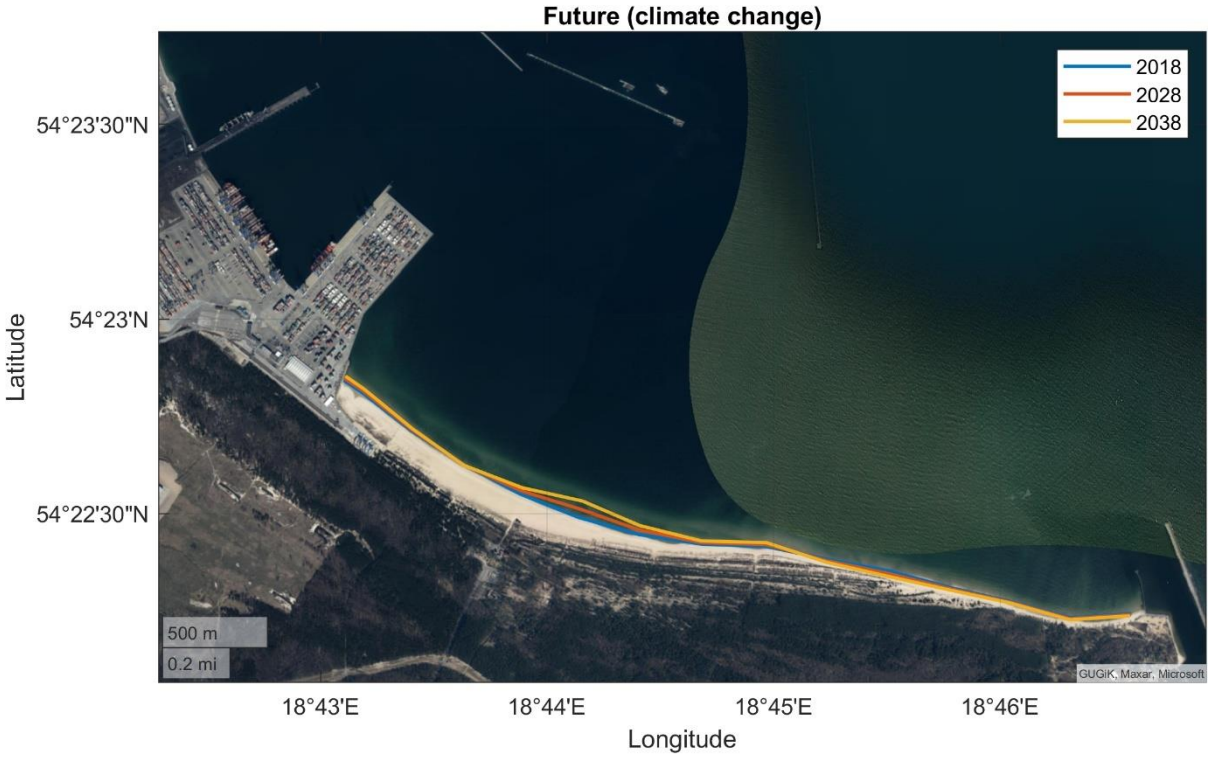


**Figure 5.20: Predicted shoreline change for the *'Future'* scenario including the effects of climate change.**

## 5.3 Conclusions

The construction of the T1 terminal in 2005 led to the accretion of the western end of Stogi Beach (adjacent to T1) at a rate of approximately 3.4 m per year from 2008 through 2018. The rate of accretion decreases with distance east of T1 and some erosion (-1.2 m per year) is seen in the central to east of central portion of the beach while the far-eastern portion of the beach is broadly stable. The rate of accretion at the western end of the beach is greater than the rate of erosion towards the centre and east of centre suggesting a net accumulation of sediment along the beach. While the source of this sediment is not clear, it most likely comes from offshore.

Results from the modelling indicate that the breakwaters that were constructed in 2020 will lead to changes to the sediment transport dynamics of Stogi Beach. They will reduce the wave driven accretion at the western end of the beach and will lead to a pattern of accretion along the central region of the beach at a rate of 2.6 m per year. Erosion and accretion patterns at the eastern end of the beach will remain largely unaffected.

The T3 development will lead to continued accretion of the shoreline in the far western end of Stogi Beach (1.5 m per year) which will be exacerbated by wind driven sand transport. The T3 reclamation will not affect sediment transport patterns on the beach to the east of this region.

The results for the three model scenarios are shown schematically in Figure 5.21 to Figure 5.23.

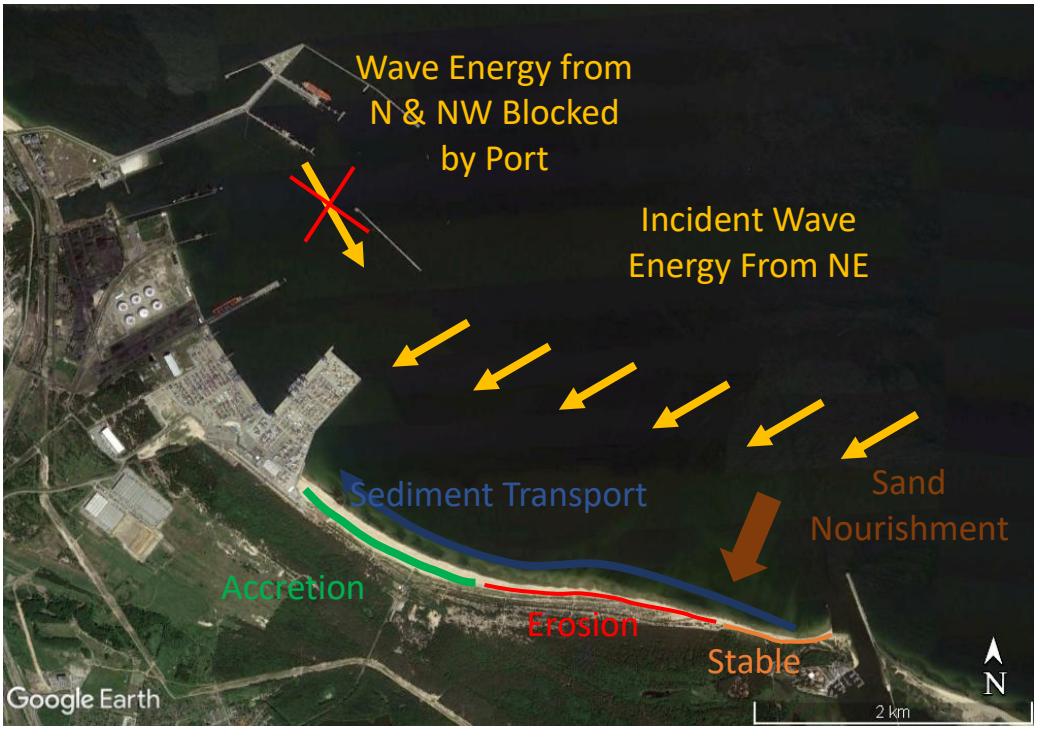


**Figure 5.21: Schematic illustration of the sediment transport scheme for the *Previous* scenario.**

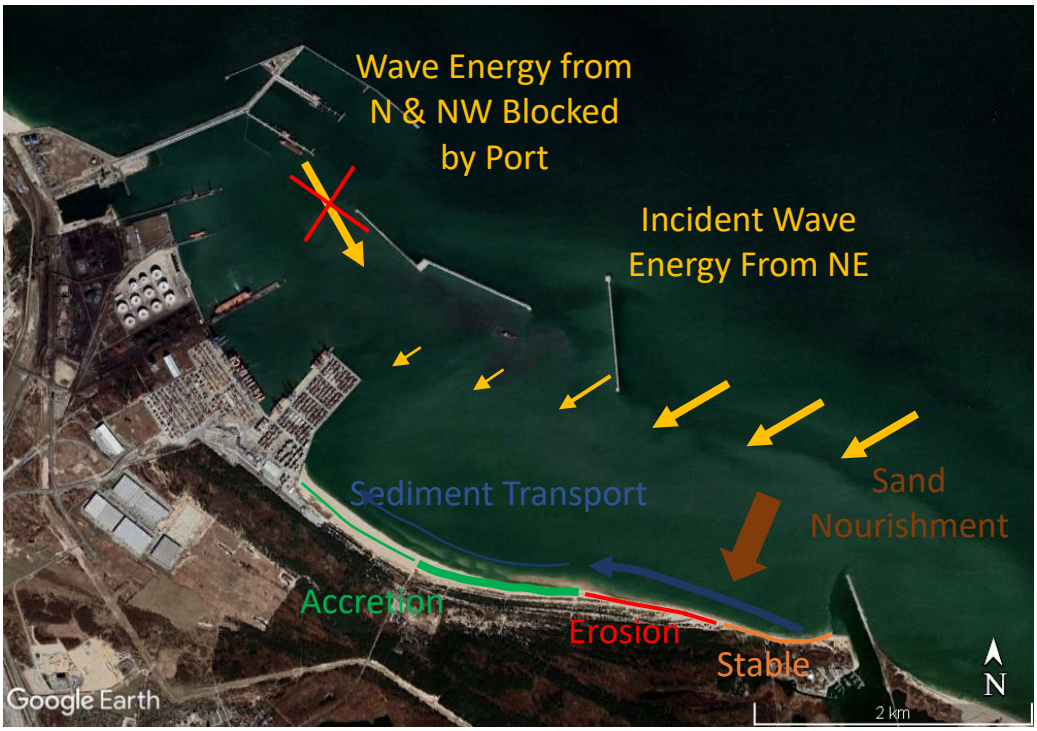


**Figure 5.22: Schematic illustration of the sediment transport scheme for the *Present* scenario.**

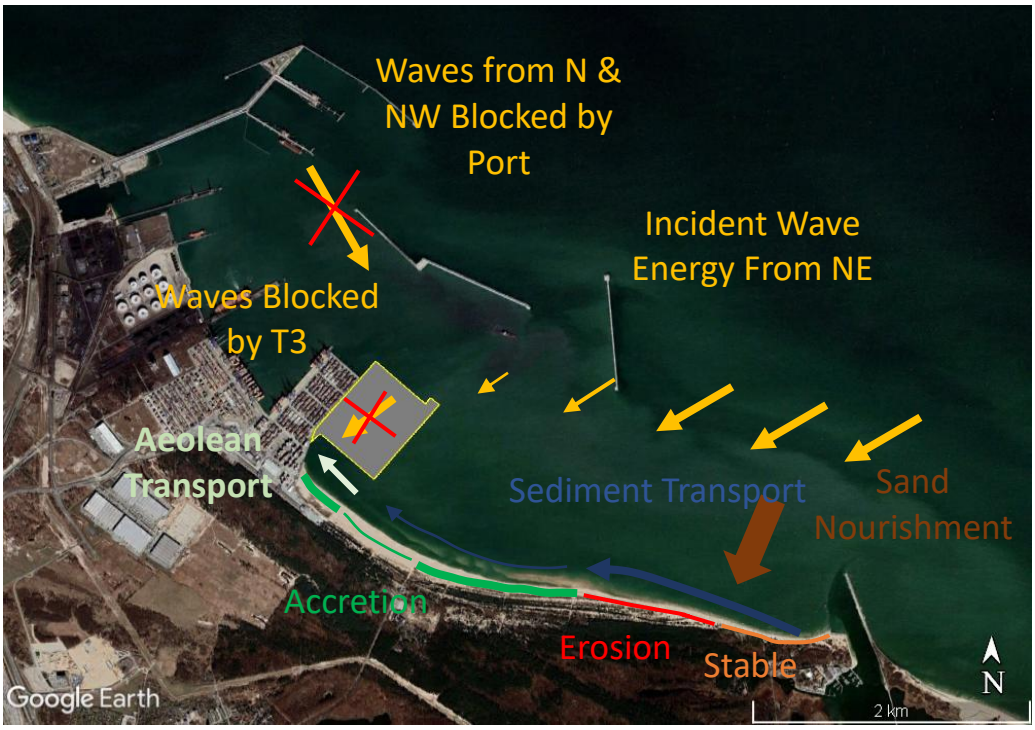


**Figure 5.23: Schematic illustration of the sediment transport scheme for the *Future* scenario.**

# 6 Water Quality Modelling

The development of the T3 terminal could lead to potential water quality issues affecting the coastal zone. This may occur due to trapping of Vistula River water or from stagnation of coastal waters. In this section the potential implications of the T3 terminal and breakwaters in the water quality of the adjoining areas are assessed.

## 6.1 Method

Effects on water quality have been investigated using a numerical modelling approach. The scenario definitions are the same as those used in the beach morphology modelling (see Section 5.1).

### 6.1.1 River Plume Modelling

The Vistula River is one of the largest rivers received by the Baltic Sea and a significant contributor of nutrients to the marine environment (Section 2). There is potential for changes in the dispersion of the river plume in the vicinity of the port due to the construction of the T3 Terminal. The modelling presented here simulates the dispersion of the river plume with and without the T3 Terminal and breakwaters in place.

The hydrodynamic modelling software used for this project is D-Flow Flexible Mesh (D-Flow FM) by Deltares which is part of the Delft3D FM Suite (Deltares, 2019). This Flexible Mesh (FM) model uses unstructured grids, with 3- to 6-sided cells and allows for irregular shapes. This grid format allows model cell shape and size to be manipulated based on the morphology in areas of interest, negating the need for multiple model domains and making simulations more accurate and efficient.

This model here was developed in 3D using five sigma-layers with layer thicknesses of 1%, 9%, 20%, 30% and 40%. The model was driven by ECMWF winds (19.0 E, 54.5 N) and freshwater input from the Vistula River. River boundary flows were derived from the Tczew flow gauge. Background and open boundary salinity was set 35 psu and river water salinity was set to 0 psu. The thinnest layers are at the water surface and they capture the buoyant river plume and surface layer wind effects. Temperature was omitted from the model as temperature derived gradients are unlikely to be strong drivers of currents near the shoreline. Tidal forcing was also omitted as tidal ranges in the Baltic Sea are negligible. The model was run for a 6-month period between 1 January and 1 August 2021 capturing periods of moderate and high flow from the Vistula River.

Model results for the *Future* scenario were scaled to reflect an estimated 18.25% climate change induced reduction in discharge from rivers (by 2081 to 2100) that terminate in the southeast of the Baltic Sea (mean of RCP 2.6, 4.5, 6.0 and 8.5) as outlined in Section 3.4.3 (Šarauskienė et al., 2017). Model results are presented in Section 6.2.1.

### 6.1.2 Flushing Rate

A potential cause of decreased water quality is stagnation of the T3 shadow zone. The T3 reclamation may lead to reduced current speeds in that area which would decrease flushing rates. This has been assessed by tracking a conservative tracer released in this region of the course of a model run for the *Present* and *Future* scenarios. The model was run using 8 scenarios for 4 cardinal (N, E, S, W) and 4 intercardinal (NE, SE, SW, NW) wind directions. Representative wind speeds were estimated by binning the long-term wind record and calculating the mean wind speed for each scenario. A spin up period of 2 days was used to initiate the hydrodynamic model. At this point a conservative tracer was released into the T3 shadow zone and allowed to disperse under the hydrodynamic conditions. The quantity of tracer remaining in the enclosed area was tracked through a weeklong model run for each wind condition with and without the T3 reclamation and associated dredging in place. Comparison plots provide an indicative quantification of the reduction in the flushing rate. Model results are presented in Section 6.2.2.

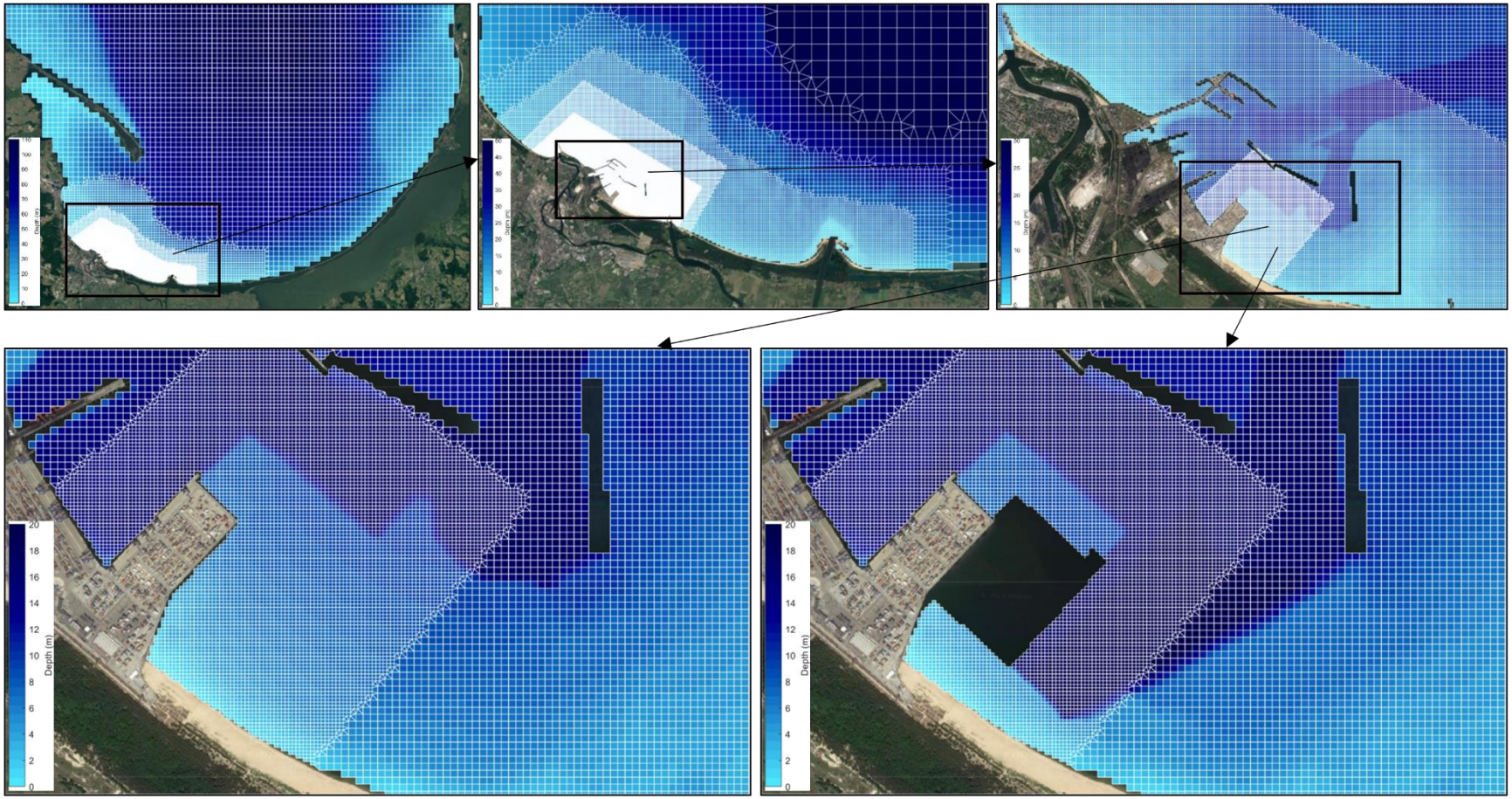


**Figure 6.1: The bathymetry grid used for the Hydrodynamic model with increasing resolution with proximity to the T1 and T3 terminals.**

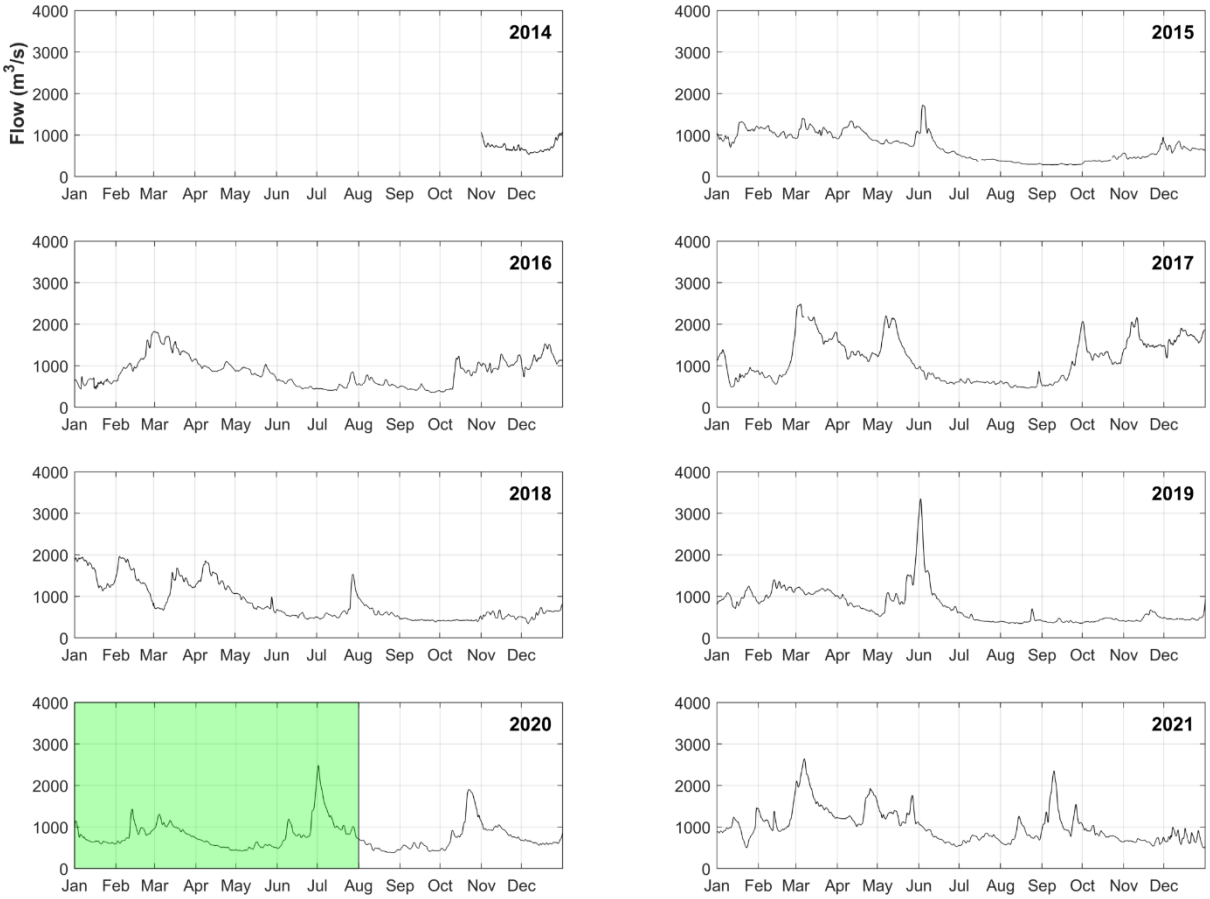


**Figure 6.2: River flow data form the Tczew gauge for the years 2014 to 2021. The green rectangle indicates the period simulated by the hydrodynamic model.**

## 6.1.3 Limitations

The hydrodynamic model does not derive current fields due to variability in broadscale temperature and salinity gradients. While salinity and temperature are important drivers of currents in the Baltic Sea, the strongest currents in the nearshore are likely to be wind driven.

Wave driven currents are not included in the hydrodynamic model. Preliminary investigations with a coupled wave model showed that they were not strong drivers of currents except very close to the shore.

A clamped 0 m sea level (MSL) was applied to the open boundary sea level and sea level variability was not included. While there is some sea level variability in the Gulf of Gdańsk, it is unlikely to be a significant driver of currents since tidal amplitudes in this area are negligible.

## 6.2 Water Quality Modelling Results

### 6.2.1 River Plume Modelling

The hydrodynamic model run simulated a period of moderate and high river flow from the Vistula River to assess the footprint of the freshwater plume in the marine environment. Modelled salinity was converted to dilution through the following relationship:

$$d = \frac{35}{35 - s}$$

Where *s* is salinity and *d* is dilution.

Minimum and median dilutions for the Previous, Present and Future scenarios are shown in Figure 6.3 and Figure 6.4 respectively. The results show that the port area is impacted by the river plume with minimum dilutions during the model run between 4 and 7-fold in the Previous scenario. The additional breakwaters in the Present scenario cause a general reduction in river water intrusion into the inner port area. In the Future scenario, the T3 terminal reduces the intrusion T3 shadow zone with minimum dilutions raising from 4-fold in the Present scenario to 6-fold in the Future scenario. The median dilution in the T3 shadow zone is approximately 20-fold for all scenarios. Overall, there is no significant difference in median dilution patterns between the three scenarios. Considering reduced river flow due to climate change projections (2081-2100), dilution throughout the model domain is higher overall (Figure 6.5). In the lee of the T3 development median dilution increases to 27-fold.

A timeseries of surface model output extracted at the western end of Stogi Beach shows salinity through the course of the model run (Figure 6.6). In the *Future* scenario, the salinity values are generally higher, more smoothed and show less short-term variability than the *Previous* and *Present* scenarios.

Residual (vector averaged) depth averaged current speeds are shown for the three scenarios in Figure 6.7. The results show a slight reduction in residual current speeds in the western end of Stogi Beach which would be expected to lead to a reduced intrusion of river water into this area.

Currents generated by the outflow of freshwater from the Vistula River mouth are largely confined to the river mouth and do not impinge on the Port area. Surface and depth averaged currents are shown in Figure 6.8 at the peak of a high flow event confirm this.

Overall, the results indicate that the addition of the T3 development will reduce the intrusion of Vistula River plume at the western end of Stogi Beach. River water is likely to be one of the largest contributors of bacterial loads to the marine environment. Construction of the T3 development is unlikely to lead to higher bacterial or pollutant concentrations at the western end of Stogi beach carried by Vistula River water.

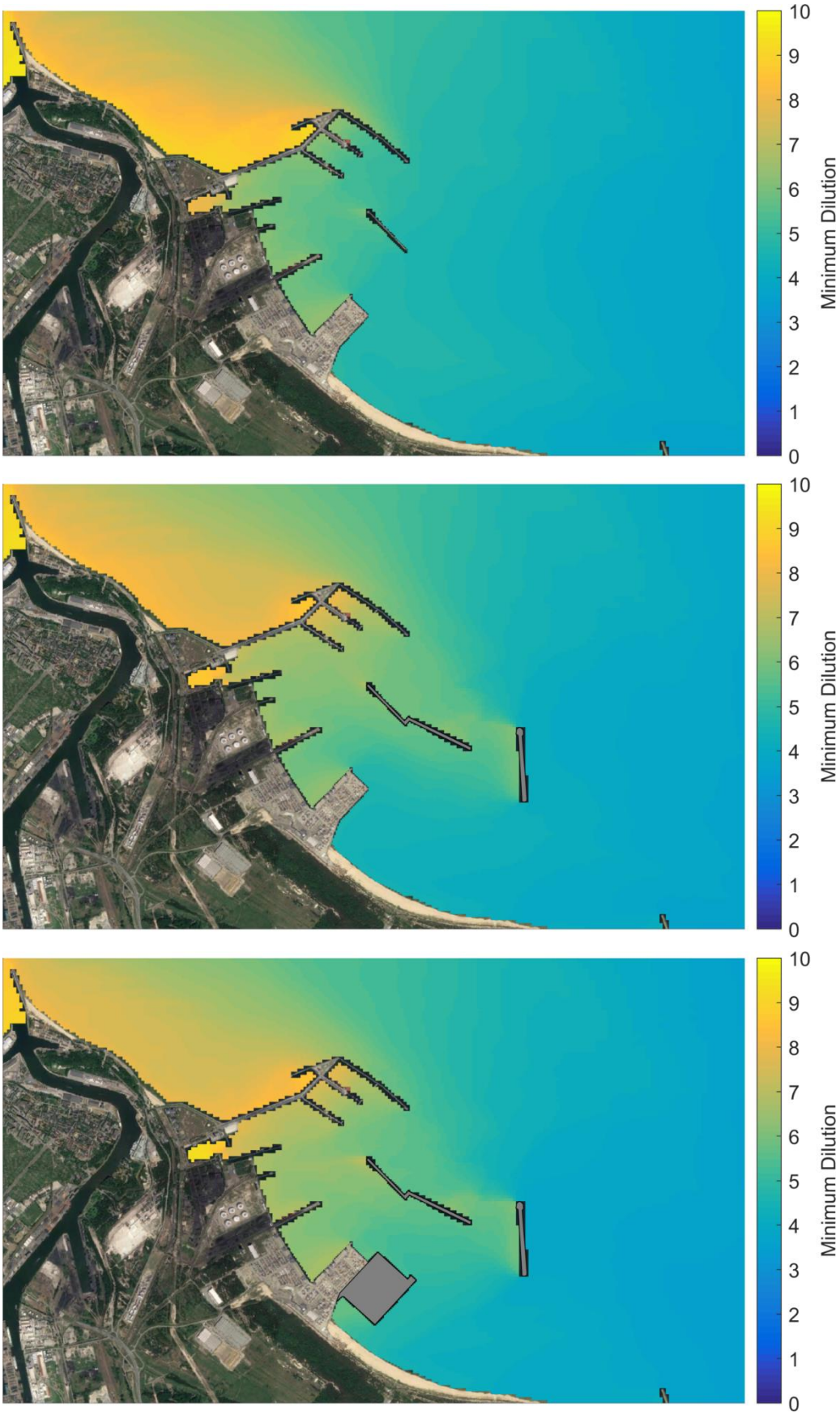


**Figure 6.3: Minimum surface layer dilution in the port area for the *Previous* (top) *Present* (middle) and *Future* scenarios (bottom).**

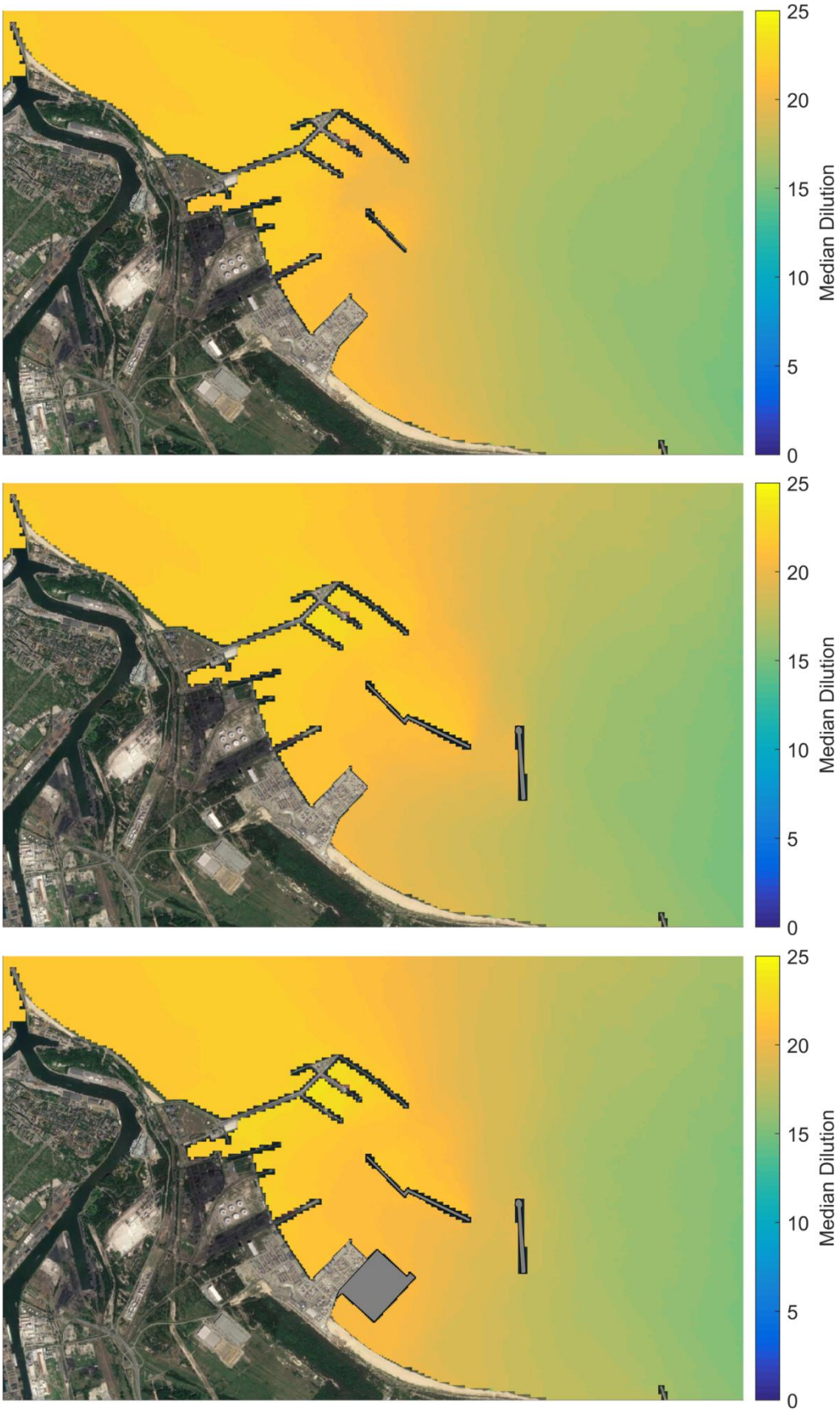


**Figure 6.4: Median dilution in the port area for the *Previous* (top) *Present* (middle) and *Future* scenarios (bottom).**

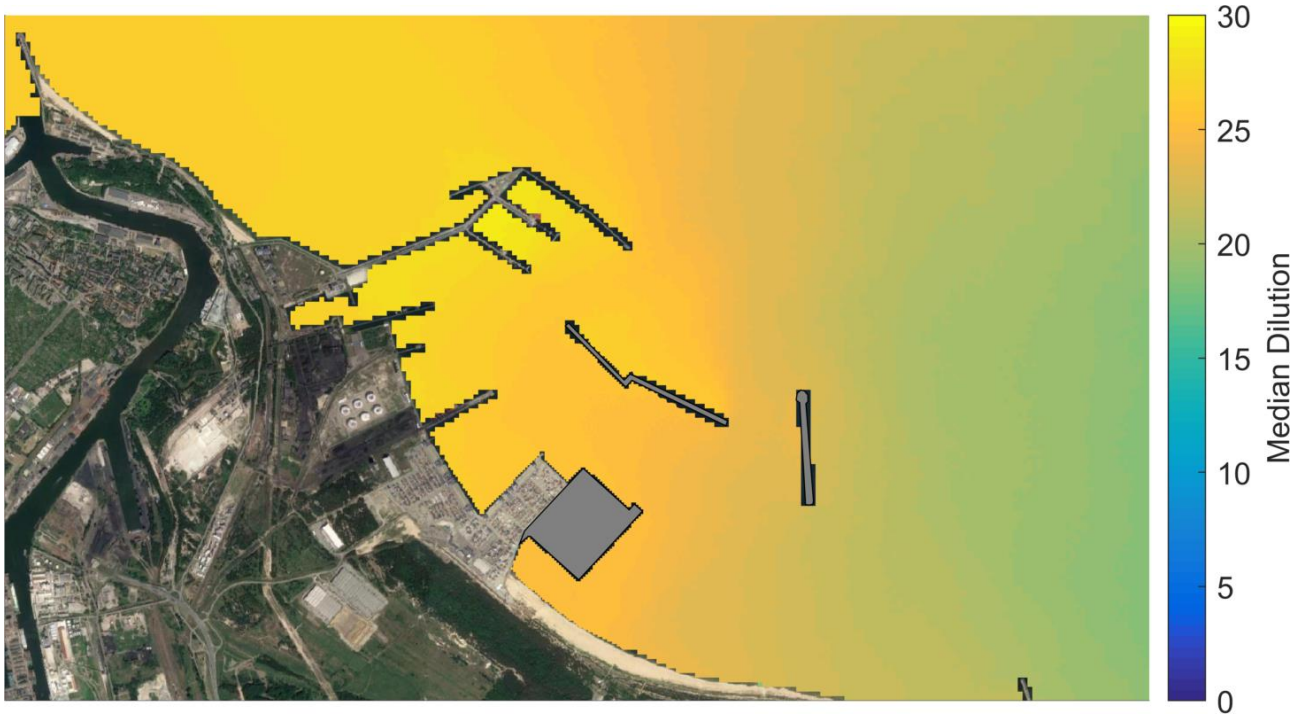


**Figure 6.5: Median dilution in the port area for the Future scenarios scaled for a predicted 18.25% reduction in river flow due to climate change effects for between 2018 and 2100.**

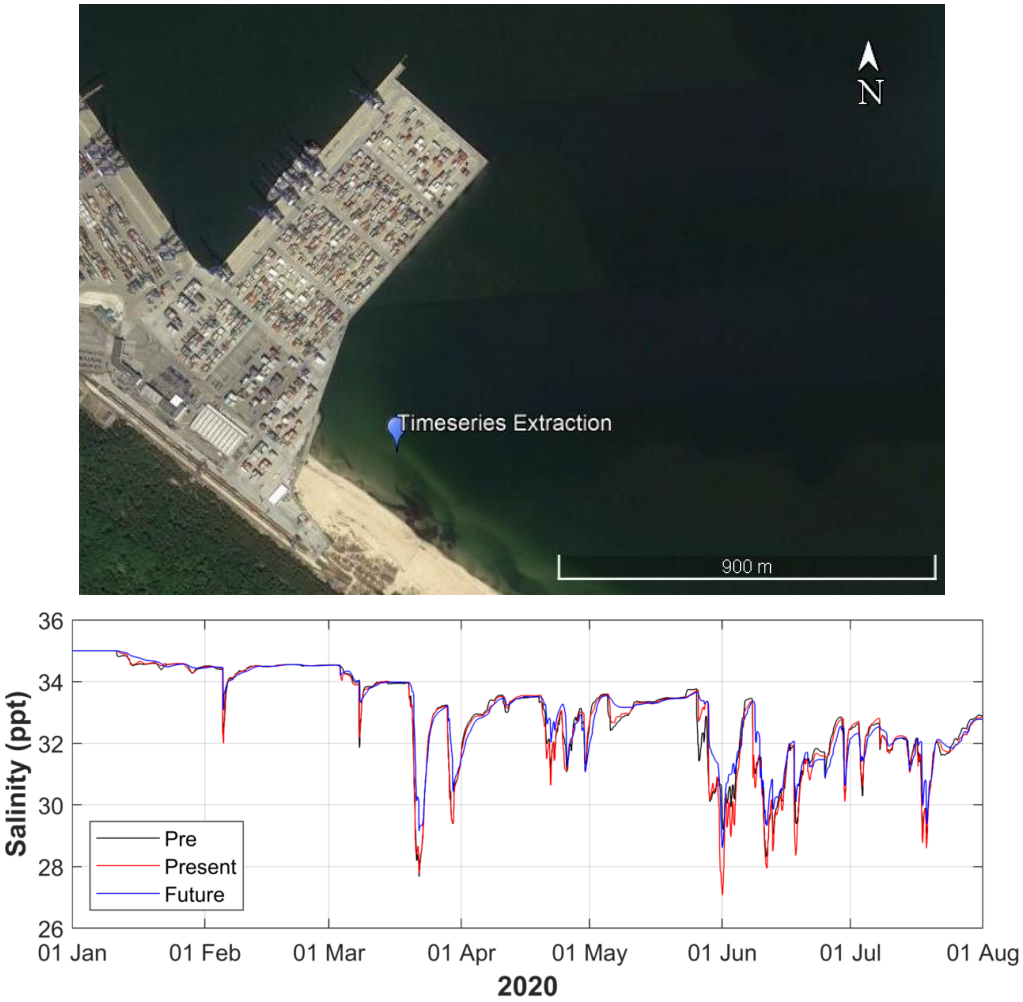


**Figure 6.6: Salinity over the course of the model runs at a single location in the area enclosed between the T3 terminal and Stogi Beach.**

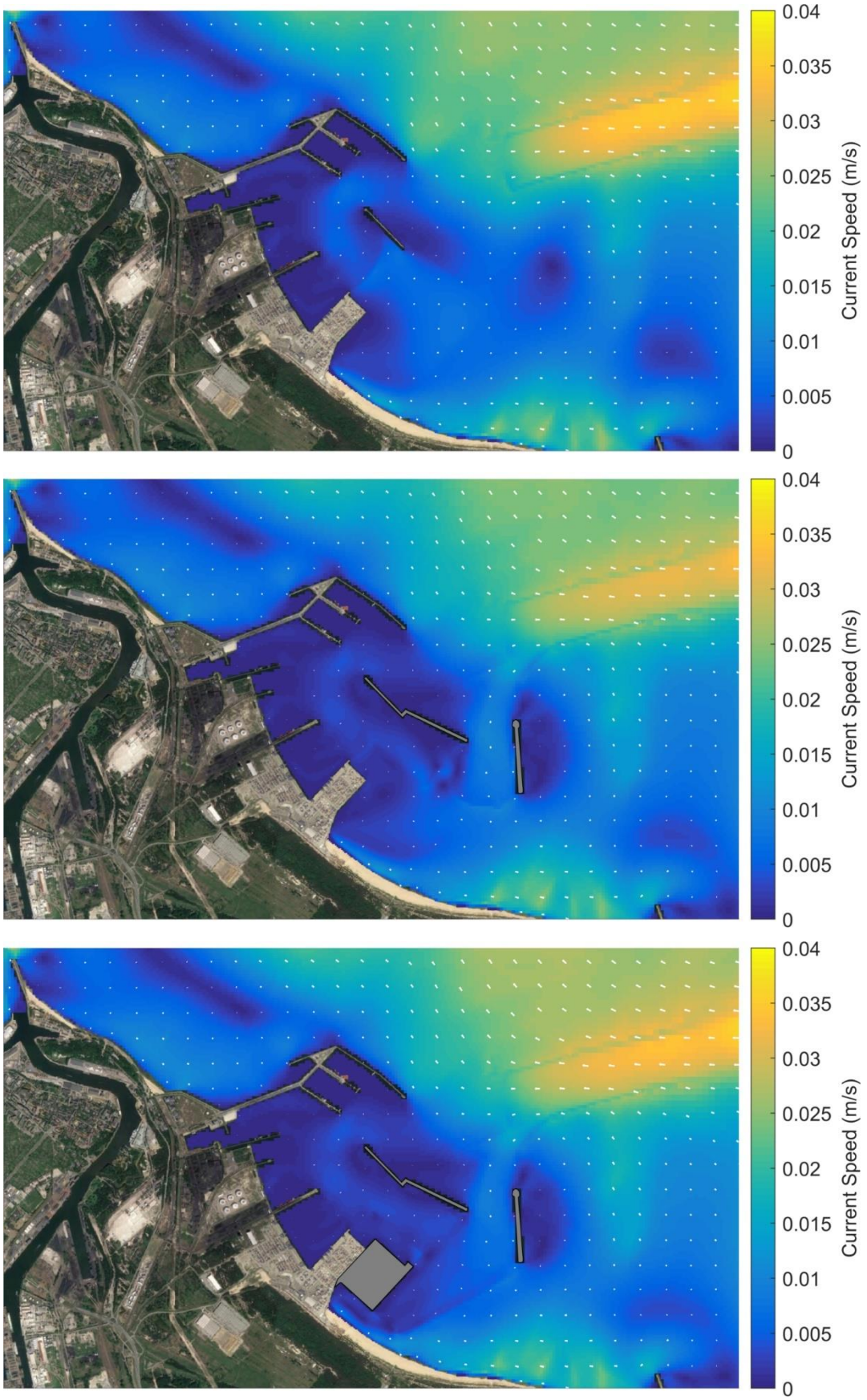


**Figure 6.7: Depth averaged residual (vector averaged) current speeds for the *Previous* (top) *Present* (middle) and *Future* scenarios (bottom).**

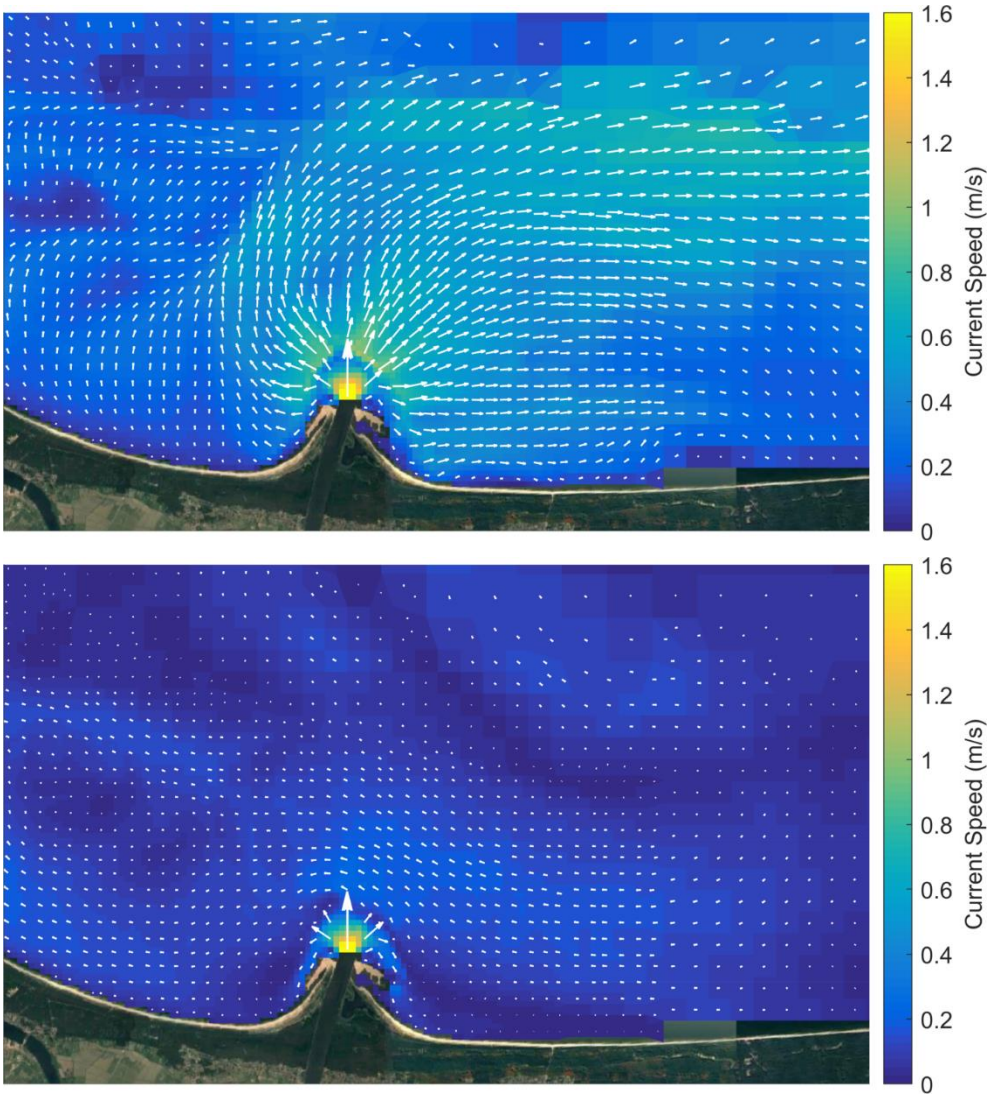


**Figure 6.8: Surface (top) and depth averaged(bottom) currents at the mouth of the Vistula River during a peak flow (2,490 m3 /s) event at 1 Jul 2020 17:00.**

## 6.2.2 Flushing

For this project, flushing is defined as the rate at which a conservative tracer is replaced by ambient water in the T3 shadow zone. Timeseries of flushing over the course of the model runs in the T3 shadow zone are shown over time in Figure 6.9 with and without the T3 terminal in place. In these plots the quantity of remaining tracer is presented as a percentage of the released tracer load. The time until 80% and 95% flushing occurs for each scenario is presented in Table 6.1. In all cases, flushing occurs most rapidly directly after the tracer release and increases tangentially towards 100%. In all cases, the flushing progresses more rapidly for the *Present* scenario than for the *Future* scenario. The mean 80% flushing time is 0.31 days for the *Present* scenario and 2.25 days for the *Future* scenario. The mean 95% flushing time is 0.70 days for the *Present* scenario and 4.68 days for the *Future* scenario. In the *Future* scenario, the most efficient flushing occurs under W winds and the least efficient occurs under NE winds. In the *Present* scenario the most efficient flushing occurs under SE winds and the least efficient occurs under NE and SW winds. The steady state surface and depth-averaged current speeds are presented for each scenario in Appendix C. Overall, with the T3 development in place, flushing in the enclosed area between the T3 terminal and Stogi Beach is reduced in all scenarios by a factor of 7 on average.

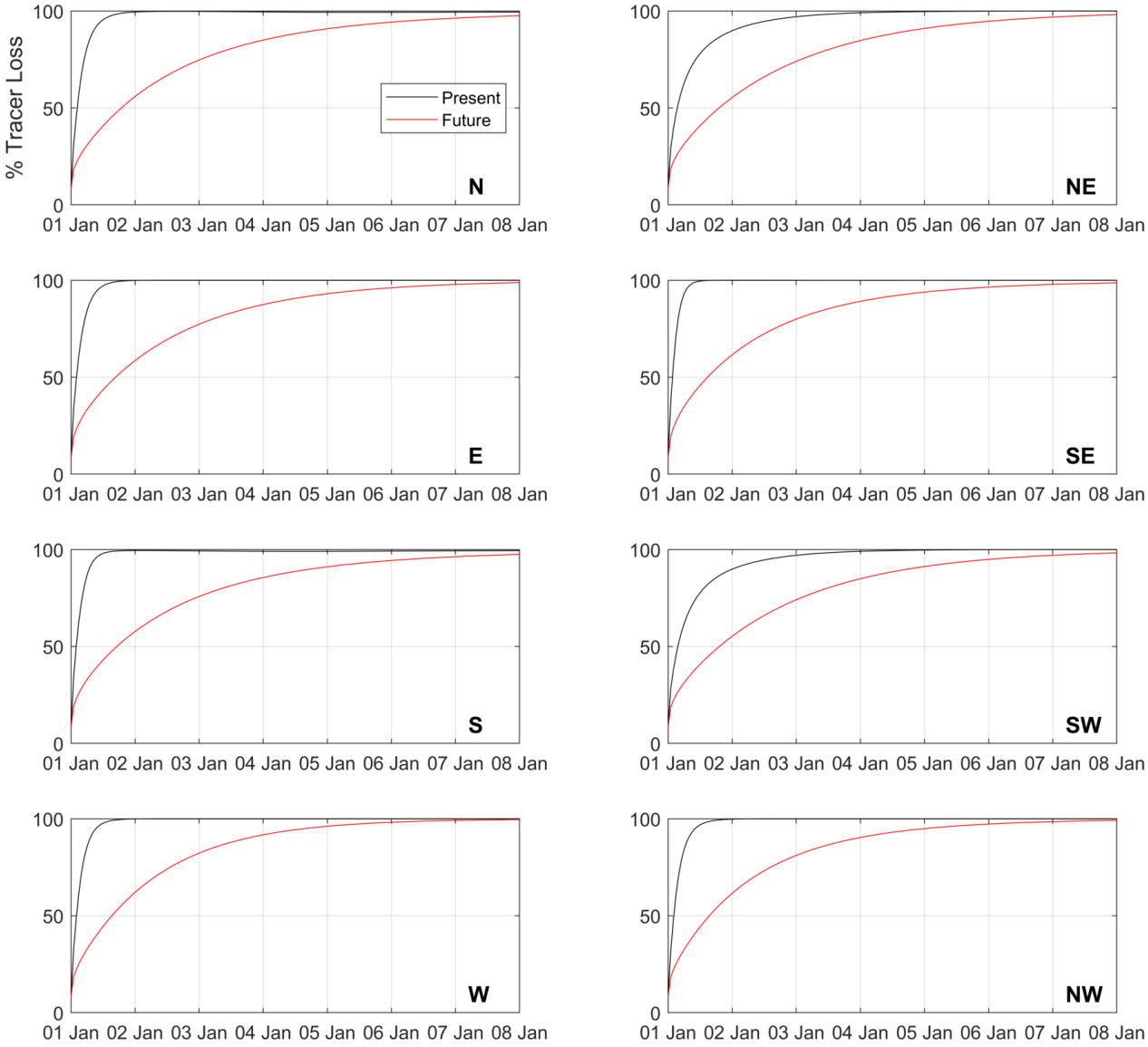


**Figure 6.9: Flushing of conservative tracer form the area enclosed by the T3 enclosed area with and without the T3 development in place.**

**Table 6.1: Flushing times for the T3 enclosed area with and without the T3 development.**

| | 80% flushing | | 95% flushing | |
|---|---|---|---|---|
| **Wind Direction** | **Present** | **Future** | **Present** | **Future** |
| **N** | 0.25 | 2.46 | 0.50 | 5.33 |
| **NE** | 0.58 | 2.50 | 1.58 | 5.13 |
| **E** | 0.25 | 2.25 | 0.42 | 4.58 |
| **SE** | 0.17 | 2.04 | 0.29 | 4.38 |
| **S** | 0.21 | 2.38 | 0.38 | 5.29 |
| **SW** | 0.58 | 2.50 | 1.58 | 5.04 |
| **W** | 0.21 | 1.88 | 0.42 | 3.67 |
| **NW** | 0.25 | 1.96 | 0.46 | 4.04 |
| **Mean** | **0.31** | **2.25** | **0.70** | **4.68** |

## 6.3 Conclusions

The modelling results indicate that the freshwater plume from the Vistula River disperses widely over the southern Gulf of Gdańsk and reaches the Port of Gdańsk particularly under high flow conditions and easterly wind conditions. The intrusion of the river water in the marine area between the T3 terminal and Stogi Beach is reduced with the T3 development in place due to its effect on ambient current patterns. River water is likely to be one of the largest contributors of bacterial loads to the marine environment. Construction of the T3 development is unlikely to lead to higher bacterial or river borne pollutant concentrations at the western end of Stogi Beach.

The modelling also shows that in the same area, while there is some variability in current patterns under different wind conditions, flushing in this area is on average 7 times slower with the T3 development in place. While Vistula River water is less likely to enter the region between the T3 terminal and Stogi beach with the T3 terminal in place, once waterborne pollutants enter this area, they will take on average 7 times as long to be removed under natural influences. There is consequently a strong likelihood that this region will become a sink for litter and debris.

# 7 References

Andrulewicz, E., & Witek, Z. (2002). Anthropogenic pressure and environmental effects on the Gulf of Gdańsk: recent management efforts. In Baltic coastal ecosystems (pp. 119-139). Springer, Berlin, Heidelberg.

Atkins (2014) Deepwater Container Terminal, Gdańsk, Poland Environmental and Social Impact Assessment (ESIA)

Bonaduce, A., Staneva, J., Behrens, A., Bidlot, J. R., & Wilcke, R. A. I. (2019). Wave climate change in the North Sea and Baltic Sea. Journal of Marine Science and Engineering, 7(6), 166.

Damrat, M., Zaborska, A., & Zajączkowski, M. (2013). Sedimentation from suspension and sediment accumulation rate in the River Vistula prodelta, Gulf of Gdańsk (Baltic Sea). Oceanologia, 55(4), 937-950.

ED, (2019), Dredging conditions in ED for T3, RDOŚ-Gd WOO.420.125.2018.AT.11

Hanson, H. and Kraus, N.C., 1989. GENESIS-Generalized model for simulating shoreline change. Vol. 1: Reference Manual and Users Guide. Tech. Rep. CERC-89-19, Coastal Engineering Research Center, U.S. Army Corps of Engineers, 247pp.

HELCOM (2021a), Input of nutrients by the seven biggest rivers in the Baltic Sea region 1995-2017. Baltic Sea Environment Proceedings No.178.

HELCOM, (2021b) Fact Sheet. Baltic Sea Environment Proceedings n°180. HELCOM/Baltic Earth 2021

HELCOM (2018), HELCOM Thematic assessment of eutrophication 2011-2016. Baltic Sea Environment Proceedings No. 156.

Hersbach, H., Bell, B., Berrisford, P., Hirahara, S., Horányi, A., Muñoz-Sabater, J., Nicolas, J., Peubey, C., Radu, R., Schepers, D., Simmons, A., Soci, C., Abdalla, S., Abellan, X., Balsamo, G., Bechtold, P., Biavati, G., Bidlot, J., Bonavita, M., De Chiara, G., Dahlgren, P., Dee, D., Diamantakis, M., Dragani, R., Flemming, J., Forbes, R., Fuentes, M., Geer, A., Haimberger, L., Healy, S., Hogan, R. J., Hólm, E., Janisková, M., Keeley, S., Laloyaux, P., Lopez, P., Lupu, C., Radnoti, G., de Rosnay, P., Rozum, I., Vamborg, F., Villaume, S., and Thépaut, J.-N.: (2020), The ERA5 global reanalysis, Q. J. Roy. Meteor. Soc., 146, 1999–2049, https://doi.org/10.1002/qj.3803, 2020.

Holthuijsen, L.H., N. Booij, A.T.M.M. Kieftenburg, R.C. Ris., A.J. van der Westhuysen, and M. Zijlema (2004) SWAN Cycle III, Version 40.41, User manual.

Inspectorate of Environmental Protection (2020). Evaluation of the condition of the Environment. Polish Marine Areas of the Baltic Sea Based on Monitoring Data from 2020.

Jakobsson, M., Stranne, C., O'Regan, M., Greenwood, S. L., Gustafsson, B., Humborg, C., & Weidner, E. (2019). Bathymetric properties of the Baltic Sea. Ocean Science, 15(4), 905-924.

Kowalewski, M. (2001). An operational hydrodynamic model of the Gulf of Gdańsk. Research works based on the ICM's UMPL numerical prediction system results.

Majewski, W. (2018). Vistula river, its characteristics and management. Int. J. Hydrol, 2(4), 493-496.

Pruszak, Z., Van Ninh, P., Szmytkiewicz, M., Hung, N. M., & Ostrowski, R. (2005). Hydrology and morphology of two river mouth regions (temperate Vistula Delta and subtropical Red River Delta). Oceanologia, 47(3).

Royal HaskoningDHV (2020). Design Criteria Report. PC1063-RHD-ZZ-ZZ-RP-CO-001, S4/P01, 27 July 2020.

Šarauskienė, D.; Akstinas, V.; Kriaučiūnienė, J.; Jakimavičius, D.; Bukantis, A.; Kažys, J.; Povilaitis, A.; Ložys, L.; Kesminas, V.; Virbickas, T.; Pliuraitė, V. (2017). Projection of Lithuanian river runoff, temperature and their extremes under climate change. Hydrology Research, nh2017007–. doi:10.2166/nh.2017.007

Sarker, Z., (2020), DCT Gdańsk – T3 Terminal Project Wave Modelling Studies, prepared by Royal HaskoningDHV for DCT Gdańsk.

Weisse, R., Dailidienė, I., Hünicke, B., Kahma, K., Madsen, K., Omstedt, A., ... & Zorita, E. (2021). Sea level dynamics and coastal erosion in the Baltic Sea region. Earth System Dynamics, 12(3), 871-898.

Witek, Z., Humborg, C., Savchuk, O., Grelowski, A., & Łysiak-Pastuszak, E. (2003). Nitrogen and phosphorus budgets of the Gulf of Gdańsk (Baltic Sea). Estuarine, Coastal and Shelf Science, 57(1-2), 239-248.

Zaborska, A., Siedlewicz, G., Szymczycha, B., Dzierzbicka-Głowacka, L., & Pazdro, K. (2019). Legacy and emerging pollutants in the Gulf of Gdańsk (southern Baltic Sea)–loads and distribution revisited. Marine pollution bulletin, 139, 238-255.

# Appendix A. Additional Satellite Imagery

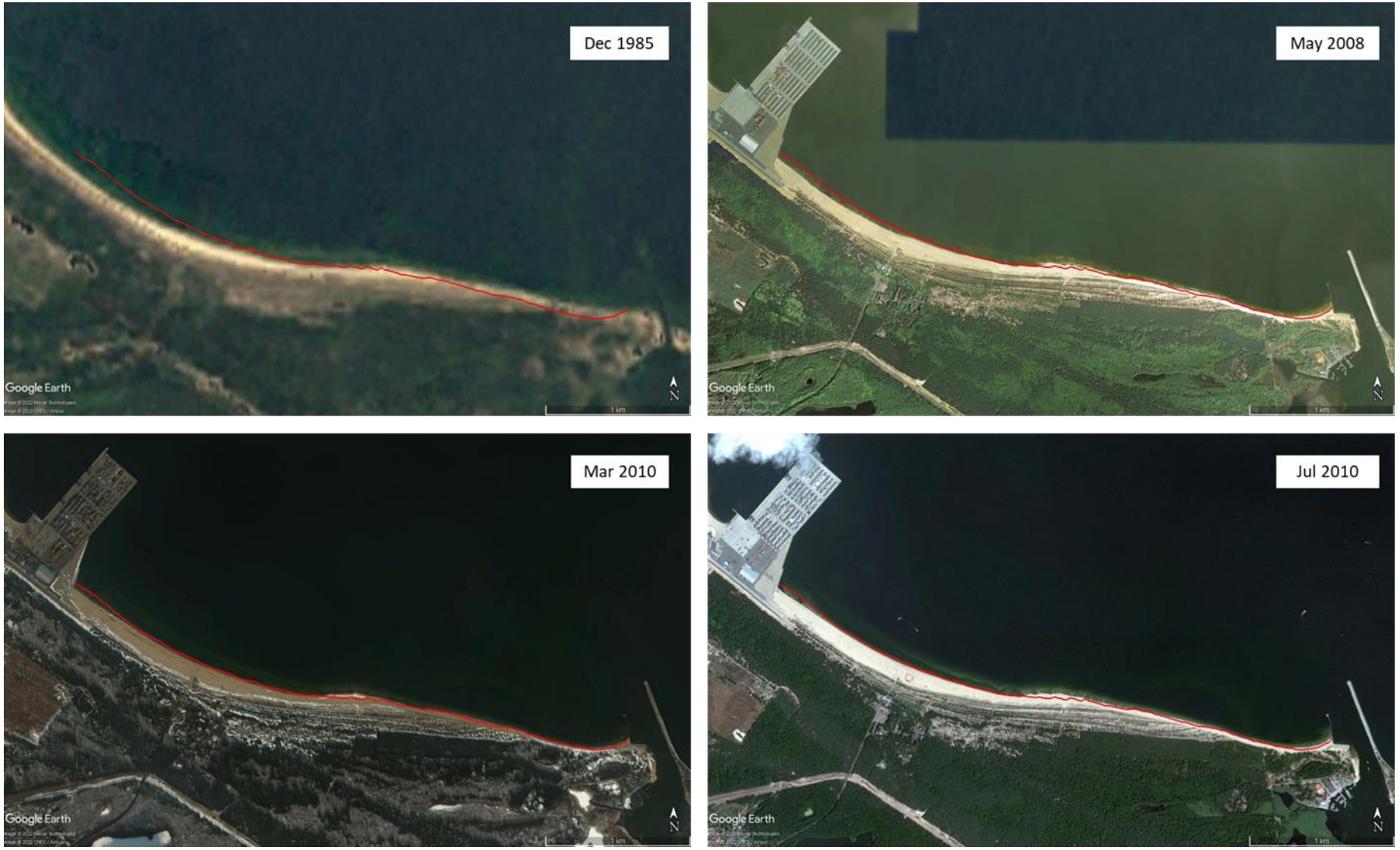


**Figure 7.1: The evolution of the Stogi Beach shoreline. The red line indicates the shoreline in May 2018 for comparison. Source: Google Earth.**

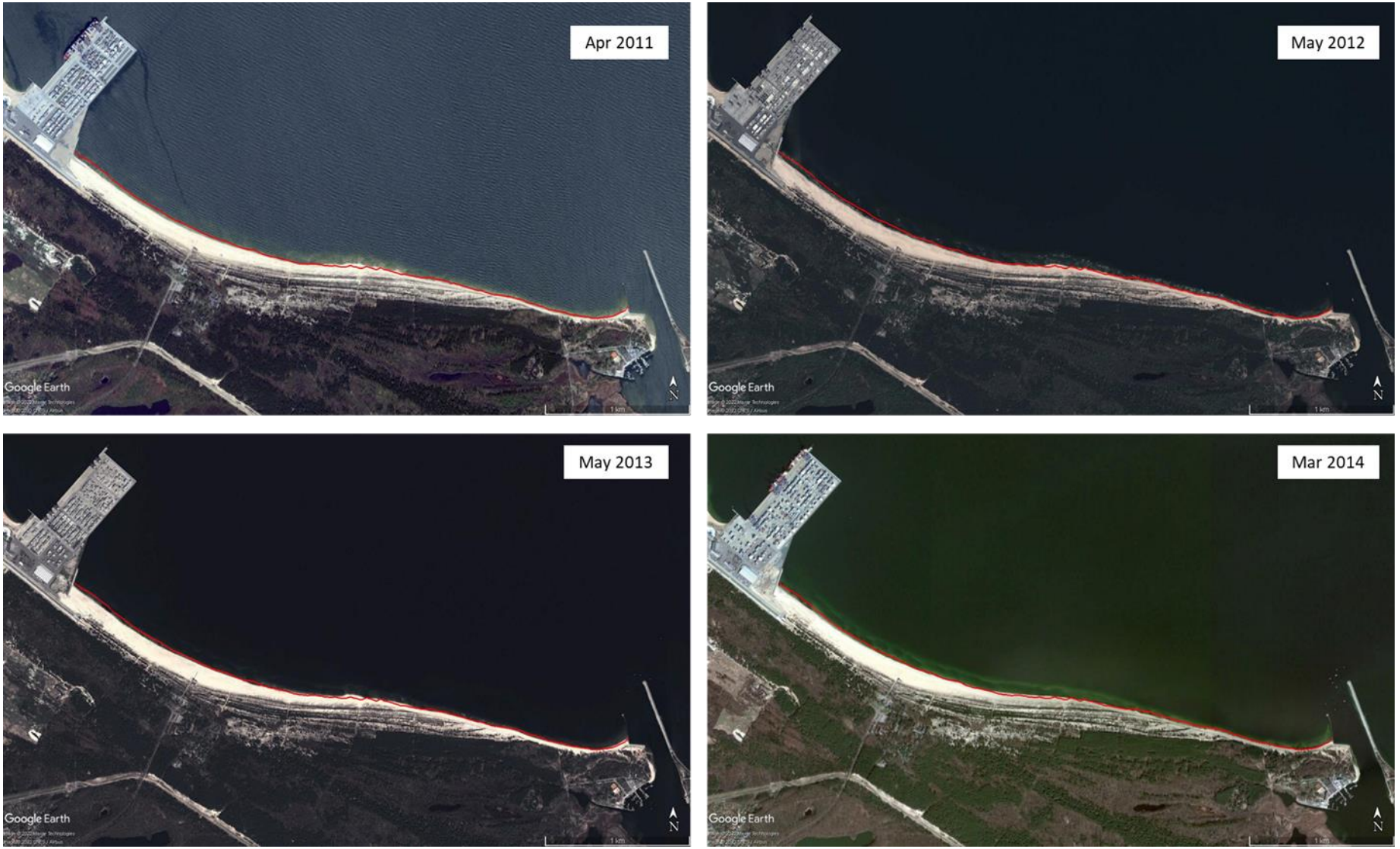


**Figure 7.2: The evolution of the Stogi Beach shoreline. The red line indicates the shoreline in May 2018 for comparison. Source: Google Earth.**


**Figure 7.3: The evolution of the Stogi Beach shoreline. The red line indicates the shoreline in May 2018 for comparison. Source: Google Earth.**

# Appendix B. Stogi Beach Width Evolution

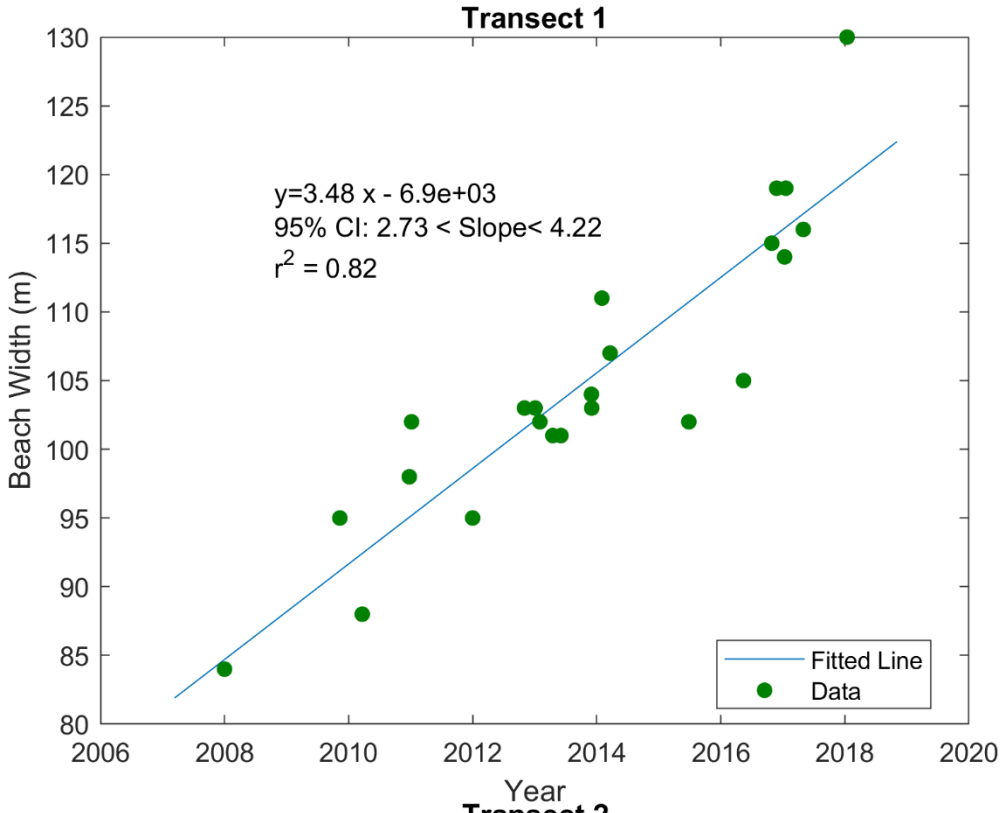
Transect 1
y=3.48 x - 6.9e+03
95% CI: 2.73 < Slope< 4.22
r2 = 0.82
Fitted Line
Data
Beach Width (m)
Year
130
125
120
115
110
105
100
95
90
85
80
2006
2008
2010
2012
2014
2016
2018
2020

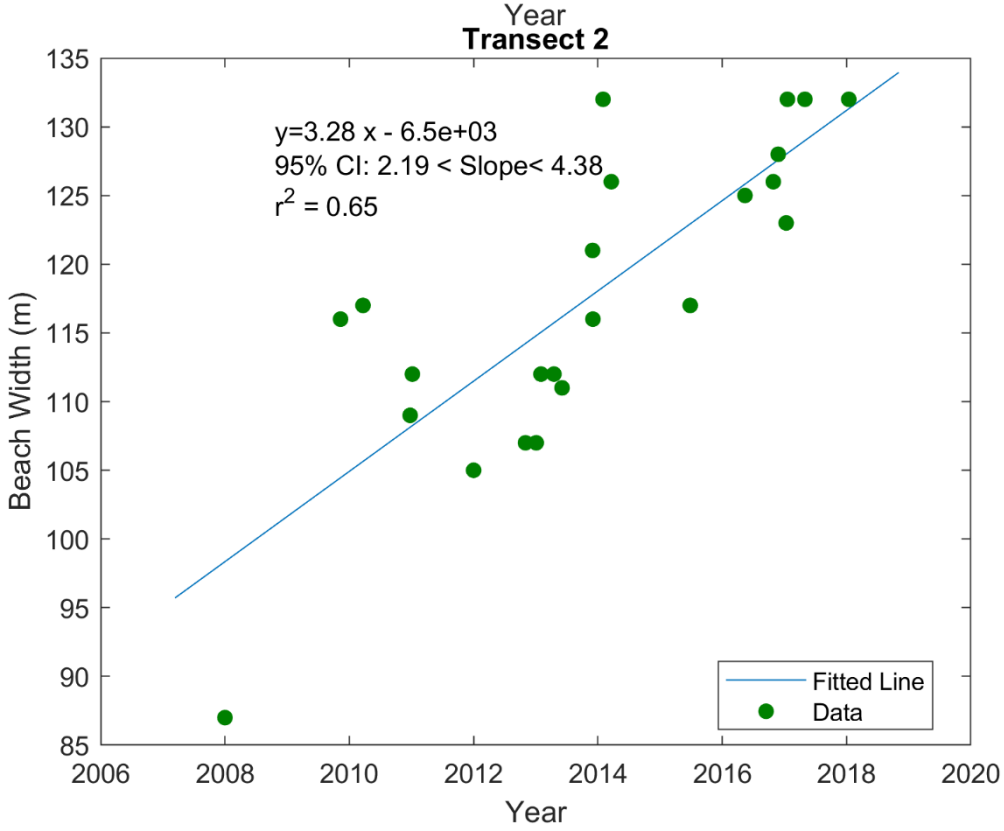
Transect 2
y=3.28 x - 6.5e+03
95% CI: 2.19 < Slope< 4.38
r2 = 0.65
Fitted Line
Data
Beach Width (m)
Year
135
130
125
120
115
110
105
100
95
90
85
2006
2008
2010
2012
2014
2016
2018
2020

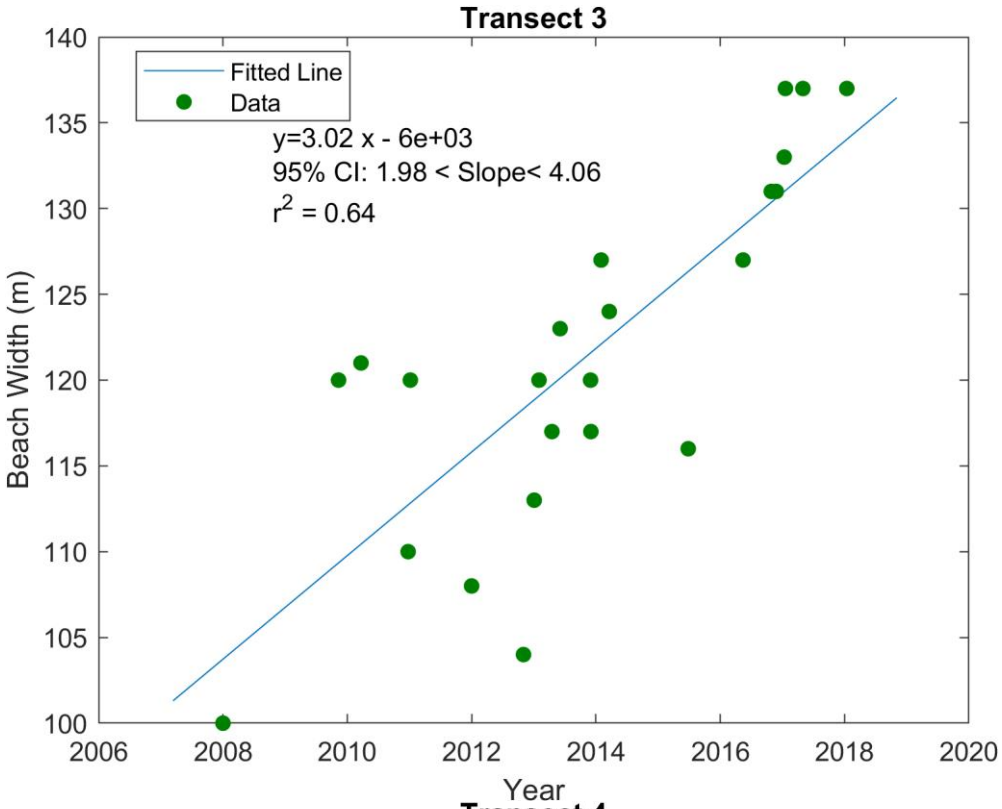
Transect 3
Fitted Line
Data
y=3.02 x - 6e+03
95% CI: 1.98 < Slope< 4.06
r2 = 0.64
Beach Width (m)
Year
140
135
130
125
120
115
110
105
100
2006
2008
2010
2012
2014
2016
2018
2020

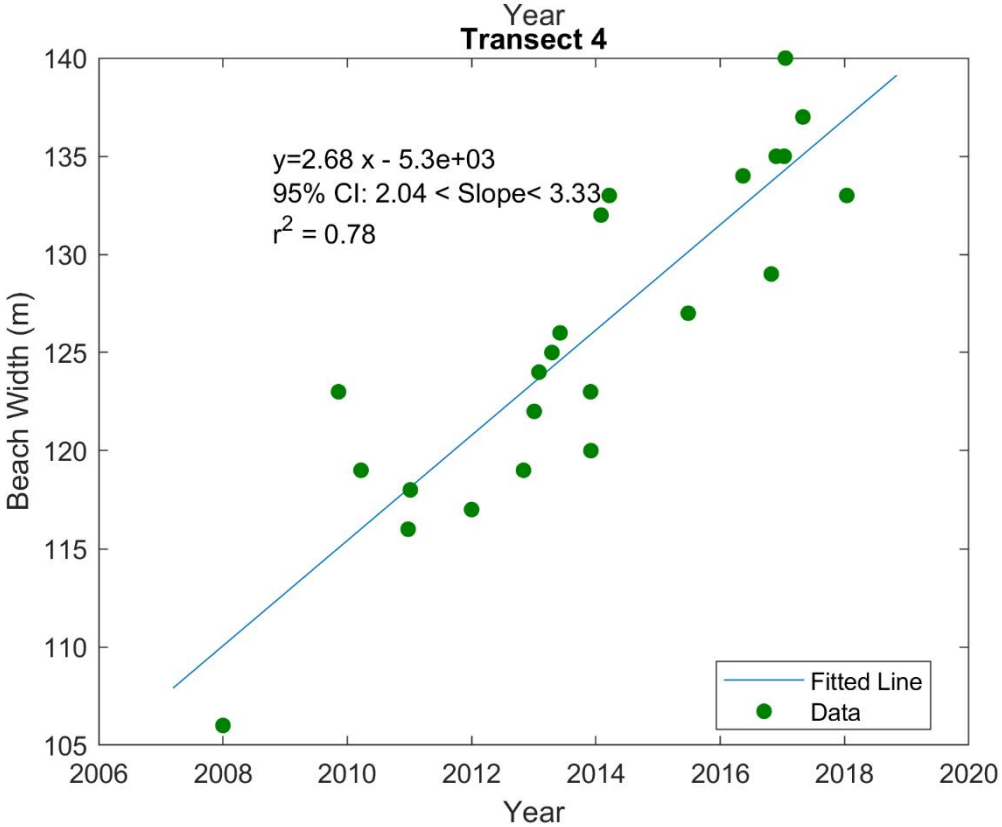
Transect 4
y=2.68 x - 5.3e+03
95% CI: 2.04 < Slope< 3.33
r2 = 0.78
Fitted Line
Data
Beach Width (m)
Year
140
135
130
125
120
115
110
105
2006
2008
2010
2012
2014
2016
2018
2020

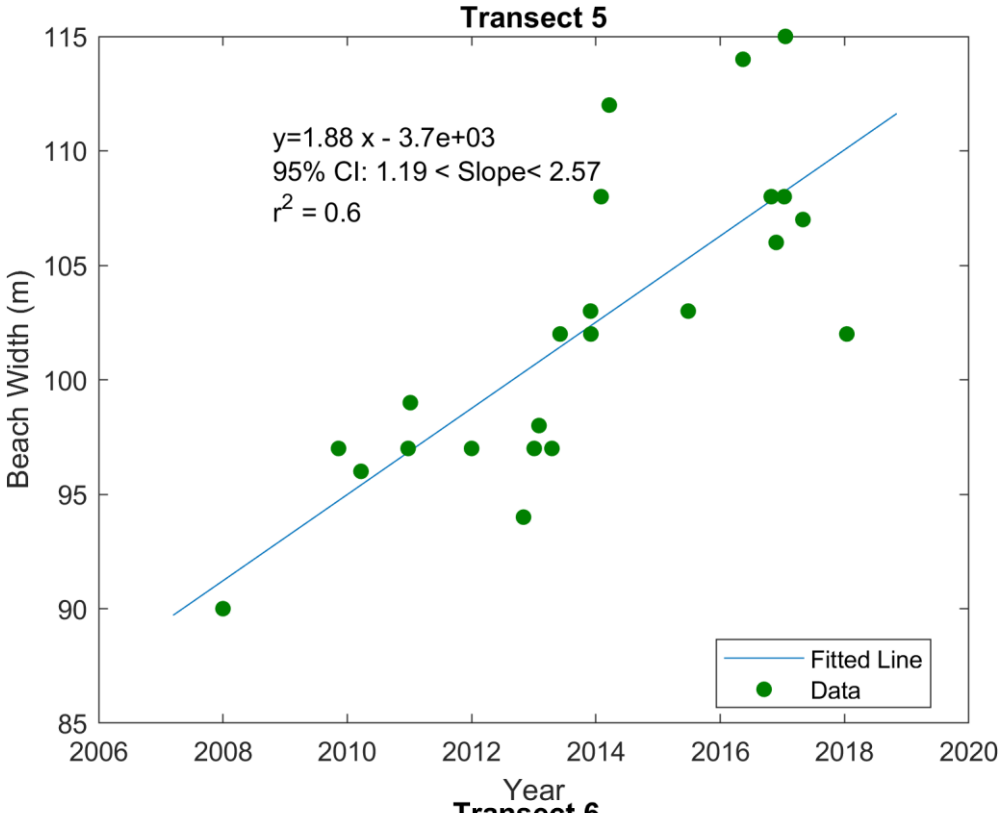
Transect 5
y=1.88 x - 3.7e+03
95% CI: 1.19 < Slope< 2.57
r2 = 0.6
Fitted Line
Data
Beach Width (m)
Year
115
110
105
100
95
90
85
2006
2008
2010
2012
2014
2016
2018
2020

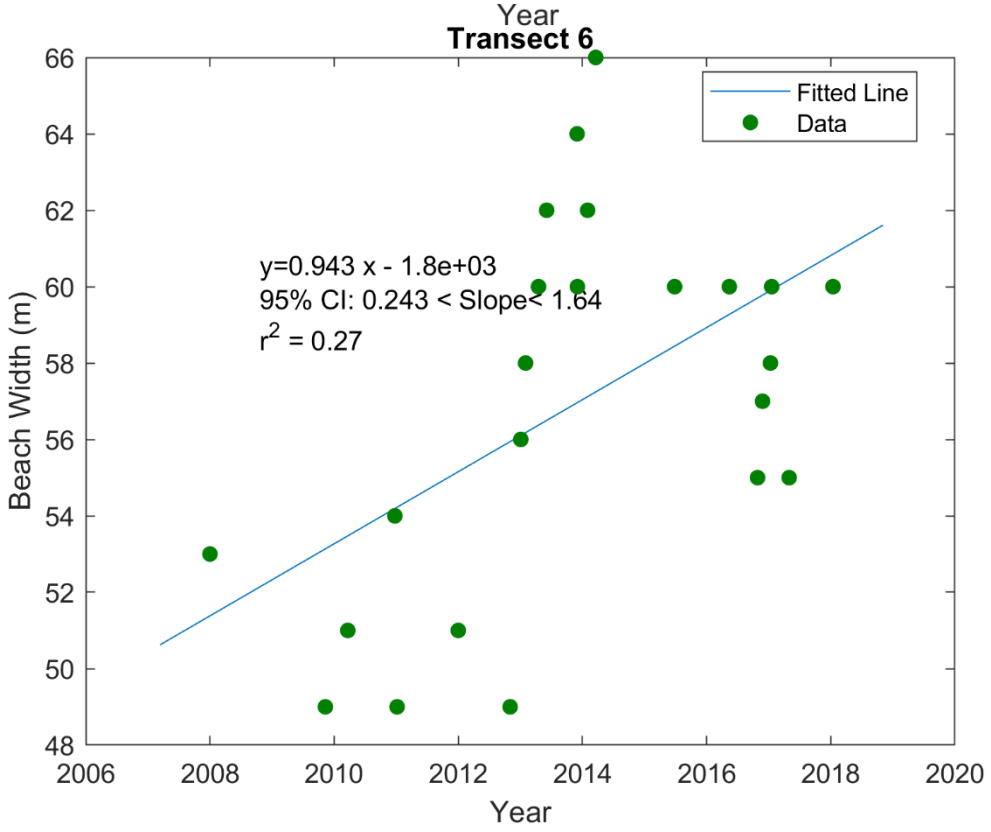
Transect 6
y=0.943 x - 1.8e+03
95% CI: 0.243 < Slope< 1.64
r2 = 0.27
Fitted Line
Data
Beach Width (m)
Year
66
64
62
60
58
56
54
52
50
48
2006
2008
2010
2012
2014
2016
2018
2020

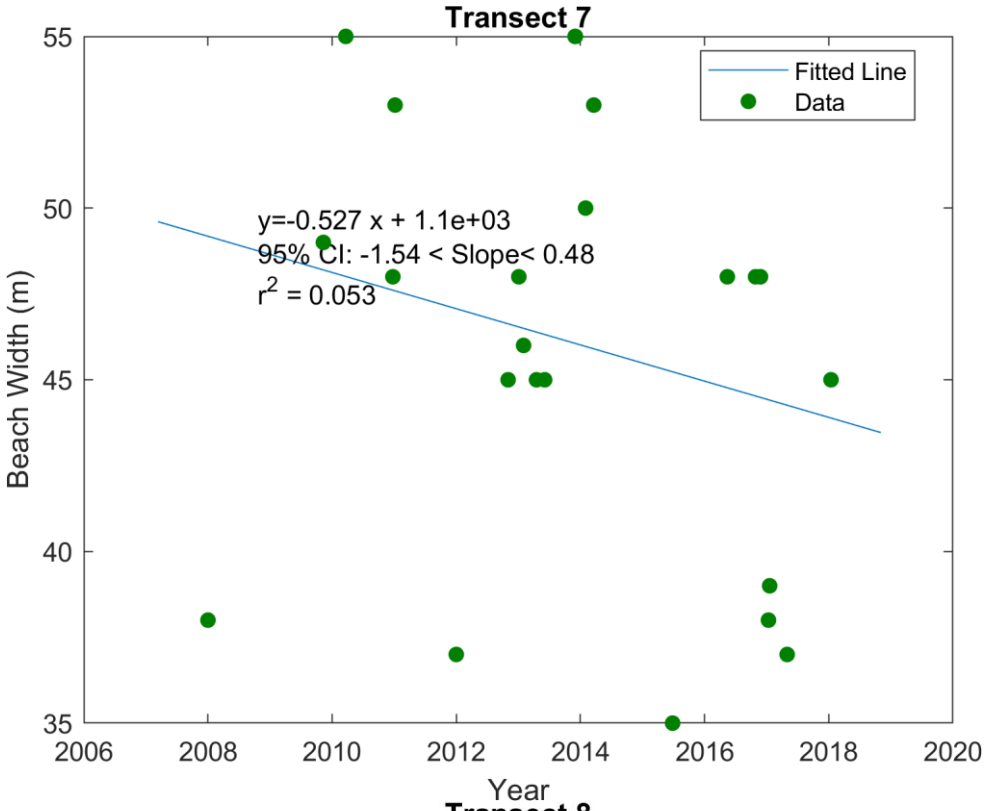
Transect 7
Fitted Line
Data
y=-0.527 x + 1.1e+03
95% CI: -1.54 < Slope< 0.48
r2 = 0.053
Beach Width (m)
Year
55
50
45
40
35
2006
2008
2010
2012
2014
2016
2018
2020

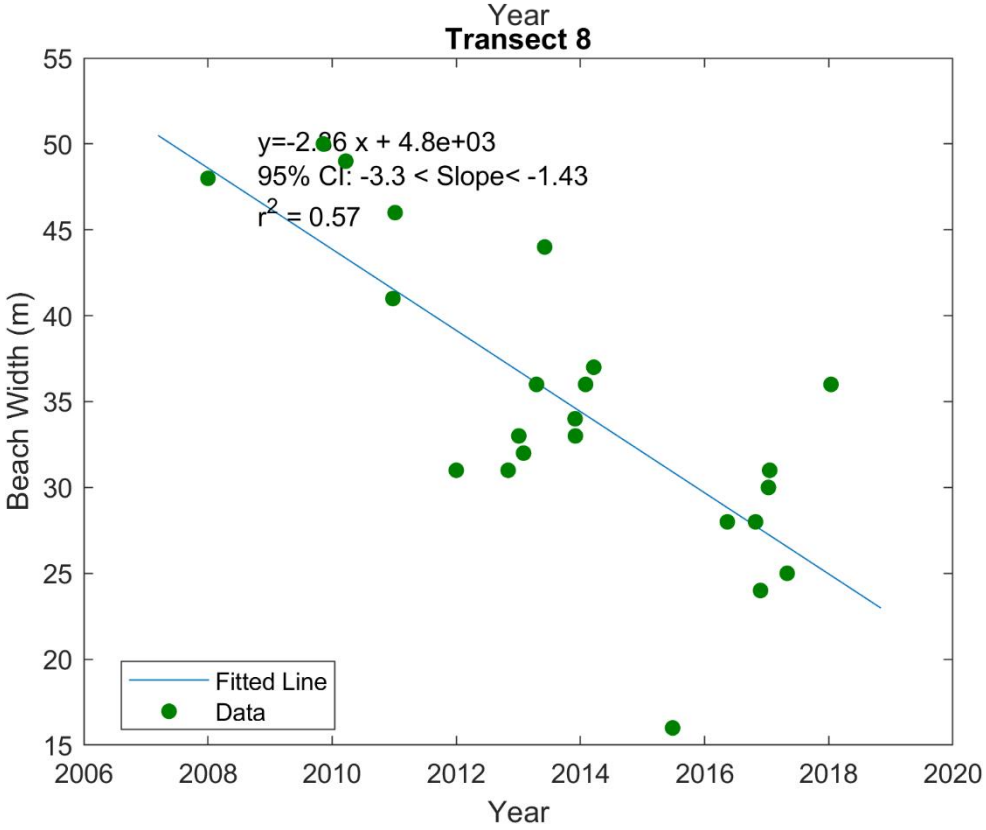
Transect 8
y=-2.86 x + 4.8e+03
95% CI: -3.3 < Slope< -1.43
r2 = 0.57
Fitted Line
Data
Beach Width (m)
Year
55
50
45
40
35
30
25
20
15
2006
2008
2010
2012
2014
2016
2018
2020

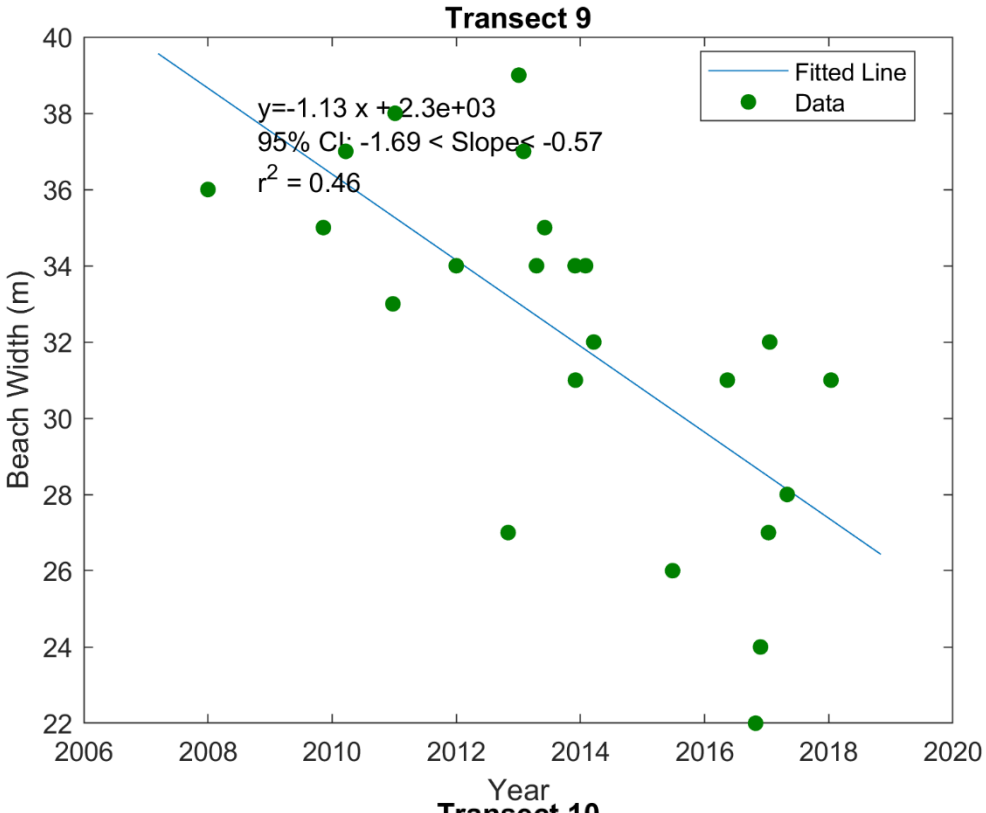
Transect 9
Fitted Line
Data
y=-1.13 x + 2.3e+03
95% CI: -1.69 < Slope< -0.57
r2 = 0.46
Beach Width (m)
Year
40
38
36
34
32
30
28
26
24
22
2006
2008
2010
2012
2014
2016
2018
2020

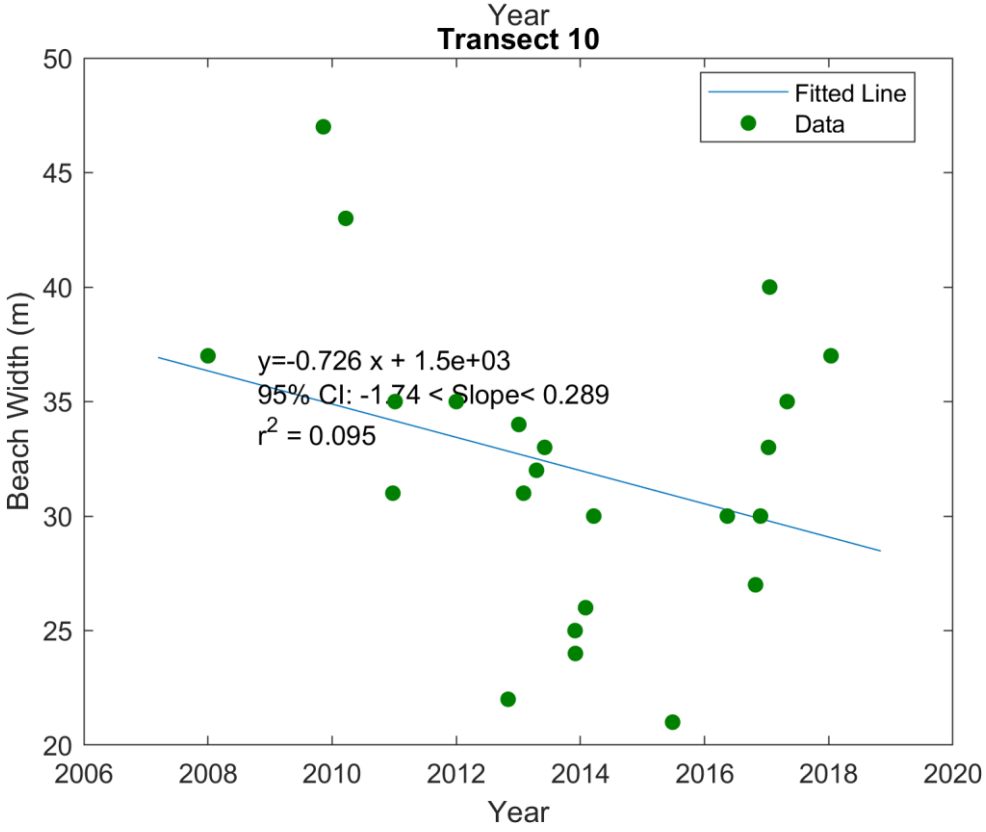
Transect 10
Fitted Line
Data
y=-0.726 x + 1.5e+03
95% CI: -1.74 < Slope< 0.289
r2 = 0.095
Beach Width (m)
Year
50
45
40
35
30
25
20
2006
2008
2010
2012
2014
2016
2018
2020

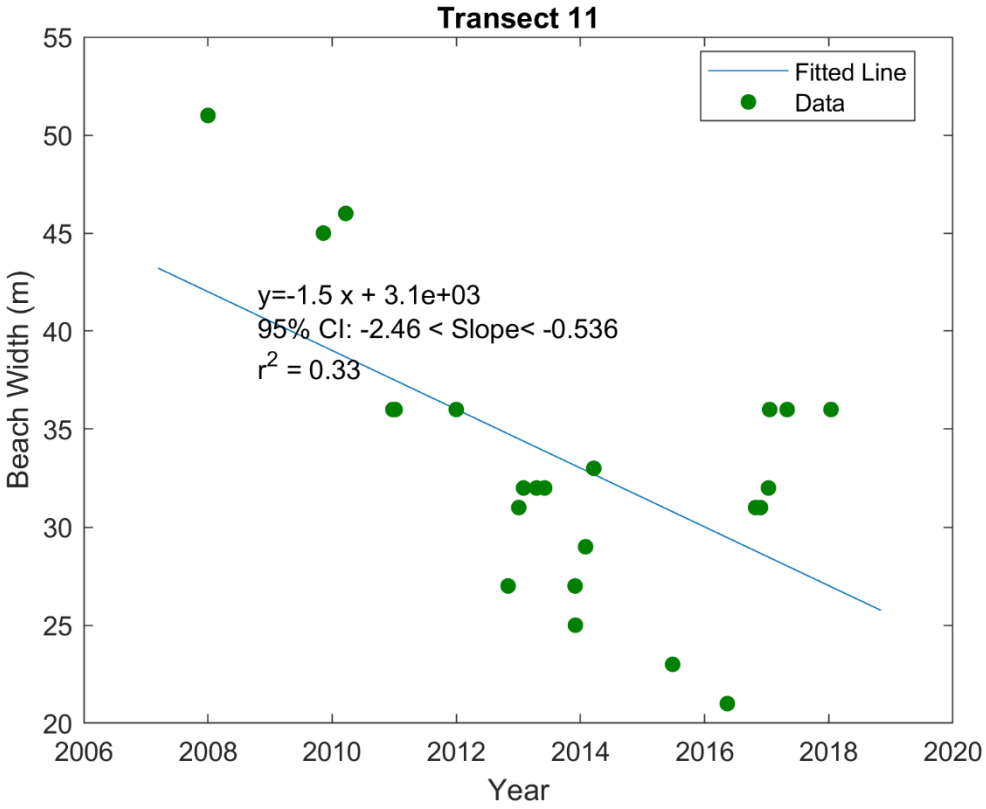
Transect 11
Fitted Line
Data
y=-1.5 x + 3.1e+03
95% CI: -2.46 < Slope< -0.536
r2 = 0.33
Beach Width (m)
Year
55
50
45
40
35
30
25
20
2006
2008
2010
2012
2014
2016
2018
2020

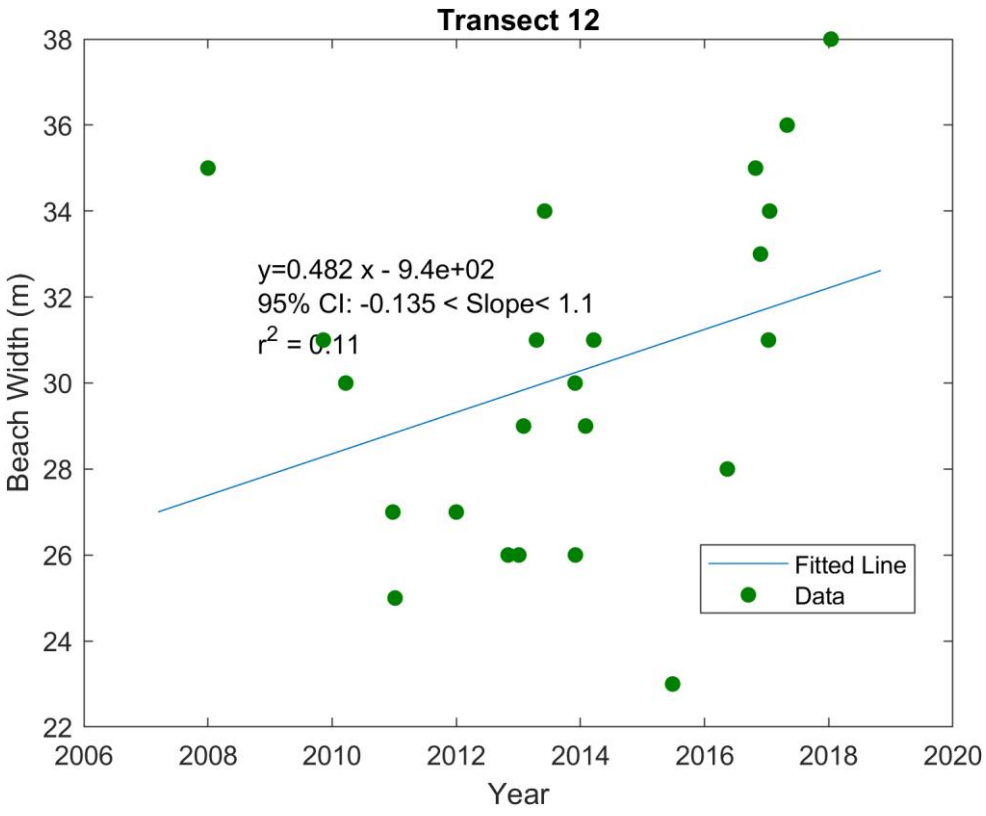
Transect 12
Fitted Line
Data
y=0.482 x - 9.4e+02
95% CI: -0.135 < Slope< 1.1
r2 = 0.11
Beach Width (m)
Year
38
36
34
32
30
28
26
24
22
2006
2008
2010
2012
2014
2016
2018
2020

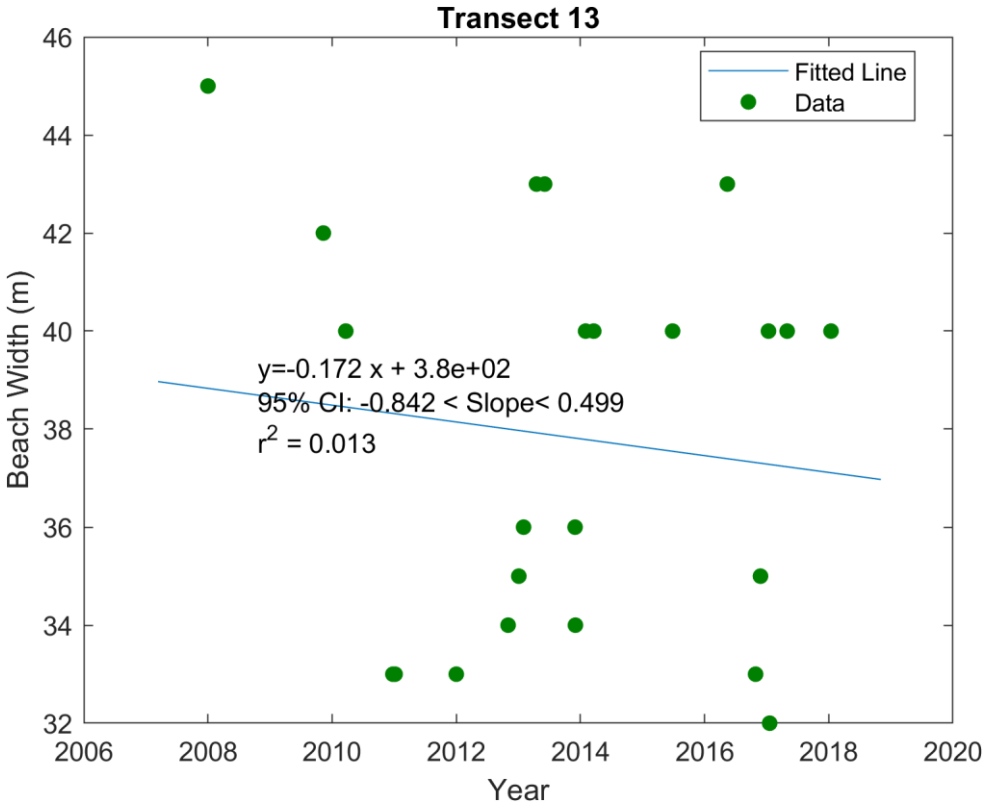
Transect 13
Fitted Line
Data
y=-0.172 x + 3.8e+02
95% CI: -0.842 < Slope< 0.499
r2 = 0.013
Beach Width (m)
Year
46
44
42
40
38
36
34
32
2006
2008
2010
2012
2014
2016
2018
2020

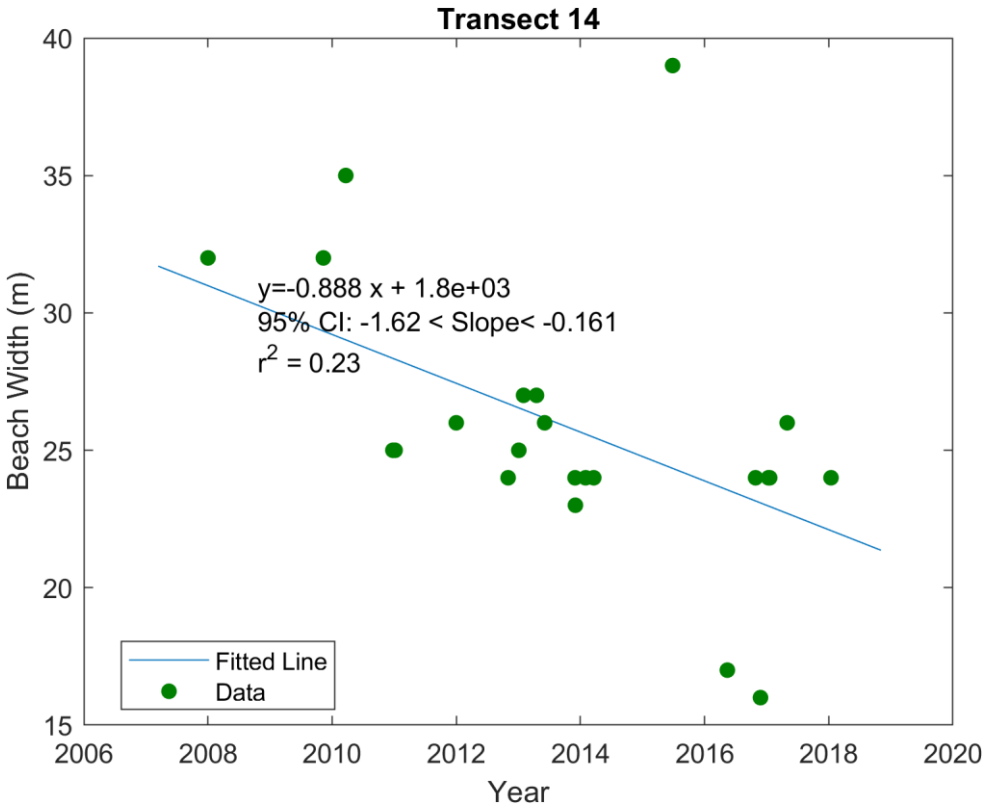
Transect 14
Fitted Line
Data
y=-0.888 x + 1.8e+03
95% CI: -1.62 < Slope< -0.161
r2 = 0.23
Beach Width (m)
Year
40
35
30
25
20
15
2006
2008
2010
2012
2014
2016
2018
2020

# Appendix C. Currents at the T3 Terminal

*Present* Scenario

Surface layer (top 1m) | Depth Averaged

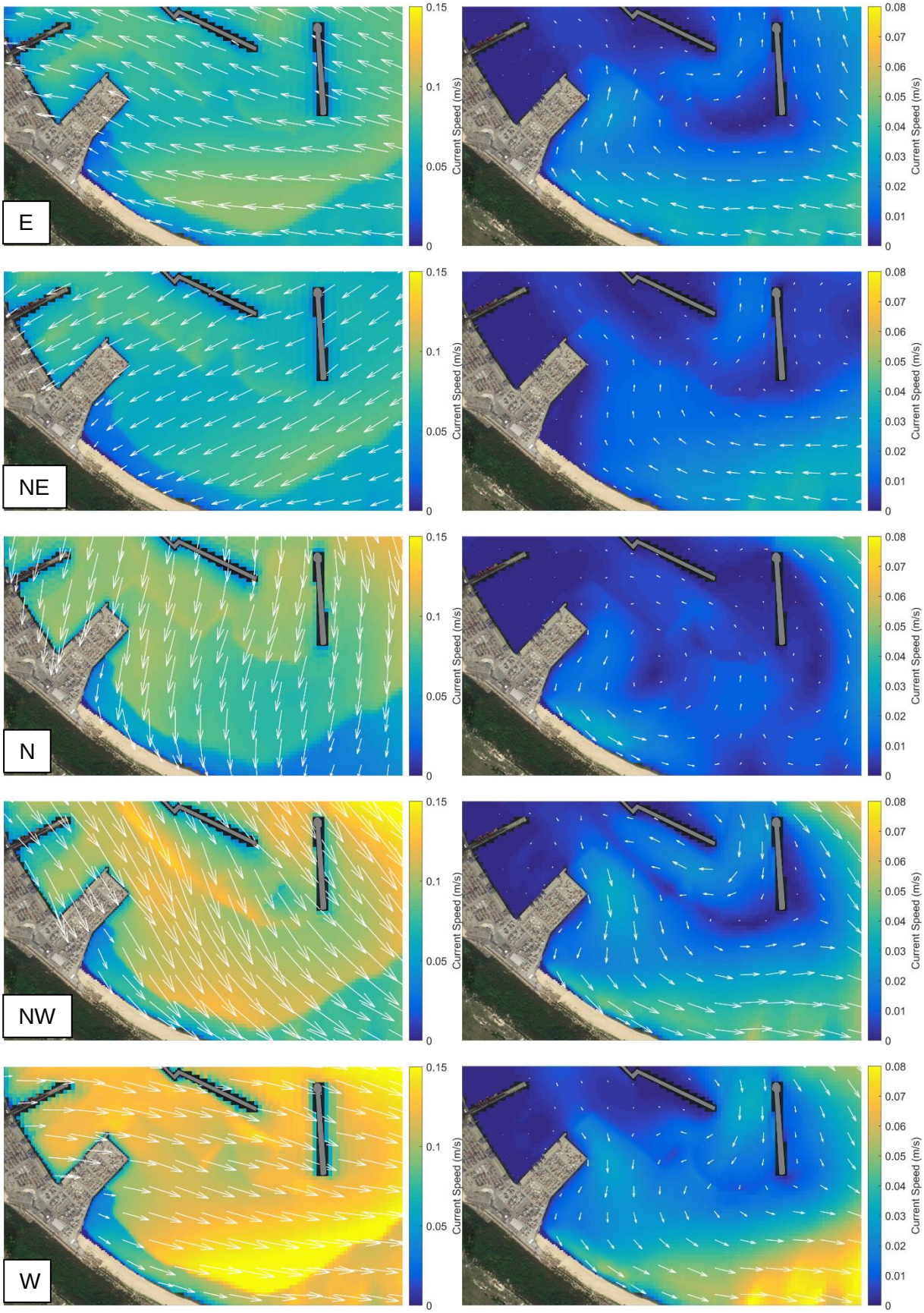

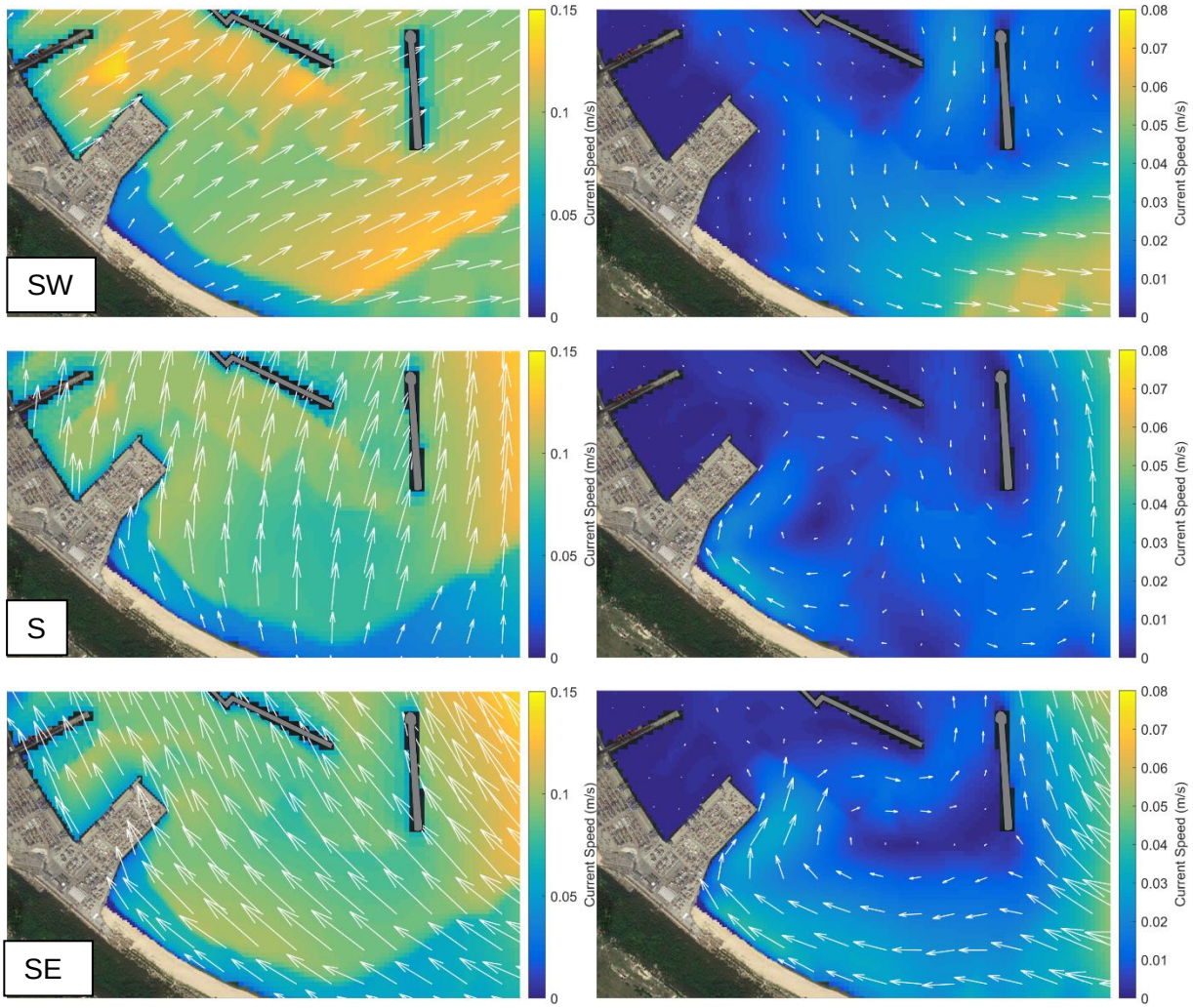
SW
S
SE
Current Speed (m/s)
0.15
0.1
0.05
0
0.08
0.07
0.06
0.05
0.04
0.03
0.02
0.01
0

*Future* Scenario

Surface layer (top 1m) | Depth Averaged

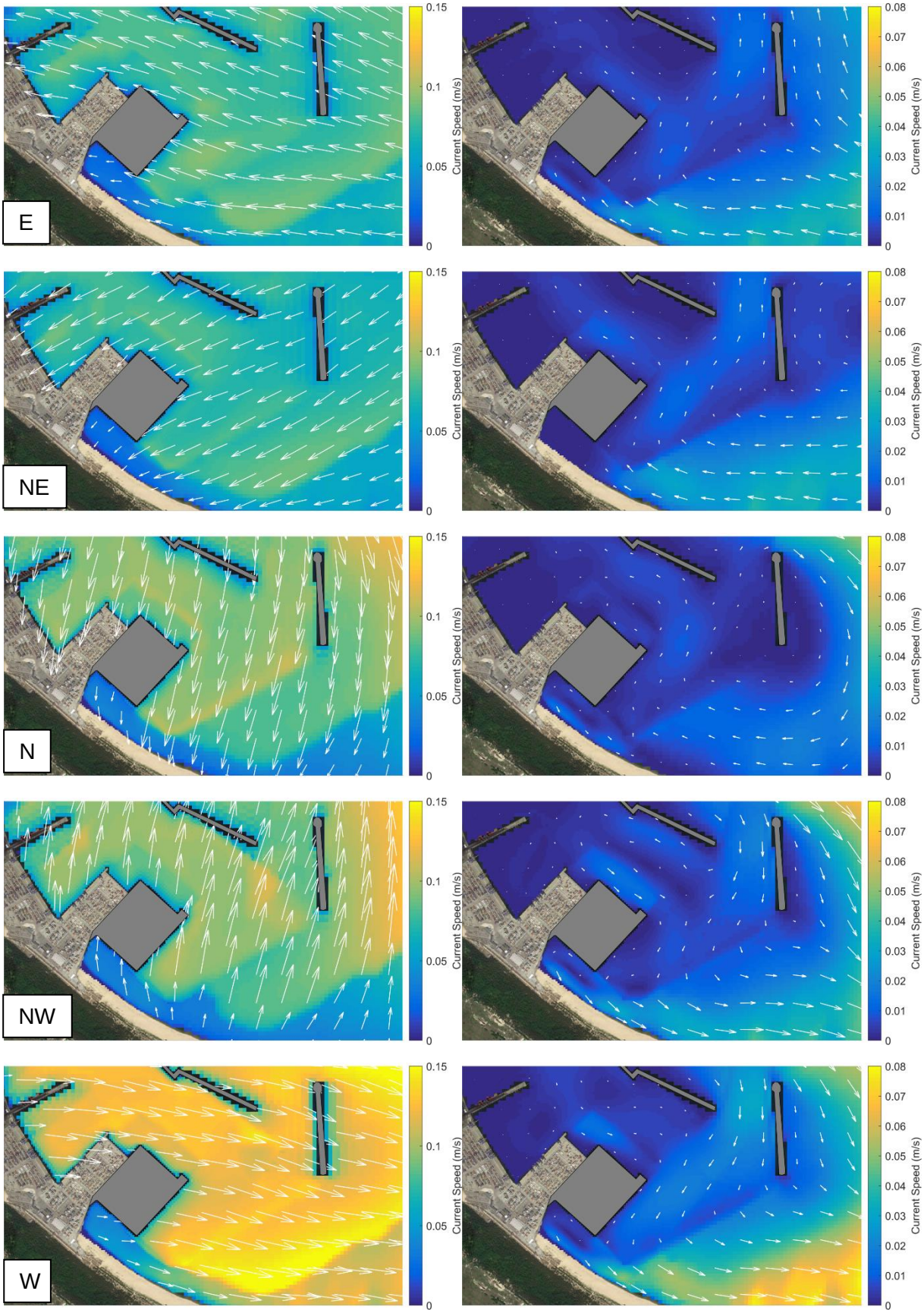

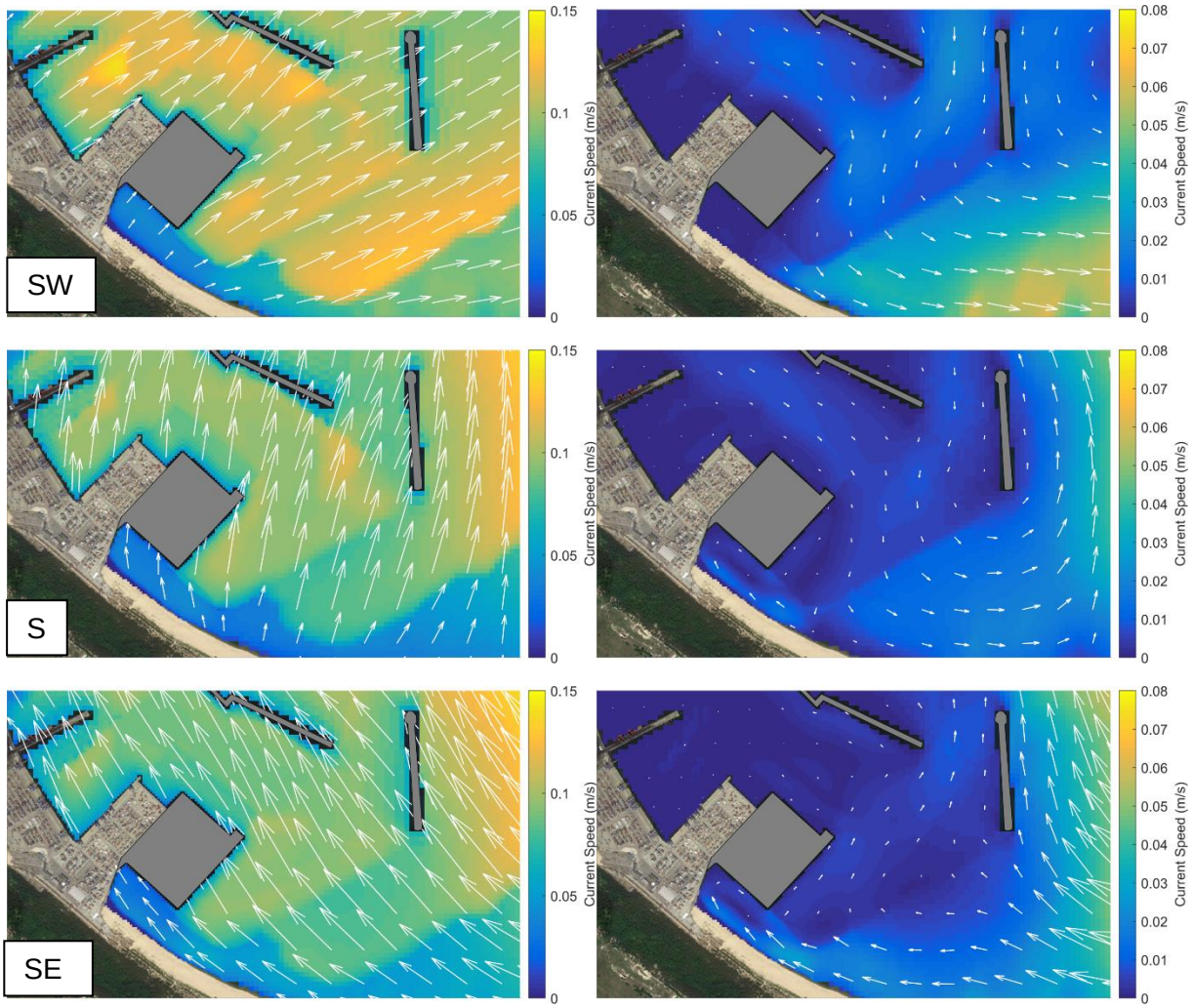
SW
S
SE
Current Speed (m/s)
0.15
0.1
0.05
0
0.08
0.07
0.06
0.05
0.04
0.03
0.02
0.01
0